Investigating the relationship between the immune response and ependymoglial activation during spinal cord regeneration in the adult and juvenile zebrafish model

by

Lidia Trzuskot

A Thesis submitted to the Faculty of Graduate Studies of

The University of Manitoba

in partial fulfilment of the requirements of the degree of

MASTER OF SCIENCE

Department of Human Anatomy & Cell Science, Rady Faculty of Health Sciences

University of Manitoba

Winnipeg

Abstract

Spinal cord injury (SCI) is a life changing condition affecting individuals within Canada and worldwide with no effective treatment to date. A limitation in humans, like other mammals, is that they cannot repair the damaged central nervous system after injury. By contrast, the zebrafish model has a remarkable ability to regenerate the spinal cord following complete transection, due to neural stem cell populations of ependymoglia. Previous work has shown that for ependymoglial-driven neural regeneration to occur, immune cells are a key requirement. However, in zebrafish the involvement of macrophages and the cytokine response during the process of spinal cord regeneration in post-larval stages remains poorly understood. In this study, I hypothesized that for functional recovery to occur, the pro-inflammatory response following SCI in zebrafish must be activated ahead of ependymoglial proliferation to initiate the regenerative process. To study this response, I developed a new juvenile model of SCI to then compare to the established adult model of SCI. By studying the spatiotemporal dynamics of immune cells post-SCI, I observed that overtime macrophages and microglia infiltrate into the injury site and contributed to cytokine release, correlating with a peak in proliferation of ependymoglia around the central canal. Interestingly, analysis of pro- and anti-inflammatory cytokines from RT-qPCR experiments demonstrated that pro-inflammatory cytokines are highly expressed shortly after injury, but are reduced to near control levels already by 3-days post-SCI. By contrast, anti-inflammatory cytokines appeared to play a minor role in the microenvironment post-SCI, remaining near control levels of expression. These findings propose that in order for successful spinal cord regeneration to occur in adult and juvenile zebrafish, a shorter pro-inflammatory response may be required to initiate ependymoglial proliferation in the spinal cord and restore functional repair.

Acknowledgements

First, I would like to thank Dr. Benjamin Lindsey for his mentorship and the opportunities he has given me. Dr. Lindsey has helped shape me into the scientist that I am today. He has gone above and beyond what a thesis supervisor is asked to do and has opened many doors for my future and for me to further grow as an individual. I will always be grateful for his support and guidance as he encouraged my independence and confidence to become a better scientist.

I would like to thank my committee members, Dr. Soheila Karimi-Abdolrezaee and Dr. Susan Logue for their support and guidance during my graduate studies. I thank the members and faculty of the Department of Human Anatomy and Cell Science for their support as well. Furthermore, I would like to acknowledge Research Manitoba for the Master's Studentship and Rady Faculty of Health Sciences Graduate Entrance Scholarship for their financial contributions to this project.

I would also like to thank Suhaila Selamat for all her assistance with the RNA extractions and RT-qPCR runs completed in my project, as well as her support, friendship and knowledge. With her help I was able to finish this thesis in a timely manner. A huge thank you to the wonderful members of the Lindsey Lab both past and present. You made coming in everyday enjoyable and fun.

Finally, I would like to thank all my family and friends whose encouragement gave me the strength to push forward and complete my studies. Thank you to my parents whose support allowed me to grow into the independent individual that I am today. Thank you to my sisters and friends for always making me laugh and distracting me from the stress of research. Your constant love made you the ultimate support system without whom I would not have gotten to where I am now.

Table of Contents

List of Figures

List of Tables

List of Acronyms & Abbreviations

ASIA	American Spinal Injury Association
BDNF	brain-derived neurotrophic factor
BMP	bone morphogenetic protein
BrdU	5-bromo-2'-deoxyuridine
CC	central canal
CNS	central nervous system
CSF	cerebrospinal fluid
Ct	cycle threshold
DAPI	4′,6-diamidino-2-phenylindole
Dpf	days post-fertilization
Dpi	days post-injury
ECM	extracellular matrix
EDTA	ethylenediaminetetraacetic acid
EdU	5-Ethynyl-2′-deoxyuridine
ESCs	embryonic stem cells
EZ	ependymal zone
FGF	fibroblast growth factor
GFAP	glial fibrillary acidic protein
GFP	green fluorescent protein
H&E	Hematoxylin and Eosin
IHC	immunohistochemistry

IL-10	interleukin-10
Il-1β	interleukin-1β
IL-4	interleukin-4
IL-8	interleukin-8
iPSCs	induced pluripotent stem cells
NSC	neural stem cells
PCNA	proliferating cell nuclear antigen
PFA	paraformaldehyde
RA	retinoic acid
RFP	red fluorescent protein
ROS	reactive oxygen species
RT	room temperature
RT-qPCR	reverse transcriptase quantitative polymerase chain reaction
SCI	spinal cord injury
SEM	standard error of the mean
SEZ	subependymal zone
Shh	sonic hedgehog
Sox2	SRY-box 2
TGF-β	transforming growth factor-β
TNFα	tumor necrosis factor α
UPR	unfolded protein response
VEGF	vascular endothelial growth factor

Chapter 1.0 Literature Review

1.1 Introduction

Spinal cord injury (SCI) in vertebrates, including humans, is defined as damage to the spinal cord from an external impact that leads to a failure in motor function (Ahuja et al., 2017). This failure results in the inability to walk or use one's legs, and can be associated with problems with voidance, and an overall loss of sensation that can impact sexual stimulation and the ability to feel pain (Mckinley et al., 1999; Hess & Hough, 2012; Shiao & Lee-Kubli, 2018). Within SCI there exist different severities that result in varying degrees of neurotrauma. Severity of SCI is classified using the American Spinal Injury Association (ASIA) Impairment Scale that is used globally to determine muscle strength and movement (Roberts et al., 2017). This allows for injury to be scored from grade A to E, with A being the most severe with a complete loss of sensation and E being the least severe with normal movement and sensation (Roberts et al., 2017). The ASIA Impairment Scale is also used to determine whether a SCI is complete, which includes a total loss of sensation below the injury level, or incomplete where there is some function retained below the injury level (Roberts et al., 2017).

Estimates show that upwards of 86,000 individuals currently live with SCI in Canada (Noonan et al., 2012) and 12,500 individuals are affected each year within North America (Alizadeh et al., 2019). Of those affected, it is common for SCI to occur in younger adults between the ages of 15-29, as a result of motor vehicle accidents or sport related injuries, or in late adulthood around the age of 50, attributed to an increased risk of falls (Lee et al., 2014; Chen et al., 2016; Ahuja et al., 2017). This neurological condition is a life-changing impairment with limited functional recovery in patients. Following SCI, the events that unfold within the microenvironment are complex and categorized into primary and secondary phases. The primary phase of injury results from a sudden

impact to the spinal cord, causing displaced bone fragments and tearing that disrupt blood vessels and axons (Kaur & Sharma, 2018; Alizadeh et al., 2019). The secondary phase is initiated minutes after initial injury and can last for months resulting in a series of cellular, molecular and biochemical events that further deteriorate tissue and impede recovery (Oyinbo, 2011; Alizadeh et al., 2019). Some of these events include inflammation, hemorrhage, apoptosis, and demyelination (Gao et al., 2020).

To date there exists no effective treatment for patients living with SCI. Mammalian models of SCI continue to reveal that some of the major barriers to spinal cord repair include glial astrocytic scarring, the role of chondroitin sulfate proteoglycans (CSPGs) in impeding axonal regeneration, and an inflammatory response that persists from acute to chronic phases of SCI (Dyck & Karimi-Abdolrezaee, 2015; Katoh et al., 2019). Several stem cell based therapeutic strategies have been developed in an effort to overcome these barriers, including the use of induced pluripotent stem cells (iPSCs) and embryonic stem cells (ESCs), stem cell transplantation, and the activation of local endogenous stem cell populations. However, the ability of stem cells to successfully undergo neuronal differentiation can only be achieved in an injury-induced environment conducive to providing the necessary signals for neuroregeneration. A clearer understanding of the relationship between the activity of transplanted or *in vivo* stem cell populations and the timeline of damage associated cues would serve as a valuable next step to define the process of successful neurorepair. To this end, taking advantage of highly neuroregenerative non-mammalian models such as the freshwater teleost, the zebrafish (*Danio rerio*), salamanders (e.g. Axolotls; *Ambystoma tigrinum*), or larvae of the African clawed frog (*Xenopus laevis)*, provide an unprecedented opportunity to further our knowledge of how successful neurorepair takes place after SCI.

My thesis research focuses on furthering this knowledge by taking advantage of the exceptional neuroregenerative ability of the zebrafish model to study the process of spinal cord repair following SCI. This research will serve to provide insight into how neural stem cells (NSC) and select immune cells work to promote functional recovery that can be later investigated in mammalian models of SCI. In the following sections, I will first review the current strategies that are used to treat SCI in human patients and their associated drawbacks that lead to the study of more effective therapies. Next, I will discuss how NSCs are regulated intrinsically within the spinal cord and through signals in the microenvironment. Within the spinal cord environment, the immune response plays a major role, thus I will review the involvement of immune cells in the inflammatory response following SCI. Finally, I will discuss what makes zebrafish an attractive model in studying successful spinal cord repair including their anatomy, the role of inflammation and the signaling pathways involved in the process of neuroregeneration.

1.2 Current Approaches to Treat SCI

The current strategies for the treatment of SCI focus on using surgical approaches to stabilize the injured area, pharmacological means to prevent further damage in the secondary phase of injury, and rehabilitation such as physical therapy to prevent or regain loss of function (Liau et al., 2020). Although these methods can improve the overall outcome of SCI in patients, they cannot stimulate regeneration in the spinal cord and as such have had limited success. This has driven researchers to study more effective strategies for the treatment of SCI including cell-based therapies such as the use of somatic cells to create iPSCs, the transplantation of stem cells to the injured spinal cord,

and activation of endogenous stem cells, such as resident ependymal cells surrounding the spinal cord central canal (Khazaei et al., 2016; Gao et al., 2020).

1.2.1 Sources of Stem Cells for Spinal Cord Repair

To repair the spinal cord after injury in humans, different sources of stem cells have been used including iPSCs, ESCs, and adult stem cells. iPSCs are a type of stem cell derived from adult somatic cells that have been reprogrammed into an embryonic stem cell-like state. These cells are pluripotent, meaning they can give rise to all cell types within the body. There are several somatic cell types that have been biopsied and used for induction including fibroblasts, keratinocytes, melanocytes, hepatocytes, adipocytes, and umbilical cord blood cells (Khazaei et al., 2016). To induce stem cells, a variety of transgenes are used and most commonly these include *Oct4*, *Sry-box 2 (Sox2)*, *Klf4*, and *c-Myc* (Takahashi & Yamanaka, 2006). While these iPSCs are capable of generating all cell types, they have commonly been used in an attempt to restore neural function through differentiation into neurons, oligodendrocytes, and astrocytes (Li & Lepski, 2013). Subtypes of neurons such as motor neurons and dopaminergic neurons can be further differentiated to treat movement disorders (Chip et al., 2012; Sances et al., 2016; Trawczynski et al., 2019). A factor that is taken into consideration when inducing stem cells is the reprogramming efficiency of the different cell types, which refers to the percentage of somatic cells reprogrammed successfully. Keratinocytes, for example, are able to be reprogrammed at higher frequencies and faster rates than fibroblasts taken from the same skin biopsies (Yee, 2010). This appears to be most likely due to the higher levels of transcription factors, *c-Myc* and *Klf4*, found in keratinocytes (Yee, 2010).

Despite the potential benefits, several drawbacks are associated with the generation of iPSCs. These include the use of viral vectors to introduce transcription factors, the decrease in efficiency seen when transitioning into a pluripotent state, and the reactivation of transgenes post-induction (Medvedev et al., 2011). First, in order to introduce transcription factors to the somatic cells, retroviral and lentiviral vectors are used. These vectors can deliver a gene of interest by infecting a cell and inserting the gene into the host DNA. The integration of retroviral DNA into the host cell genome occurs randomly and so the copy number of the retroviral DNA that ends up integrated varies (Medvedev et al., 2011). Another issue that arises is that the transcription level of *Oct4*, *Sox2*, *Klf4*, and *c-Myc* decreases when the cell transitions to a pluripotent state and as a result decreases the efficiency of stable iPSC line production (Medvedev et al., 2011). Finally, studies have shown that the transcription of transgenes can resume in cells that are derived from iPSCs (Medvedev et al., 2011). Reactivation of these transgenes can cause tumors and as such cannot be used in clinical trials (Yee, 2010).

ESCs are similar to iPSCs in the sense that they are able to differentiate into any cell type of the body. A major difference however is that these cells are isolated from blastocyst-stage early embryos rather than induced from somatic cells (Gepstein, 2002). ESCs retain the ability to differentiate into the three germ layers and as such are a promising candidate to generate cells for replacement. However, deriving such cells has led to ethical controversy and there is the challenge of acquiring the cells due to the limited supply of donor embryos. Using ESCs as a therapeutic strategy can result in teratomas due to uncontrollable cell proliferation. Further, they may be prone to rejection by adult tissue leading to the use of immunosuppression which increases the risk of cancer and infection (Nussbaum et al., 2007; Shiras et al., 2009; Rong et al., 2014).

A way to overcome the ethical concerns and challenges of acquisition is to employ more mature multipotent stem cells phenotypes that retain the capacity to develop into multiple specialized cells, as an alternative strategy for cell replacement therapy. Stem cells such as NSCs, mesenchymal stem cells, oligodendrocyte precursor cells, and olfactory ensheathing cells are commonly used in stem cell therapies (Nandoe Tewarie et al., 2009; Assinck et al., 2017). These cells are easier to gain ethical approval for, can be isolated from adult tissue without the need of embryos, and have been the focus of research in many animal models (Hernández et al., 2011). However, there is a decrease in the number of available proliferating adult stem cells with increasing age, and with senescence, cellular function may decrease with ageing of the stem cell niche microenvironment (Mariano et al., 2015). While each stem cell type, including adult stem cells, ESCs, and iPSCs are associated with advantages and disadvantages, common across all is that they have been delivered through stem cell transplantation methods in an effort to improve spinal cord repair.

1.2.2 Stem Cell Transplantation

Cell transplantation as an intervention for SCI has been studied by researchers for many years. This therapy works through *in vivo* or *in vitro* transplantation where various sources of stem cells can be delivered to treat injuries or diseases. *In vivo* transplantation occurs by direct transplantation of stem cells into the body whereby signaling molecules within the environment will guide the cells into a mature cell type (Li & Lepski, 2013). By contrast, *in vitro* transplantation consists of isolating the cells, culturing, purifying and finally amplifying them to be induced into the necessary cell type before transplantation (Li & Lepski, 2013). Since both ESCs and iPSCs are capable of

differentiating into all cell types under the proper conditions *in vitro*, a common approach is to transplant the derived cell lines from these stem cells, rather than directly applying lost cell types (Li & Lepski, 2013). Like this method, there exists direct reprogramming of somatic cells into the desired cell for transplantation without first dedifferentiating into a pluripotent state (Kim & Tae, 2016). These methods reduces the risk of generating teratomas (Coutts & Keirstead, 2008). In addition to ESCs and iPSCs, more differentiated adult stem cells can serve as sources for stem cell transplantation, but due to their multipotency, are limited in their ability to differentiate into different cell phenotypes (Nandoe Tewarie et al., 2009; Assinck et al., 2017).

Using cell transplantation as a therapeutic strategy may encourage regeneration post-SCI through means of secreting neurotrophic molecules at the site of injury, creating a scaffold for axons to regenerate, and replacing cell types lost to injury (Li & Lepski, 2013). Many stem cell types including those derived from iPSCs, are able to secrete trophic factors and cytokines (Hawryluk et al., 2012; Assinck et al., 2017). These trophic factors stimulate proliferation and differentiation of existing neural precursor cells following SCI, and enhance axonal regrowth, remyelination and neuronal plasticity (Gordon et al., 2010; Hawryluk et al., 2012; Li & Lepski, 2013; Cooney et al., 2016). A study in rats using mesenchymal stem cells found that when compared to control groups, mesenchymal stem cells transplants contained more neurofilament labeling which demonstrated an axon growth-supportive scaffold (Ankeny et al., 2004). They also found that the transplants provided directional guidance, orienting them to ascend and descend along the longitudinal axis of the spinal cord (Ankeny et al., 2004). While stem cell transplantation may hold great promise in the treatment of SCI, there are factors that need to be considered in using this approach including

ethical concerns, the number of cells to be transplanted, and the window of time for treatment following SCI (Nandoe Tewarie et al., 2009).

A downside in utilizing ESCs for transplantation is the possible formation of teratomas from uncontrollable cell proliferation. Additionally, ESCs may be prone to rejection by adult tissue leading to the use of immunosuppression which increases the risk of cancer and infection (Nussbaum et al., 2007; Shiras et al., 2009; Rong et al., 2014). To avoid this, more differentiated adult stem cells can be used with caution since these cells show decreased differentiation over time (Wright et al., 2006). Nevertheless, using mature stem cells usually does not result in the formation of tumors as they are more differentiated than ESCs and the risk of rejection is lower if the cells are derived from the patient, consisting of the same genetic makeup (Coutts & Keirstead, 2008; Jin et al., 2016; Goulão & Lepore, 2016).

Regardless of the source of stem cells used in attempt to improve recovery following SCI, a sufficient number of transplanted cells is necessary to maximize the therapeutic effect. With this said, a greater number of cells may not always result in better outcomes for patients, and the number of transplanted cells may interact differently with the microenvironment (Iwai et al., 2014; Piltti et al., 2017). This was seen in a study that found no correlation with the number of cells transplanted in an SCI mouse model and cell survival (Iwai et al., 2014). In addition, the number of transplanted NSCs had no effect on differentiation (Piltti et al., 2017). For example, oligodendrocyte differentiation was unaffected through either the low-dose or high-dose group (Piltti et al., 2017). These results indicate that there exist optimal thresholds of the number of transplanted stem cells which can affect the differentiation of target cells.

Across researchers, the consensus varies as to the appropriate window of time post-SCI to perform stem cell transplantation. Some believe that early administration is beneficial in reducing the effects of secondary injury such as acute inflammation, glial scarring, and regulating glial cells and macrophages (Nakajima et al., 2012; Watanabe et al., 2015; All et al., 2015). Early intervention of NSCs has also been shown to provide neuroprotection and improvement in neurological performance (Watanabe et al., 2016). On the other hand, it has been proposed that prolonging the start of stem cell administration may lead to better survival of transplanted cells due to a larger number of neurotoxins that are produced from macrophages early after SCI in mammals and humans (Kigerl et al., 2009). Obstacles arising from ethical concerns, insufficient cell number and drawbacks in the timing cell transplantation could be avoided if there were ways to harness the ability of endogenous stem cells within the spinal cord itself.

1.2.3 Endogenous Potential of NSCs

While stem cell transplantation has great potential for the treatment of SCI, there exist concerns over ethics, number of donors, and rejection by the immune response (Gao et al., 2020). As an alternative to transplantation, harnessing endogenous stem cells to treat SCI overcomes these concerns and the challenges regarding cell delivery (Ahuja et al., 2020). NSCs are one of many common stem cells used for the treatment of SCI due to their multipotentiality and ability to differentiate into specific neuronal and glial cells (Huang et al., 2021). These cells can divide asymmetrically to self-renew and produce a daughter cell that will take the identity of a neuron, oligodendrocyte or astrocyte to restore cells lost to injury within mammals (Ahuja et al., 2020). The endogenous NSCs in non-mammalian vertebrates such as axolotls, zebrafish, and even the

freshwater turtle *Trachemys dorbignyi* have the potential to repair their damaged spinal cords due to their powerful neurogenic capacity after injury (Becker & Becker, 2008; Rehermann et al., 2009; Sabin et al., 2015).

This powerful neurogenic capacity in non-mammalian vertebrates may stem from the different factors post-SCI that can stimulate regenerative neurogenesis by the proliferation of NSCs. These factors, similarly, found in mammals could also hold the potential for recovery in a non-regenerative environment. For example, in the adult central nervous system (CNS), NSCs neighbor endothelial cells and proliferate around dividing capillaries, otherwise known as vascular niches (Carmeliet, 2003). By using vascular endothelial growth factor (VEGF), Liu and colleagues (2018), were able to trigger NSCs of the rat spinal cord to proliferate and maintain self-renewal to significantly increase the number of activated NSCs. Similar studies in rats have shown suggestive results using fibroblast growth factor (FGF) or brain-derived neurotrophic factor (BDNF) to increase proliferation and stem cell survival (Kojima & Tator, 2000; Hachem et al., 2015). Direct application of growth factors, however, can lead to unregulated cell growth so there is a need for other forms of activation (Hachem et al., 2020).

More recently some studies have examined the secreted factors and vesicles arising from stem cells known as the secretome, to trigger a regenerative effect (Pinho et al., 2020). This procedure involves culturing cells, priming them through hypoxia, apoptotic or inflammatory stimuli, and collecting the factors released (Pinho et al., 2020). The composition of the secretome can include VEGF, BDNF, FGF, glial-derived neurotrophic factor, and nerve growth factor (Pinho et al., 2020). Despite current research to enhance the potential for stem cells to repair post-SCI, more

work is required to achieve greater levels of activation and neuronal differentiation in mammals. Comparing spinal cord anatomy, NSC populations, and injury-induced signals following SCI between mammalian and non-mammalian models, such as the zebrafish, may provide new clues for better patient treatments for spinal cord recovery.

1.3 Spinal Cord Anatomy and NSC Regulation Post-SCI

The adult vertebrate spinal cord serves to relay sensory information and motor instructions between the brain and the peripheral nervous system (Leung & Shimeld, 2019). This is protected by the vertebral column, which is also involved in maintaining body posture (Cho, 2015). Below the vertebral column lies three layers of tissue termed the meninges of the spinal cord, whose function is to provide a supportive framework and protect the spinal cord from damage (Dasgupta & Jeong, 2019). These layers consist of the pia mater, arachnoid mater, and the dura mater (Sehgal & Das, 2021). The pia mater is the deepest layer that forms a thin sheath immediately around the spinal cord and helps maintain its compact structure while the arachnoid functions to maintain the cerebrospinal fluid (CSF) metabolism (Sehgal & Das, 2021). The most superficial and strongest layer is the dura mater, sitting adjacent the vertebrae (Sehgal & Das, 2021).

Viewed in cross section, two areas of the spinal cord are visible. These include the inner grey matter that is made up of a collection of cell bodies from both neurons and glia, and the outer white matter consisting of mainly axon fibers tracts (Khan & Lui, 2021). In mammals, motor neurons and interneurons are located in the ventral horn of the grey matter and help fine-tune motor output. The grey matter also consists of the dorsal horn which contains sensory neurons and interneurons that receive different inputs to recognize pain, light touch and temperature (Cho, 2015). Similarly,

in zebrafish the dorsal horn contains sensory neurons and interneurons that excite the motor neurons and interneurons in the ventral horn (Hale et al., 2001; Reimer et al., 2008; Björnfors & El Manira, 2016; Henderson et al., 2019). Within the grey matter the central canal extends the length of the spinal cord and makes up a cavity of CSF lined by ependymal cells (Hamilton et al., 2009; Saker et al., 2016). These ependymal cells, which act as endogenous NSCs, are one of the many cell populations located within the vertebrate spinal cord.

1.3.1 Cell Populations of the Spinal Cord

During embryonic development, the mammalian vertebrate CNS is formed by neuroepithelial cells that line the neural tube (Subramanian et al., 2017). Around the time that neurogenesis begins, neuroepithelial cells begin to take on glial features, becoming radial glia (Kriegstein & Alvarez-Buylla, 2009; Paridaen & Huttner, 2014). Throughout development, radial glia, that function as neural progenitor cells, undergo asymmetric division to generate neurons and oligodendrocytes (Kriegstein & Alvarez-Buylla, 2009). Some of these radial glia then convert into ependymal cells and astrocytes neonatally (Kriegstein & Alvarez-Buylla, 2009). The transition to adulthood in the mammalian spinal cord includes radial glia differentiating into ependymal cells that will line the central canal of the spinal cord throughout life (**Fig. 1A**; Kriegstein & Alvarez-Buylla, 2009; Sabelström et al., 2014). This ependymal lining of the central canal is a feature shared by all amniotes. Ependymal cells in adult mammals have a cuboidal, multi-ciliated morphology. Under homeostatic conditions in mammals, ependymal cells self-renew *in vivo*, but are limited in proliferation beyond postnatal development with only residual activity persisting into adulthood (Bruni, 1998; Meletis et al., 2008).

In anamniotes, such as salamanders and zebrafish, similar to mammals, radial glial cells are also derived from initial neuroepithelial populations during early development and will give rise to neurons and glia (Lewis & Eisen, 2003; Than-Trong & Bally-Cuif, 2015; Ghosh & Hui, 2016; Tazaki et al., 2017; Zambusi & Ninkovic, 2020). However, a major difference compared to amniotes is that both neuroepithelial and radial glial populations persist into adulthood and serve lifelong as the two major NSC populations of the zebrafish CNS (Lindsey et al., 2018). Specifically, in the mature spinal cord, salamanders and zebrafish both have populations of oligodendrocytes and ependymal cells. However, throughout the literature several different terms have been used to describe the cells sitting adjacent to the central canal, including radial glia, ependymal cells, ependymal radial glia and ependymoglia (Briona & Dorsky, 2014; Hui et al., 2015; Ribeiro et al., 2017). For simplicity, moving forward I will refer to the cells encircling the spinal cord central canal of non-mammalian models as ependymoglia due to their combination of ependymal and radial glial-like characteristics (**Fig. 1B**; Lewis & Eisen, 2003; Grupp et al., 2010; Cardozo et al., 2017; Tazaki et al., 2017). These characteristics include quiescence under physiological conditions, a feature shared by mammalian ependymal cells, and long processes that are seen among glial cells (Zambusi & Ninkovic, 2020). This quiescent state refers to reversible cell cycle arrest, where quiescent cells are non-proliferative but with appropriate stimuli can re-enter the cell cycle, self-renew and give rise to daughter cells (Urbán et al., 2019). In mammalian ependymal cells, the quiescent stem cell population under homeostasis, increases with proliferation after injury to generate new progeny (Barnabé -Heider et al., 2010). This is seen by larger amounts of incorporated 5-bromo-2'-deoxyuridine (BrdU), a thymidine analog that is taken up by cells in the S-phase of the cell cycle, to label for proliferation that results in ependymal cells, oligodendrocytes, and astrocytes (Barnabé -Heider et al., 2010).

Figure 1

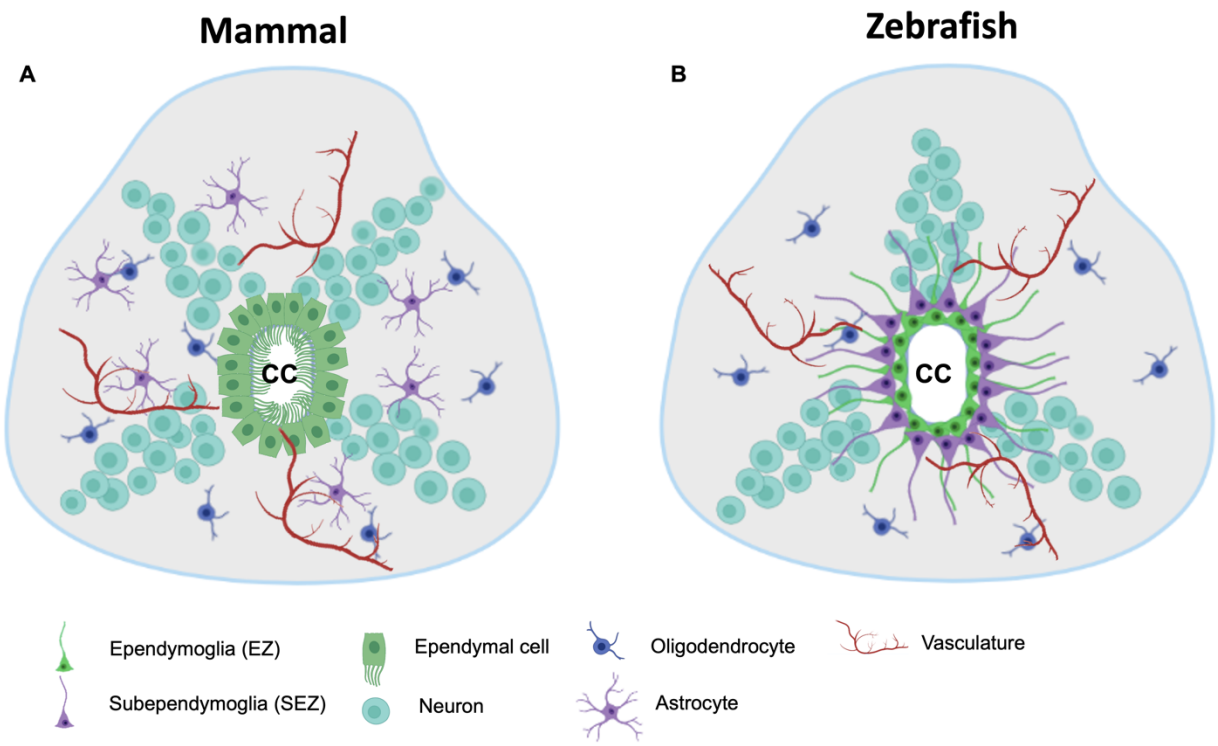

Figure 1. Cellular populations in the mammalian and zebrafish spinal cord. (**A**) Uninjured mammalian spinal cord consists of ependymal cells surrounding the central canal (CC) and neurons within the two dorsal and two ventral horns. The two dorsal horns consist of sensory neurons and interneurons while the ventral horns contain motor neurons and interneurons. Oligodendrocytes, astrocytes and vasculature can be found throughout the parenchyma. (**B**) Within the zebrafish spinal cord there are layers of ependymoglia sitting adjacent to the central canal. Neurons reside in the singular dorsal and two ventral horns. Similar to the mammalian spinal cord, the dorsal horn contains sensory and interneurons, and the ventral horns contain motor neurons and interneurons. Oligodendrocytes and vasculature are seen within the parenchyma.

While a subpopulation of glial cells with astrocytic features exist in the salamander spinal cord, it's undetermined if similar mammalian astrocytes exist (Tazaki et al., 2017). In the zebrafish model, it has been proposed that astrocytes are absent and instead ependymoglia serve the role of astrocytes (Grupp et al., 2010; Goldshmit et al., 2012). However, recently a cell type found throughout the larval zebrafish CNS that is similar to mammalian astrocytes has been characterized by Chen et al. (2020). This undescribed glial cell type has similar characteristics to that of mammalian astrocytes, some of which include morphology, expression of astrocytic markers like glutamate astrocyte-specific transporter and glutamine synthetase (GS), and close association with synapses (Chen et al., 2020). These cells were shown to transform from traditional radial glia to astrocyte-like cells, but since they have been identified only in larval zebrafish it remains unknown whether these cells persist beyond larval development or how they differ from ependymoglia.

In vitro, ependymal cells have been confirmed to be multipotent and form neurospheres that can give rise to neurons, oligodendrocytes and astrocytes after injury (Liu & Chen, 2019). Rather, *in vivo*, rodent models of SCI demonstrate that ependymal cells react post-SCI to proliferate and produce oligodendrocytes, and even more astrocytes which then migrate to the injury site and contribute to the glial scar (Meletis et al., 2008). This difference in cell production *in vitro* compared to *in vivo* implicates the inhibitory environment post-SCI in blocking the path towards neuroregeneration.

The scarring that results in mammalian SCI is made up of a heterogeneous population of cells including reactive astrocytes, oligodendrocyte precursor cells, microglia, fibroblasts, and pericytes (Alizadeh et al., 2019). This scar formation is beneficial as it limits the spread of inflammation to

protect uninjured tissue around the injury site (Sofroniew, 2015). However, despite this protective role, it also inhibits regeneration by acting as a barrier for axonal regrowth and creating an inhibitory extracellular matrix (ECM) through the production of CSPGs (Yang et al., 2020). Thus, regardless of the increase in cell cycle activity of ependymal cells post-SCI, mammalian spinal cords are not able to recover and regenerate neurons. This is large in part, a consequence of cues in the damaged microenvironment that include the inflammatory response, and inhibitory signals arising from the ECM and glial scar formation that impedes regenerative neurogenesis (Lee-Liu et al., 2013; Vajn et al., 2013; Bradbury & Burnside, 2019).

1.3.2 Intrinsic Regulation of NSCs Post-SCI

Functional recovery post-SCI can be regulated by cell intrinsic factors that aid in NSC proliferation, some of which include upregulation of signaling pathways, expression of genes involved in SCI, the unfolded protein response (UPR), and cell metabolism. These factors appear to provide the ependymoglia of lower vertebrates, including axolotl, zebrafish and eels to not only proliferate, but replace motor neurons for functional recovery after SCI (McDonough & Martinez-Cerdeño, 2012). However, in mammals, since differentiation to replace lost cells does not occur, functional recovery is absent, suggesting that a different set of factors regulate mammalian ependymal cells post-SCI (McDonough & Martinez-Cerdeño, 2012).

Different signaling pathways are required for proliferation to occur in vertebrates around the central canal, some of which include Notch, FGF, bone morphogenetic protein (BMP), Wnt/β-catenin, and retinoic acid (RA) (Wilson et al., 2004; del Corral & Storey, 2004; Yeo & Chitnis, 2007). Notch signaling functions to maintain cells in a quiescent state, but through this can impede

regeneration post-SCI. In zebrafish, it has been shown that increased Notch signaling attenuates the regeneration of spinal cord motor neurons and pharmacologically inhibiting Notch increases neurogenesis (Dias et al., 2012). FGF signaling in both zebrafish and mammals controls glial cell activation, specifically in mammals activating an elongated morphology in astrocytes similar to the glial cells seen in zebrafish (Goldshmit et al., 2012). BMP signaling in mammals following SCI shows an upregulation that is involved in glial cell differentiation, contribution to cell death, increase in macrophage infiltration, and an improvement in astrocytic proliferation (Al-Sammarraie & Ray, 2020). In zebrafish ependymoglia, Wnt/β-catenin signaling is activated following SCI and when inhibited, reduces neurogenesis and axonal regeneration (Briona et al., 2015). Studies in motor neuron regeneration has suggested that RA signaling plays an important role because of the increase in RA associated genes in the zebrafish spinal cord (Reimer et al., 2009). Furthermore, studies in rat SCI found that RA signaling participates in physiological responses of neurons, macrophages, astrocytes and oligodendrocytes through the increase in retinoid receptors post-SCI (Schrage et al., 2006).

In addition to the involvement of signaling pathways, SCI has been correlated with changes in gene expression. For example, it has been shown that following SCI, astrocytes in mammals exhibit a significant downregulation of Alpha-synuclein (Yu et al., 2019). This gene encodes for proteins involved in synaptic vesicles and has been implicated in SCI (Wang et al., 2016). Due to the downregulation seen in astrocytes it has been proposed that Alpha-Synuclein may play a role in inhibiting glial scar formation and be a novel gene target to explore mechanisms of mammalian spinal cord repair. Moreover, it has also been previously established that the transcription factor, Sox9, upregulates an array of genes associated with the formation of glial scar seen in mammals

(McKillops et al., 2013). Knocking out Sox9 has led to reduced expression of CSGPs that are found within the glial scar (McKillops et al., 2013). While not many genes have been studied in zebrafish following SCI, Sasagawa and colleagues (2016), demonstrated that e2f4, a coordinator of cell cycle dependent gene transcription was activated after SCI and promoted neuronal regeneration and recovery.

Recently, there have been studies examining the relationship between cellular stress and SCI. Following SCI, the events taking place in the secondary phase of injury can trigger endoplasmic reticulum stress (Penas et al., 2007). Under physiological conditions, the endoplasmic reticulum is the site of protein synthesis, folding and maturation occurs (Hetz et al., 2015). The UPR, which is a new and emerging signaling pathway that has been the focus of growing SCI studies, works to preserve organelle function through the transmembrane proteins: protein kinase RNA-like endoplasmic reticulum kinase, inositol-requiring protein-1 and activating transcription factor-6 (Ohri et al., 2011). When the endoplasmic reticulum is stressed due to injury, the result is an accumulation of abnormal proteins that will activate the UPR (Matsuyama et al., 2014). If the recovery of homeostasis does not occur through the resolution of endoplasmic reticulum stress, apoptosis is triggered (Hetz et al., 2015). A study in mice demonstrated UPR activation post-SCI, specifically in neurons, oligodendrocytes, and astrocytes (Ohri et al., 2011). These findings raised the possibility of using small molecule modulators of the UPR to restore endoplasmic reticulum stress to increase functional outcomes post-SCI (Ohri et al., 2013). Recently in a amyotrophic lateral sclerosis zebrafish model, elevated activating transcription factor-6 activity was found in spinal cord interneurons, indicating that the UPR in spinal cord cells could be a new approach in studying SCI using a non-mammalian model (Clark et al.,

2020). Therefore, further investigating cellular stress in SCI may provide a new therapeutic strategy for functional regeneration.

SCI often results in mitochondrial dysfunction that leads to disorders in metabolism which in turn affect cell survival (Hu et al., 2021). For example, the events that lead to axonal regeneration, including the resealing of injured terminals, reconstructing the cytoskeleton, and synthesizing building materials, require energy through adenosine triphosphate (Han et al., 2020). This energetically demanding process can be resolved by enhancing mitochondrial transport in axons found in murine spinal cords (Han et al., 2020). Since mitochondrial damage can affect glucose metabolism in cells, it is necessary to promote glucose uptake and increase production of mitochondria. Researchers found that glucose metabolism within the spinal cord was regulated by zinc and this promoted functional recovery through the AMP-activated protein kinase pathway that is closely related to glucose transport (Hu et al., 2021). The necessity for proper mitochondrial function has been demonstrated in the zebrafish model that showed injured axons with a greater regenerative ability also maintained greater mitochondrial motility within that area (Xu et al., 2017). Further examining mitochondria and glucose uptake may provide better strategies in achieving recovery through cellular metabolism.

1.3.3 Effects of Injury-Induced Environmental Signals on NSCs

In vitro studies of isolated mammalian spinal cord ependymal cells demonstrate that these cells possess the intrinsic capacity to generate newborn neurons (Liu & Chen, 2019). However, this is not the case within the *in vivo* environment post-SCI (Meletis et al., 2008). Therefore, it is essential to examine the extrinsic factors within the injured spinal cord environment that prevent

regeneration in mammals but promote this fate in lower vertebrates. The microenvironment of the spinal cord largely controls regeneration through signaling arising from local vascularization, the ECM, and immune cells.

Within the vertebrate spinal cord niche, NSCs and blood vessels share a close proximity to each other whereby blood vessels deliver oxygen and nutrients, and remove metabolic waste (Oudega, 2012). Changes in vasculature post-SCI is unfavorable to regeneration because of the resulting hemorrhaging that occurs at the epicenter of the injury site, furthering the loss of tissue (Oudega, 2012). In addition, damaged blood vessels cause hyperpermeability through the blood-spinal cord barrier, which acts to regulate and restrict the movement of molecules in the CNS. (Mautes et al., 2000; Oudega, 2012). This exposes the spinal cord to toxic molecules such as calcium and free radicals, and inflammatory cells that further impede regeneration (Mautes et al., 2000; Oudega, 2012). VEGF released from vascular endothelial cells lining the blood vessels, exerts a protective effect on neurons and stimulates angiogenesis. For instance, when VEGF was injected into the spinal cords of rats, NSCs were activated and differentiated into neurons and astrocytes (Liu et al., 2019). Furthermore, the inflammatory response in rats was inhibited by VEGF which decreased the levels of inflammatory cytokines such as interleukin-1β (IL-1β), interleukin-10 (IL-10), and tumor necrosis factor α (TNFα) (Wang et al., 2015). This indicates that VEGF is an important factor in neuroprotection and overall functional outcome post-SCI.

Another key component of the vertebrate spinal cord niche is the ECM which provides support and structure to cells. In addition, the ECM provides cues to maintain nervous tissue through synaptogenesis, regulate the migration of cells, and guide axons to downstream targets (Haggerty

et al., 2017). In the uninjured spinal cord, the ECM is essential in preserving proper function of the CNS by its involvement in providing regulatory signals and acting as a reservoir for growth factors and molecules (Haggerty et al., 2017). Within the ECM of mammalian and zebrafish spinal cords, there exist CSPGs that play crucial roles in both development and adulthood (Dyck & Karimi-Abdolrezaee, 2015; Lee et al., 2020). After SCI, neutrophils, microglia or macrophages, secrete ECM components including proteoglycans, glycoproteins, and proteins, in addition to matrix metalloproteinases that continue to destroy the ECM. In mammalian SCI, there is an abundant upregulation of CSPGs from activated astrocytes within the glial scar that contribute to the inhibition of axonal regeneration, replacement of cells, and remyelination (Dyck & Karimi-Abdolrezaee, 2015; Lee et al., 2020). Studies have shown that optimizing the injured microenvironment using growth factors and chondroitinase ABC, an enzyme that degrades CSPGs, improves proliferation of NSCs and reduces their differentiation towards an astrocytic lineage (Karimi-Abdolrezaee et al., 2012). This ECM targeted approach provides a promising avenue to regeneration through optimizing the microenvironment.

Finally, the inflammatory response elicited from immune cells in the injured microenvironment can be both beneficial to regeneration and detrimental if prolonged. Under homeostasis, non-activated immune cells relay environmental information to neurons and glial cells, like astrocytes (Ousman & Kubes, 2012). Immune cells, like microglia and lymphocytes, survey the environment of the spinal cord and under injury, elicit an inflammatory response. Some of the cell types involved in the inflammatory response include neutrophils, resident microglia, astrocytes in mammals, macrophages, and lymphocytes. This innate immune response recruits and activates more immune cells, such as neutrophils, to the injury site to help clear debris while also activating

astrocytes, microglia and neuroinflammation (Alizadeh et al., 2019). Other cells like macrophages and microglia promote repair through phagocytosis, scavenging of damaged cells and expressing growth factors (Ousman & Kubes, 2012). Astrocytes play a large role in the formation of the glial scar which protects the spread of the injury to healthy tissue but at the same time impedes axonal regeneration (Alizadeh et al., 2019). When these immune cells are eliminated the recovery process is disrupted, suggesting that new mechanisms are needed to modulate the detrimental aspects of inflammation post-SCI and promote the beneficial effects. One of the largest differences in the ability of lower vertebrates to regenerate and the inability of mammals is the effect of the immune response.

1.4 The Inflammatory Response

Inflammation is a response to harmful stimuli that works to begin the body's healing process. Harmful stimuli that can trigger the inflammatory response include pathogens, damaged cells or toxic compounds (Chen et al., 2018). The common mechanisms of the inflammatory response are cell surface pattern receptors that recognize harmful stimuli, activation of inflammatory pathways, release of inflammatory markers, and recruitment of immune cells (Chen et al., 2018). Upon injury, damaged tissue release endogenous molecules, termed alarmins, that are sensed by the immune system and further activate it to initiate inflammation (Osuka et al., 2014). These alarmins are detected by pattern recognition receptors, found on innate or adaptive immune cells (Amarante-Mendes et al., 2018). These receptors also bind exogenous antigens called pathogen-associated molecular pattern molecules, and damage-associated molecular patterns released by damaged cells (Amarante-Mendes et al., 2018). Inflammatory stimuli, such as microbial products, mediate inflammation through pattern recognition receptors that then trigger intracellular signaling

pathways such as the mitogen-activated protein kinase, nuclear factor kappa-β, and Janus kinase-signal transducer and activator of transcription pathway (Chen et al., 2018). These pathways further the regulation of cytokine production, as well as the recruitment of local and peripheral immune cells including neutrophils, B- and T-lymphocytes, microglia, and macrophages, that collectively contribute to the immune response.

1.4.1 Activity of Local and Peripheral Immune Cells

Following injury, there are various peripheral immune cells that migrate into areas of injury, and local immune cells found within the spinal cord. The first phase of inflammation in mammals lasts 0-2 days post-injury (dpi) and begins with the recruitment of resident microglia and astrocytes, and neutrophils to the injury site. The next phase occurs near 3dpi when blood-born macrophages and lymphocytes are recruited (Alizadeh et al., 2019). Across vertebrates, neutrophils are one of the first responders and are found in the spinal cord within the first few hours after injury. These cells phagocytize and clear debris, secrete proteases, and release reactive oxygen species (ROS) that combat invading pathogens (Gadani et al., 2015). Neutrophils have been viewed as potentially detrimental due to the release of inflammatory cytokines, proteases and free radicals that contribute to secondary damage (Alizadeh et al., 2019). However, studies show that depleting these immune cells in mice resulted in worse functional hindlimb recovery and a delay in activation of astrocytes (Stirling et al., 2009). This indicates that neutrophils have a dual role in the inflammatory response.

After neutrophil recruitment, local microglia and peripheral macrophages infiltrate the injured spinal cord. In a healthy CNS, the resident immune cells, microglia, survey the microenvironment and have a branched morphology along with low immune and cytokine activity (Kroner &

Almanza, 2019). In response to injury, they become activated and their morphology changes to a round amoeboid shape with shorter processes (Kroner & Almanza, 2019). Microglia have both detrimental and beneficial functions following SCI. These cells contribute to secondary damage through their release of reactive oxygen species and pro-inflammatory cytokines. On the other hand, their protective effects include debris clearance, production of anti-inflammatory cytokines, and sealing the injury site to prevent further spread of damage (Hines et al., 2009).

Following a SCI when the blood-brain/spinal cord barrier is damaged, monocytes are able to infiltrate the spinal cord tissue and transform into macrophages (Zhou et al., 2014). Upon activation, there exist subsets of macrophages termed M1- or M2-type macrophages that take on an amoeboid-like morphology as compared to their ramified morphology under homeostasis (Fernández-Arjona et al., 2017). When discussing polarization within the literature, the term 'macrophages' is commonly used to refer to both the infiltrating macrophages and the resident microglia. M1 macrophages are a pro-inflammatory, early-stage immune cell that are detected during the acute response to injury and activated by interferon-γ (Gensel & Zhang, 2015; Park et al., 2018). These cells enter the injury epicenter to phagocytize apoptotic and necrotic cells, and clear tissue debris (Gensel & Zhang, 2015). In addition, they release ROS and pro-inflammatory cytokines that facilitate the inflammatory response leading to further damage and inflammation (Zhou et al., 2020). In contrast, M2 macrophages are activated by interleukin-4 (IL-4) and display tissue repair characteristics through their attenuated production of pro-inflammatory cytokines and ROS, while secreting anti-inflammatory cytokines (Liu et al., 2014; Gensel & Zhang, 2015).

When the injured site is cleared of debris and pathogens, the M1 polarized macrophages undergo a switch to the M2 polarization in response to anti-inflammatory signals like IL-4, released from mast cells, basophils, and eosinophils (Orekhov et al., 2019). Therefore, the immune cells involved in SCI follow a successful acute inflammatory response when damaged cells, debris and pathogens are eliminated which is then followed by a resolution and repair phase (Medzhitov, 2008). However, when this acute response is not resolved it results in chronic inflammation. This prolonged inflammation can be detrimental due to the occurrence of apoptosis, glial scar formation in mammals, and a reduction in neuronal function, leading to poor recovery in mammals (Yong et al., 2019).

1.4.2 Pro-inflammatory Cytokines

Cytokines are small secreted proteins mainly released from immune cells, including macrophages, monocytes, and lymphocytes, but may be produced by non-immune cells such as mast cells, endothelial cells and glia (Zhang & An, 2007). These proteins work through autocrine or paracrine action to help modulate the immune response and regulate inflammation. Macrophages are one of the main producers of cytokines and based on their polarization of an M1 pro-inflammatory or M2 anti-inflammatory phenotypes, can release pro- or anti-inflammatory cytokines, respectively (Zhang & An, 2007; Ren & Young, 2013; Kong & Gao, 2017). Cytokines have neuromodulatory functions, but also have the capability of furthering damage if pro-inflammatory cytokines are uncontrolled at high concentrations.

A common cytokine seen among vertebrates following SCI is TNFα. This cytokine exerts both neuromodulatory effects such as neuroprotection or apoptosis and has been implicated as a factor

involved in the limited recovery seen in mammals (Huie et al., 2012). Specifically, it increases neutrophil infiltration, inhibits survival of neurons and oligodendrocytes, and limits remyelination (Ren et al., 2018). In mammals, the effects of TNFα on axonal regeneration are unclear, but in larval zebrafish it has been shown to promote regeneration by reducing levels of neutrophils (Tsarouchas et al., 2018). In addition, the notable pro-inflammatory cytokine, IL-1β, increases its expression after injury and acts by activating the immune response by elevating the production of inflammatory cytokines (Boato et al., 2013). For IL-1β to first become activated, the inflammasome is required (Martín-Sánchez et al., 2016). The inflammasome is a multiprotein complex found within a cell that will be activated by pathogen associated molecular patterns and damage associated molecular patterns (Martín-Sánchez et al., 2016). The inflammasome next activates the enzyme caspase-1 to process IL-1β into a bioactive form (Martín-Sánchez et al., 2016). This pro-inflammatory cytokine is sourced from microglia and astrocytes and is rapidly expressed in mice following SCI (Pineau & Lacroix, 2006). In a study using larval zebrafish, initial inflammation and the presence of IL-1β promoted axon bridging, whereas at later timepoints needed to be decreased to not exert detrimental effects on regeneration (Tsarouchas et al., 2018). Another cytokine of the interleukin family, interleukin-8 (IL-8), is synthesized from macrophages, endothelial cells and neutrophils, exerting pro-inflammatory effects through the activation of further neutrophils (Morganti-Kossmann et al., 1997). Pro-inflammatory cytokines are beneficial at low concentrations due to their induction of neurotrophin expression, but at higher concentrations activate transcription factors that stimulate neurotoxic genes which cause further damage (Garcia et al., 2016).

1.4.3 Anti-inflammatory Cytokines

In SCI, anti-inflammatory cytokines are crucial for reducing pro-inflammatory cytokines, thus promoting regeneration and protection of injured tissue. Although anti-inflammatory cytokines can reduce the number of pro-inflammatory cytokines, they exist at low levels or are absent immediately after SCI, prolonging inflammation (Hellenbrand et al., 2021). In mammals, anti-inflammatory cytokines are commonly induced later in recovery. Interestingly however, in a study of axolotl limb regeneration anti-inflammatory cytokines were increased simultaneously with pro-inflammatory cytokines (Godwin et al., 2013). Transforming growth factor-β (TGF-β) is a family of anti-inflammatory cytokines important in inflammation, ECM formation and scar formation in mammals (Buss et al., 2007). TGF-β1 showed a rapid induction both extracellularly and intracellularly in macrophages, astrocytes and neutrophils, indicating it plays a role in early inflammation within the human spinal cord (Buss et al., 2007). The role of TGF-β1 is bi-directional due to the pro-inflammatory effects it has on inactivated cells initially after injury and the anti-inflammatory effects it has on activated cells later during inflammation (Buss et al., 2007). Another cytokine that belongs to the TGF family is TGF-β3, which works through the FGF pathway to reset astrocytes into a non-reactive state in mammals and has been shown to reduce scarring in rat pups (Gottipati et al., 2020). Combining TGF-β3 with mesenchymal stem cells in rabbits, enhanced the ability to regenerate post-SCI and increased the healing rate (Feldman & McCauley, 2018). Therefore, focusing on early enhancement of these proteins as a therapeutic strategy may aid in reducing inflammation and promoting recovery in mammalian models of SCI.

1.5 Zebrafish as a Leading Regenerative Model to Study SCI

Zebrafish, in contrast to mammals, have been used as a model system in which regeneration can be studied due to their remarkable ability to not only repair the spinal cord after SCI but also repair other tissue types, including the brain, fins, heart, kidneys, and retina (Vihtelic & Hyde, 2000; Poss et al., 2002; Poss et al., 2003; Diep et al., 2011; Kyritsis et al., 2012). Zebrafish possess key differences from mammals, such as the presence of ependymoglia around the central canal that act as NSCs, and the extent of inflammation post-injury. However, the exact relationship between ependymoglia and the immune cell response is still unclear.

Mammals and zebrafish differ dramatically in their regenerative response but do share a small number of overlapping features. One notable similarity is that NSCs in both mammalian and zebrafish spinal cords are non-proliferative under homeostasis, but increase following SCI (Meletis et al., 2008; Cigliola et al., 2020). While both models show an increase in proliferation, their functional recovery remains different. The spinal cord in mammals is irreversibly impaired due to the disruption of axons, neuronal cell death, and formation of scar tissue that inhibits regeneration of axons (Möllmert et al., 2020). In zebrafish, the loss of function seen following SCI is not permanent. When a SCI occurs, zebrafish respond with the production of new motor neurons originating from proliferating ependymoglia, and the promotion of growth in axons with the help of fibroblast-like cells that accumulate to the injury site (Reimer et al., 2008; Wehner et al., 2017). These key differences at the cellular level allow for functional recovery in zebrafish and make for an ideal model in the field of regenerative medicine.

1.5.1 Injury Models Used in Zebrafish SCI

To study SCI in zebrafish there exist different injury models, some of which include transection models and compression models. The commonly used full transection model consists of a complete severance of the spinal cord and has been used across both adult and larval zebrafish (Becker et al., 1997; Reimer et al., 2009; Briona & Dorsky, 2014). This is useful for studying axonal regeneration, scaffolds to bridge the gap of the severed spinal cord, and the role of motor and sensory circuits in recovery of locomotion (Alizadeh et al., 2019). This model is easy to reproduce but is less relevant in translation to human SCI. To perform transection injuries in adults, the spinal cord is cut using micro-dissecting scissors after the fish has been anesthetized while full transections in larval models only require a scalpel rather than scissors due to their smaller body size (Fang et al., 2012; Briona & Dorsky, 2014). In addition, larval SCI is commonly performed by mounting the zebrafish in low-melt agarose after being anesthetized. Overall, performing SCI on zebrafish is a simple process that takes less than 5 minutes to perform under a dissecting microscope (Fang et al., 2012). A variation of the transection model is a hemi-section where only part of the spinal cord is severed. In larvae, this injury model has been induced by lasers (Dehnisch Ellström et al., 2019). Hemi-sections are useful in studying plasticity, grafting of nerves and comparing injured vs. non-injured pathways within the same animal (Cheriyan et al., 2014). However, this injury can be less severe or lead to spontaneous recovery and are harder to keep consistent across different animals (Cheriyan et al., 2014).

Compression models, which involve prolonged compression of the spinal cord, are more relevant to human SCI. The most common way of inducing a compression injury is through clip compression where a clip is applied for a certain period of time. An advantage to this method is

that it's inexpensive and can be used to block blood supply to inflict ischemia seen in human SCI (Cheriyan et al., 2014). Few have utilized this injury model in zebrafish, however, a study examining the regeneration of ependymoglia in the spinal cord exposed the vertebral column and compressed the spinal cord dorsoventrally with forceps to create a compression injury (Riberio et al., 2017). While this exact type of injury is not commonly seen when using zebrafish, a crush injury was induced using forceps in adult zebrafish to study the cellular response, similar to the compression model (Hui et al., 2010). This injury resulted in a loss of movement similar to transections, that began to recover around 2 weeks post-SCI until a full recovery at around 1 month (Hui et al., 2010). Compression models are considered the most relevant when translating to human SCI because they better simulate the neuropathology, whereas transection is valuable in anatomic regeneration and commonly seen among zebrafish SCI.

1.5.2 Techniques Used to Facilitate the Study of SCI in Zebrafish

The zebrafish model was first used in developmental biology due to the transparency of embryos and external fertilization/development (Veldman & Lin, 2008). In addition, zebrafish can be kept in large numbers due to their size and female zebrafish are able to lay up to 300 eggs at a time, allowing thousands of embryos from a single reproductive cycle (Aleström et al., 2020). Together with zebrafish reaching sexual maturity and adulthood near 3 months, this model allows for large scale studies to be conducted (Singleman & Holtzman, 2014).

Following their use in development, zebrafish expanded into other fields, notably being used in regenerative studies. As a result, there exists numerous tools to assist in the study of zebrafish, including a number of molecular and genetic approaches, and behavioural tests to examine

functional recovery and motor activity (Kabashi et al., 2011; Babin et al., 2014). To date, the zebrafish genome has been fully sequenced and has allowed for new discoveries in genetics through comparison with the human genome (Howe et al., 2013). For example, gain- and loss-of-function techniques can be used to manipulate homologs of human genes through injection of anti-sense morpholino oligonucleotides (Kabashi et al., 2011). Using this method, researchers have been able to replace zebrafish genes with human genes by injecting zebrafish embryos with human mRNA with the anti-sense morpholino oligonucleotides that targets the zebrafish sequence (Kabashi et al., 2011). This has allowed for the study of degenerative brain/spinal cord disorders and developmental disorders such as amyotrophic lateral sclerosis, spinal muscular atrophy, Parkinson's, Huntington's, epilepsy and validation of mutations involved with autism (Kabashi et al., 2011).

Most recently, CRISPR/Cas9-based technologies has allowed for the identification of pro-regenerative genes in larval zebrafish SCI (Keatinge et al., 2021). Using genome wide expression profiling, researchers have further discovered genes expressed at different times following SCI in the adult zebrafish, in line with the process of spinal cord regeneration (Hui et al., 2014). Therefore, there exist different genetic methods to study SCI across stages of neurorepair. In addition, an important tool used in the study of SCI includes the use of transgenics to view cell specific expression in various tissues before and after injury. Reporter expression can be visualized in both single or double-transgenic lines to study neurons, immune cells, glia, vasculature and even signaling pathways using reporters such as green fluorescent protein (GFP) and red fluorescent protein (RFP; DsRed) (Lawson & Weinstein, 2002; Arkhipova et al., 2012; Fang et al., 2013). With these beneficial reporter lines, researchers do not have to rely on antibodies for labelling

experiments and large quantities of transgenic lines can be created due to the high number of embryos produced in facilities. Additionally, as a result of their transparency, zebrafish larvae are often used for live-confocal imaging of SCI regeneration (Huemer et al., 2017). After the first 10 days, zebrafish are no longer transparent and as such, this imaging technique cannot be used on older larvae, juvenile and adult stages.

In studying the regeneration and differentiation of cells following SCI, lineage tracing can be useful in visualizing stem cell progeny. One method of lineage tracing involves the Cre/*loxP* system which permanently labels progeny cells by modifying the parent cells' genome with fluorescent reporter proteins (Brown et al., 2018). By temporally controlling the induction of Cre/*loxP* with commonly used tamoxifen, an estrogen receptor modulator, parent cells containing a gene of interest can be induced to give rise to progeny with a different reporter following SCI. A more advanced technique that requires Cre-*loxP* is Zebrabrow, or Zebrafish Brainbow, that creates combinations of different fluorescent colours in adjacent cells that are then inherited by daughter cells (Pan et al., 2013). This technique also allows for lineage tracing of cells to obtain direct evidence of the lineage from the parent NSC to the daughter progenitor cells that differentiate into newborn neurons post-SCI.

In the last 10 years several new ways to study zebrafish behavioural phenotypes and activity have been created (Kalueff et al., 2013). In studying regeneration, behaviour can be successfully examined using zebrafish due to the absence of movement as a result of a complete transection of the spinal cord (Becker & Becker, 2006). This, in combination with the fact that uninjured zebrafish swim constantly allows for one to accurately monitor and quantitate behaviour post-

injury, as well as recovery which has been shown to occur at 6 weeks post-SCI in adult zebrafish (Becker & Becker, 2006; Noorimotlagh et al., 2017).

1.5.3 Anatomy of the Zebrafish Spinal Cord

The main cell populations present in the zebrafish spinal cord include ependymoglia, neurons, oligodendrocytes and microglia (**Fig. 1B**). Ependymoglia in particular, are functional orthologs of ependymal cells found in mammals and are the key cells involved in the regenerative response (Zambusi & Ninkovic, 2020). These cells have a combination of ependymal cell bodies and radial glial-like characteristics such as elongated processes (Lewis & Eisen, 2003; Grupp et al., 2010; Cardozo et al., 2017; Tazaki et al., 2017). Under homeostasis, high levels of Notch signaling keep the ependymoglial populations in a quiescent state (Dias et al., 2012). Under injury or with lower levels of Notch signaling, these cells re-enter the cell cycle and self-renew or generate new neurons, all of which can be identified using different cell specific markers (Dias et al., 2012).

To examine ependymoglia researchers have used astrocytic and glial markers such as glial fibrillary acidic protein (GFAP), GS, S100 calcium-binding protein β, brain lipid-binding protein (BLBP), and vimentin (Hui et al., 2015; Johnson et al., 2016; Cigliola et al., 2020; Chen et al., 2020). In addition, the NSC marker Sox2, neural progenitor cell marker nestin, and ependymal marker, Foxj1a have also been used to mark these cells (Goldshmit et al., 2012; Hui et al., 2015; Ribeiro et al., 2017; Zambusi & Ninkovic, 2020). Expression of Foxj1a is upregulated in the injured spinal cord within the ependymoglia surrounding the spinal cord and in their respective daughter progenitor cells (Ribeiro et al., 2017). Following injury, the ependymoglial cells express high levels of nestin indicating the progenitor feature these cells hold (Goldshmit et al., 2012).

Additional studies have shown Sox2 and nestin co-labelling in the ependymoglia around the central canal of embryonic larvae (Johnson et al., 2016). Therefore, using different transgenic lines and markers can display co-expression of glial and NSC features in these ependymoglia.

To identify dividing cells within the spinal cord, researchers often use 5-Ethynyl-2′-deoxyuridine (EdU), BrdU and proliferating cell nuclear antigen (PCNA). EdU and BrdU are both incorporated into nuclear DNA during the S-phase of the cell cycle, but a key difference is that BrdU requires an antibody and DNA denaturing to stain for proliferation which can affect image quality and cell morphology (Salic & Mitchison, 2008; Crane & Bhattacharya, 2013). EdU uses a proliferation assay where it is detected by a click reaction of an azide-alkyne that can access the DNA without denaturing (Salic & Mitchison, 2008). A different method in studying proliferation is by looking at by marking against antigens expressed during proliferation with the use of primary antibodies. PCNA is a common marker to label proliferation expressed across early G1 phase and S phase of the cell cycle, however, staining for it provides a snapshot on proliferating cells at a given timepoint. This is opposed to EdU/BrdU that is incorporated into the DNA of cells and their progeny providing information on proliferation over a period of time. EdU, BrdU and PCNA have all been commonly used to stain for proliferation in larval and adult zebrafish following SCI (Reimer et al., 2008; Hui et al., 2010; Goldshmit et al., 2012; Briona & Dorsky, 2014; Hui et al., 2015; Ohnmacht et al., 2016; Nelson et al., 2019; Vandestadt et al., 2019). Using these markers to identify ependymoglial proliferative activity following SCI is important to understand their activation and regulation to initiate regenerative neurogenesis.

1.5.4 Cell Intrinsic Factors Required for Recovery in Zebrafish SCI

Functional regeneration has been observed in a variety of zebrafish tissues by the activation of signaling pathways, gene expression and cellular metabolism. In the zebrafish model, mechanisms that are involved in the regulation of proliferation in development seem to be similarly upregulated after SCI (Cardozo et al., 2017). For example, signaling pathways such as Sonic hedgehog (Shh), Wnt, FGF, RA, and Notch are key players in the development of the spinal cord and have been studied in the context of SCI. Shh, which plays crucial roles in axon guidance and connectivity, has been shown to be upregulated in ependymoglia during development and when inhibited in adult zebrafish affects the generation of new motor neurons after injury (Reimer et al., 2009). In addition, Foxj1a upregulation following SCI was seen to be dependent on Shh activity, indicating that regeneration relied on similar cues seen during development (Ribeiro et al., 2017). Wnt signaling is critical for development because it regulates cell fate choice, proliferation and growth (Cardozo et al., 2017). In zebrafish larvae, ependymoglia exhibit Wnt signaling that plays a role in axonal regeneration post-SCI (Briona et al., 2015). This signaling is conserved in adult zebrafish as inhibiting the Wnt pathway led to impairment in locomotor recovery (Strand et al., 2016).

The FGF pathway in zebrafish SCI has been shown to be upregulated in neurons and glia and be involved in the formation of a glial bridge that facilitates axon regeneration by acting as a scaffold (Goldshmit et al., 2012). Additionally, RA is an important signal involved in cell communication both within development and adulthood. During zebrafish SCI, RA is upregulated after a lesion but the exact role in regeneration is unclear (Reimer et al., 2009). In the unlesioned spinal cord there is little Notch expression or neurogenesis observed. However, induction of Notch signaling in the injured spinal cord of adult zebrafish attenuates proliferation and motor neuron generation

(Dias et al., 2012). This indicates low levels of Notch activity keeps cells in a quiescent state such that precise regulation of Notch is needed to allow for proliferation and neurogenesis to occur, similar to what is seen in mammalian SCI models.

While signaling pathways play an important role in regeneration post-SCI, genes are also involved and differentially expressed during spinal cord regeneration. A master coordinator of cell cycle dependent gene transcription, e2f4, was activated after SCI and promoted neuronal regeneration and recovery in larval SCI (Sasagawa et al., 2016). In addition, profiling of the adult zebrafish genome during spinal cord regeneration revealed a number of upregulated genes involved in cell proliferation, death, migration, neurogenesis and axon growth (Hui et al., 2014). For example, stat3, a gene that controls proliferation and apoptosis, was increased in the early phases of injury while the genes in the Sox family were upregulated across different timepoints (Hui et al., 2014). Sox2 fold changes were also most noticeable in 3dpi spinal cords and co-labelling of this gene with HuC/D confirmed its involvement in neurogenesis (Hui et al., 2014). Therefore, many signaling pathways and genes are upregulated for functional spinal cord recovery to occur in the regenerative zebrafish model.

1.5.5 Extrinsic Cues in the Injury-Induced Environment following SCI

The injured environment of the zebrafish CNS provides cues to ependymoglia for regeneration to take place through the immune response, vasculature and ECM that together form a highly permissive, pro-regenerative environment. To date, most of what is known stems from the immune response, with less knowledge on the vasculature and ECM.

Inflammation has been shown to promote functional regeneration in the spinal cord through the dynamic control of macrophages (Tsarouchas et al., 2018). In larval SCI, treatment with Dexamethasone, an immunosuppressant, decreased the number of immune cells such as neutrophils, macrophages and microglia, and as a result inhibited axonal regrowth (Tsarouchas et al., 2018). Activating the immune system using bacterial lipopolysaccharides had the opposite effect on the growth of axons and number of immune cells (Tsarouchas et al., 2018). Similarly, the immune cell response has also been shown to be involved in axon regeneration of the adult spinal cord as shown by Becker & Becker, 2001, who described a macrophage/microglial response after 2 days-post spinal cord transection. Therefore, the immune cell response appears to be a requirement for spinal cord regeneration through the regrowth of axons.

Through studying regeneration in the brain, Kyritsis et al. (2012), showed a connection between inflammation due to injury and regeneration. Specifically, they used adult zebrafish to perform telencephalon injuries and determined that inducing sterile inflammation without an injury, using zymosan A, showed similar outcomes in proliferation levels and neuronal production as a physical injury (Kyritsis et al., 2012). This indicated that inflammation itself appears required for activation of NSCs to initiate the reparative process. By next using Dexamethasone, researchers showed that exposure of brain injured zebrafish to the immunosuppressant resulted in a significant decrease in proliferation and neurogenesis as compared to control. This further confirmed the necessity of the immune response and inflammation in a traumatic brain injury (Kyritsis et al, 2012).

Within the inflammatory response, cytokines play a large role in promoting and regulating inflammation after injury. The study of cytokines is now emerging in the zebrafish model and can

allow for more insight into how the injury induced environment controls regeneration. Looking further into the effects of the immune system, it was determined through reverse transcriptase quantitative polymerase chain reaction (RT-qPCR) that pro-inflammatory cytokines, IL-1β and TNFα, and anti-inflammatory cytokines, TGF-β1a and TGF-β3, play a role in regeneration (Tsarouchas et al., 2018). Specifically, these cytokines work in a bi-phasic manner where pro-inflammatory cytokines are expressed early and for a short period of time followed by anti-inflammatory cytokines (Tsarouchas et al., 2018). This has been similarly seen in mammalian SCI where a majority of pro-inflammatory cytokines including IL-1β, interleukin-6 and TNFα, are upregulated in the early phases of SCI (Hellenbrand et al., 2021). However, IL-10, an anti-inflammatory cytokine, appears to increase the most around 7dpi in mammals while the anti-inflammatory cytokine IL-4 shows no observable change (Hellenbrand et al., 2021). However, within the zebrafish model there is little understanding about the production of anti-inflammatory cytokines. Thus, there is a clear need to better understand how cytokines and immune cells play a role in the recovery of zebrafish following SCI.

The vasculature in the spinal cord plays an important role in SCI, but there is little studied to date within the zebrafish model. Vasculature within the spinal cord requires a scaffold for the organization of blood vessels. This scaffold is the ECM which is involved in helping create the permissive environment for regeneration in zebrafish. In zebrafish, knocking down CSPGs sped up the regeneration of the spinal cord in larvae and adults which suggests that this ECM component is conserved across mammals and zebrafish (Sahu et al., 2019). In mammals, CSPGs inhibit axon growth, however, zebrafish exhibit CSPGs yet show a pro-regenerative environment. This could be due to shorter pro-inflammatory responses and more growth permissive components expressed,

such as connective tissue growth factors, that are upregulated in and around glial cells to promote bridging for axonal regeneration (Mokalled et al., 2016). In addition, it was demonstrated in larval SCI that through fibroblast-like cells, Wnt signaling controls the components of the ECM, specifically the deposition of collagen XII which promotes axonal regeneration (Wehner et al., 2017). This further supports the notion that zebrafish have a pro-regenerative environment through the inflammatory response, vasculature and growth permitting ECM components resulting in functional recovery. However, there is still a need to better understand the series of events that occur within the NSC environment of zebrafish SCI to promote the functional recovery seen in this regenerative model.

Chapter 2.0 Rationale, Hypothesis and Objectives

2.1 Rationale

Despite the growing use of zebrafish for regenerative studies, there exist significant gaps in our required knowledge to fully take advantage of the zebrafish model of SCI for translation to human SCI. Most knowledge on SCI in zebrafish originates from larval models and as such, there is no information on the relation between macrophages, microglia and neutrophils, and NSC behaviour in post-larval stages. The immune response, involving macrophages, microglia, neutrophils and cytokines, following SCI has been documented in larval zebrafish and the general timeline of regeneration in adult models, but the exact relationship between these two processes is unclear. Thus, in order to better understand regeneration, it is necessary to understand SCI at later developmental stages post-larvae and develop a zebrafish model more translatable to humans.

Following SCI in zebrafish and mammals, the events that take place are closely related but are defined by major differences. Work in mammalian SCI has exhibited a prolonged inflammatory response and glial scarring that results in an anti-regenerative environment. However, zebrafish have been shown to regenerate the spinal cord after injury, and larval studies have demonstrated a shortened pro-inflammatory response with no resulting glial scar to restrict axonal regrowth (Tsarouchas et al., 2018). Attenuation of the inflammatory response in these studies was shown to interrupt spinal cord repair, furthering the notion that the inflammatory response is required for regeneration. While it has become clear that zebrafish appear to have a highly permissive microenvironment following SCI, little is known concerning the temporal relationship between proliferative ependymoglia and the immune cell response post-SCI.

In studying SCI, larval and adult zebrafish are the most common developmental stages used. Around only 5% of SCI occur in infants and children so the larval zebrafish model is not the most representative (Basu, 2012). SCI in older populations commonly occurs during young adulthood, between the ages of 15-29 and in late adulthood, around the age of 50 (Ahuja et al., 2017). Using zebrafish models of SCI at later developmental stages, such as adults (4-months to 1-year) and juveniles (1- to 3- months), could allow for a more relevant understanding in how immune cells and NSCs function together to repair the damaged spinal cord. Moreover, if such comparative studies show similarities between developmental stages, juveniles could act as a quicker representative model and replace the adult model of SCI.

Although researchers have studied the activation of the immune cell response in the context of SCI and how critical it is to trigger the events necessary for successful repair, there are still limitations in our knowledge. Specifically, there is little understanding in post-larval stages regarding the infiltration and recruitment of immune cells, such as macrophages and microglia, towards the injury site, and how this is temporally controlled with the proliferative response of resident NSCs surrounding the spinal cord central canal. In addition, knowledge of the timeline of cytokine release within adult zebrafish SCI is lacking, including data on both pro- anti-inflammatory cytokines. As such, strict timing of the macrophage response and cytokine activity may be crucial to form the permissive environment that stimulates the ependymoglial cells around the central canal to initiate the process of successful spinal cord repair. These current gaps in knowledge form the basis of my project hypothesis.

2.2 Hypothesis and Study Objectives

Hypothesis: I hypothesize that in order for functional recovery to occur in adult and juvenile zebrafish following SCI, the pro-inflammatory response must peak ahead of ependymoglial proliferation. I will directly address this hypothesis using two study objectives:

Objective 1: To develop a new juvenile model of SCI and compare its timeline of events for spinal cord regeneration with the adult model of SCI.

Objective 2: To examine the temporal relationship between the macrophage response and ependymoglial proliferation and neuronal differentiation for functional spinal cord repair.

Objectives 1 and 2 will be studied using a combination of behavioural analysis, H&E staining, proliferation assays, labelling experiments, and quantitative RT-qPCR. First, I will establish the adult and juvenile SCI models to compare the extent of injury behaviourally and anatomically. Following this, I will investigate the timeline of proliferation in ependymoglia and the generation of newborn neurons. Next, the inflammatory response will be investigated through the study of microglial recruitment, infiltration of macrophages, and pro- and anti-inflammatory cytokines across multiple timepoints. Finally, functional recovery will be assessed and compared as juvenile locomotor recovery has yet to be documented. These findings will provide more insight into how inflammation regulates the regenerative response in adult and juvenile zebrafish to better understand the relationship between immune cells and local NSC populations. This will further develop our knowledge of how successful regeneration occurs for future application in mammalian SCI.

Chapter 3.0 Methodology

3.1 Zebrafish Husbandry

All zebrafish were housed and bred in our Zebrafish Facility at the University of Manitoba, Bannatyne Campus, Rady Faculty of Health Sciences. Zebrafish were kept on a 12hr light/dark cycle in a standalone recirculating system with ultraviolet and carbon filters (Tecniplast Inc., Italy). Water parameters were maintained near 28°C, 500 conductivity, and pH 7.4. Zebrafish were fed a minimum of three times a day (8:00am, 12:00pm and 5:00pm) with a combination of pellet food (Skretting, Gemma Micro 300, 150 and 75), brine shrimp, and rotifers. Animals were given a diet of 75 μm, 150 μm, and 300 μm pellets according to larval, juvenile and adult developmental stages, respectively. In addition, juvenile and adult zebrafish were fed brine shrimp (Brine Shrimp Direct) once a day (12:00pm) and larvae received rotifers (Reed Mariculture) until 30 days post-fertilization (dpf).

Zebrafish breeding was set up between 3:00-5:00pm using 1 L regular breeding tanks and 1.7 L beached tanks that had a shallow end to replicate their natural habitat. Males and females were either separated using dividers or allowed to interact in tanks that included imitation plastic plants that provided spawning sites to replicate their natural environment. Dividers were removed just after 7:00am the next morning near the beginning of the light cycle to simulate dawn. Zebrafish were then left to breed until for a maximum of 2 hours. Thereafter, embryos were collected using a strainer and transferred into a petri dish (Fisherbrand®, FB0875712) filled with embryo medium to suppress fungal growth. A maximum of 20 embryos per dish were kept in the dark in an incubator (Forma™ Direct Heat CO_2 Incubator, Thermo Fisher™) at 28°C until 5dpf. At 6dpf when larvae depleted their yolk sac of nutrients, they were transferred into 1.1 L tanks in our Zebrafish Facility with no water drip. Upon reaching the juvenile stage at 30dpf, animals were

transitioned to 3.5 L tanks with a constant water flow. Adult zebrafish (≥ 3 months) were housed in 3.5 L tanks or 8 L tanks.

Experimental juvenile zebrafish were between 1- and 3-months old and adult zebrafish were between 4-months to 1-year old. The experimental lines used included wildtype (AB strain), Tg(mpeg1:eGFP) that marks for macrophages/microglia, Tg(gfap:GFP) that marks for GFAP, Tg(hb9:eGFP) that marks for motor neurons, Tg(Olig2:eGFP) that marks for oligodendrocytes, and Tg(Fli1a:eGFP) that marks endothelial cells (Lawson & Weinstein, 2002; Shin et al., 2003; Flanagan-Street et al., 2005; Bernardos & Raymond, 2006; Ellet et al., 2011). Animal ethics and experiments were approved by the University of Manitoba Animal Care Committee and in accordance with the Canadian Council for Animal Care.

3.2 Spinal Cord Injury and Sham Protocol

To perform SCI, a 0.4% tricaine solution of 4.2 ml of tricaine (anesthetic) per 100 mL of system water and a recovery tank of system water were prepared in order to anesthetize the animals. Individual adult and juvenile zebrafish were transferred into the 0.4% tricaine and observed until breathing had slowed and no response to tail pressure was present (zebrafish stage 4 anesthesia). Using a spoon, zebrafish were then gently transferred from the tricaine solution onto a Petri dish where the injury was performed. Under a dissecting microscope (Leica EZ4 W), zebrafish were held with tissue forceps and the injury performed using micro-dissecting scissors in the second quarter of the spinal cord, rostral to the dorsal fin. Continuous, small incisions were made in the muscle layer, and consecutive cuts were made until the spinal cord was visible. A complete transection through the spinal cord was then completed using the micro-dissecting scissors. The

bodies of adult zebrafish were approximately 2 cm in length and required more snips to get through the layers of skin and muscle as compared to juvenile zebrafish. Juveniles, whose bodies measured at around 1.4 cm, did not require as many cuts to reach the spinal cord due to their smaller body size. Thus, the transection was performed as needed on adults and juveniles, but the rest of the protocol was performed similarly. To perform a sham injury, the incision was made only to the skin and muscle layer, with the spinal cord left fully intact. The SCI or sham injury took ~30 seconds to be performed and afterwards the zebrafish were placed into the recovery tank while a pipette was used to gently aerate the gills by pulsing water to promote breathing and the removal of tricaine from their system. The zebrafish were left in the recovery tank for approximately 5 minutes until normal breathing had returned. The SCI was visually confirmed when the zebrafish attempted swimming and could only move the upper halves of their body. Sham injuries were confirmed when swimming was consistent with uninjured zebrafish. Once recovered from anaesthesia, the zebrafish were netted back into individual recovery tanks, and not fed for 3dpi since fish cannot swim to the surface to feed and leftover food could lead to infection at the injury site.

3.3 Behavioural Tracking

Behavioural tracking was used to validate the SCI model and also to study functional swimming recovery following SCI. To specifically assess the SCI model, using control (uninjured), sham, and SCI groups of adult and juvenile zebrafish, swimming ability was measured at 1dpi using an open-field tracking system that consisted of four walls with a free area to swim in (Ethovision XT, Noldus). Two glass tanks (28 cm x 23.5 cm x 20 cm; Into the Blue Aquarium Services Inc., Winnipeg) were filled with 2 L of system water, placed on a light box to illuminate the tanks from

bellow for better contrast against the zebrafish, and separated with laminated paper to allow for n=2 fish to be recorded per trial and control for visual cues. Zebrafish were acclimated in tanks for 30 minutes prior to recording. Each behavioural trial, for both validating the SCI model and measuring recovery, consisted of one zebrafish per tank, for a total of two zebrafish per trial, which were then recorded and analyzed for 5 minutes to obtain the total distance travelled in centimeters. For validating the SCI model, n=4 zebrafish were recorded per group (control, sham, SCI) at 10:00am (**Fig. 2**). When tracking behavioural recovery post-SCI, similar parameters were used as above and n=4-10 zebrafish were recorded at 1:00pm approximately every other day beginning on the day of injury (day 0) until 28dpi (**Fig. 11**).

3.4 Cell Cycle Labelling

To study cell proliferation dynamics of ependymoglial cells following SCI, EdU, which marks cells in the S-phase of the cell cycle, was administered through a 10 mM bath solution, made by dissolving EdU powder (E10187, ThermoFisher Scientific™) with system water (Lindsey et al., 2018). Juvenile zebrafish were bathed in a 6-well culture plate with n=1-2 zebrafish per well while adult zebrafish were placed in 100 mL of 10 mM EdU. Animals were exposed to EdU solution for 12 hours to obtain a snapshot of the dividing cell population post-SCI and in control (uninjured) spinal cords. The following morning, zebrafish were euthanized through an overdose of 0.4% tricaine, post-EdU bath to then be used for IHC.

EdU labelling was also used to perform pulse-chase experiments where zebrafish were pulsed with EdU for 24 hours in an EdU bath. During the chase, EdU is incorporated into the DNA of cells and as these cells proliferate, EdU is passed along to the progeny, providing information on

proliferation over a period of time. This method is used to determine the number of proliferating cells over a longer span of time but does not provide lineage information. Following this, co-labelling with other markers can be used to determine newly divided cells, such as newly generated neurons when stained for EdU and the pan-neuronal marker HuC/D. EdU baths for chase experiments were performed for 24 hours at the peak of cell proliferation; adult zebrafish at 7dpi, and juvenile zebrafish at 3dpi. Zebrafish were removed from the EdU bath the following morning at 9:00am and placed back into individual tanks with system water until they were euthanized.

3.5 Spinal Cord Dissection

Zebrafish were euthanized by immersion in 0.4% tricaine. Zebrafish were next placed in a silicone dissecting dish and stabilized using tungsten pins to orient the specimen dorsally under a brightfield dissecting microscope. Fine forceps and micro-scissors were used to cut through the skin and expose muscle along the dorsal body wall. The spinal cord was then further exposed in situ by removing surrounding muscle with tissue forceps. For downstream processing of adult spinal cord tissue, a scalpel blade was next used caudal to the dorsal fin such that tissue consisted of brain and the first two quarters of the spinal cord. For juvenile zebrafish, once the spinal cord was exposed *in situ*, the entire body was kept for tissue processing. Tissue was then immediately transferred to a fresh ice-cold solution of 2% paraformaldehyde (PFA) for tissue processing.

3.6 Tissue Processing

After dissection, segments of juvenile and adult spinal cord were fixed *in situ* in 10 mL fresh, ice-cold, 2% PFA solution in a 15 mL Falcon tube. Tubes were placed on a rocker in the dark at 4ºC and was gently rocked overnight for approximately 12 hours or alternatively placed on a rocker at

room temperature (RT) for 6 hours. Fixed tissue was next transferred into a solution of 20% Sucrose/Ethylenediaminetetraacetic acid (EDTA) for 24-48 hours on a tissue rocker at 4°C to break down cartilage.

Cryo-embedding of spinal cord samples was completed using a solution of 8% fish gelatin, placed on a bed of crushed dry ice to facilitate freezing. Peel-A-Way® Disposable Embedding Molds (Polysciences, Inc, T-12) were used for all adult or juvenile zebrafish tissue. These molds were labelled prior to embedding with the sample number, date and treatment group, and filled with enough 8% gelatine solution such that it fully covered the specimen, before being placed onto the bed of dry ice. Using tissue forceps, the tissue was oriented in a sagittal or vertical plane depending on the downstream experiment. Once the gelatine solution was frozen, the peel-away molds were stored in the -80ºC ultra-low freezer (Thermo Scientific™ Forma™ 89000) in boxes labelled by treatment groups until cryosectioning.

3.7 Cryosectioning

Prior to sectioning tissue, the object temperature and chamber temperature of the cryostat (Leica CM3050 S) were set to -30°C. These temperatures refer to the block that holds the embedded tissue in place and the ambient temperature of the cryostat, respectively. Blocks of tissue were placed in the cryostat to equilibrate to -30°C from -80°C. Using O.C.T compound (Tissue-Tek, 4583) the blocks were frozen onto metal ‘chucks’ and mounted onto the microtome for cutting. The blocks were first trimmed at 30 µm until tissue was visible in block and then switched to a cutting thickness of 20 µm. Sectioned tissue was collected sequentially, rostral to caudal within the 2nd quarter of the spinal cord and 3 mm before and after the injury site. This was similarly done in

control uninjured spinal cords. Sectioned tissue was collected onto RT microscope slides (Fisherbrand, Superfrost Plus) to allow tissue to quickly adhere to slides. Each slide held 8-10 spinal cord sections and a total of ~8 slides were used per adult zebrafish and ~6 slides per juvenile zebrafish. The microscope slides were dried flat for 1-hour before being stored in a -80°C ultra-low freezer (Thermo Scientific™ Forma™ 89000).

3.8 Immunohistochemistry (IHC)

IHC was used for experiments where I stained for neurons (HuC/D), motor neurons (HB9), NSCs (Sox2) and microglia (4C4) (**Supplemental Table S1**). First, cryosectioned slides were removed from our -80°C ultra-low freezer (Thermo Scientific™ Forma™ 89000) and dried at RT for 1-hour inside a slide box kept moist with 1x PBS. Slides were rehydrated using PBS-Tx for 15 minutes at RT. Incubation occurred overnight (12-14 hours) in the primary antibody (HuC/D, HB9 or 4C4). diluted in PBS-Tx at 4°C in the dark. The following day, slides were briefly rinsed and then washed with PBS-Tx thrice for 10 minutes before being incubated for 1-hour in the dark at RT with the secondary antibody diluted (1:750) in PBS-Tx with 4′,6-diamidino-2-phenylindole (DAPI) nuclear counterstain. Thereafter, the slides were rinsed with 1x PBS 3 times for 10 minutes per wash before mounting with Immu-Mount™ (Shandon™, ThermoScientific™) and cover slipped.

Specifically, for staining with the pan-neuronal primary antibody HuC/D staining followed the above protocol in addition to an antigen retrieval step to expose antibody binding sites. Antigen Fretrieval consisted of an incubation in 50 mM Tris buffer for 30 minutes at 80-85°C in a tissue incubator followed by a rinse with PDT 3 times for 5 minutes per wash. The sections were blocked

for 1-hour at RT before being incubated with the primary antibody. In situations where IHC was done in combination with EdU staining, EdU staining was completed first.

3.9 EdU Staining

To stain for cell proliferation in ependymoglia, EdU staining consisted of a 15-minute rehydration using PBS-Tx followed by a 30-minute RT incubation in the dark using an EdU staining solution (186.75 µL of 1x-PBS with Dapi (1:10,000), 50 µL of 0.5M L-Ascorbic Acid in MilliQ water, 12.5 µL of 2M Tris buffer (pH 8.5), 0.5 µL of 100mM Azide-Fluor 555 and 0.25 µL of copper sulphate; per slide) that was spread across slides using parafilm. This was followed with a quick rinse using PBS-Tx and washed 4 times for 10 minutes with 1x-PBS prior to mounting.

3.10 Hematoxylin and Eosin (H&E) Staining

To stain for the anatomy of spinal cord tissue, hematoxylin and eosin staining on cryosectioned spinal cord tissue was completed by the Histomorphology & Ultrastructural Imaging Platform, located within the Department of Human Anatomy and Cell Science. Sagittal spinal cord slides were allowed to dry for a minimum of 1-hour before using PBS-Tx to rehydrate for 15 minutes. Slides were then water washed before using a Hematoxylin nuclear stain. This was followed by differentiation in acid alcohol, more washing with water and the nuclear stain was completed with a blueing solution. After washing, the eosin counter stain was applied and then washed to remove any unbound staining. The slides were passed through an alcohol dehydration series, clearing solution and mounted in a toluene-based medium before being cover slipped.

3.11 Harvesting of 4C4 Primary Antibody from Hybridoma Cells

To differentiate between macrophages and microglia in our Tg(mpeg1:eGFP) line, the 4C4 antibody, that stains for microglia, needed to be isolated from the supernatant of a cultured hybridoma cell line. We first prepared a 10% media using 435 mL Dulbecco's Modified Eagle Medium (DMEM) (Millipore-Sigma cat # D5796), 5 mL 2mM L-Glutamine – GlutaMAX™-I (Life Technologies cat #35050-061), 10 mL 50X HT supplement (Life Technologies cat # 41065012) and 50 mL fetal bovine serum (Millipore-Sigma cat # F2442-500ML). This was filtered using a 0.22 μm PES filter and stored at 4°C. Next, 6 mL of media that had been warmed in a 37°C water bath was added to a T25 flask and the hybridoma cells (7.4.C4 – ECACC) (Millipore-Sigma cat # 92092321) were removed from liquid nitrogen. The cells were mixed with the media in a 15 mL conical tube and centrifuged at 1000 rpm for 5 minutes. Resuspended cells were added into fresh media within the T25 flask and incubated overnight at 37°C with 8% CO_2.

Following this, the growth of cells was monitored every few days through cell counting and topped up with fresh media. When necessary, cells were sub-cultured into T75 and T175 flasks to allow room for growth. Once the number of cells plateaued, the media was slowly changed from 10% to 5% in order for cell death to occur and for the antibody to be released. Antibody collection began when the supernatant changed colour from red to yellow, indicative of a high level of cell death. The supernatant was mixed with 1/20 volume of 1M Tris (pH 8.0) and centrifuged at 1000 rpm for 10 minutes. This was filtered using a 0.22 μm PES filter, aliquoted into microcentrifuge tubes and stored at -20°C.

To validate that this antibody is specifically staining for microglia a negative control was completed such that the 4C4 antibody was omitted from the IHC protocol. In addition, a serum control was used in place of the primary to ensure that the serum from which the cells were cultured is not falsely staining. These controls both resulted in an absence of microglial staining (**Fig. S1**).

3.12 Imaging

Confocal imaging was completed using a Zeiss LSM 880 Airyscan inverted confocal microscope with a 20X non-immersion, 40X water immersion and 63X oil immersion lenses at the Kleysen Institute for Advanced Medicine. For all images, z-stacks were taken at 1 μm intervals at a resolution of 1024 for downstream analysis and cell quantification. Virtual zoom was applied in cases where co-localization was investigated. To image H&E staining, a Zeiss Axio Imager M2 was used in the Human Anatomy and Cell Science Imaging Facility. All brightfield images were taken at 5X and cropped to show region of interest. Cross-section images were shown with dorsal oriented upwards and sagittal images were shown oriented rostral to the left and caudal to the right as proximal to the injury site as possible.

3.13 Cell Counting and Analysis

All quantifications were done by counting through z-stacks taken at 63X magnification for proliferation experiments and 40X magnification for differentiation experiments. Cells were counted using FIJI/ImageJ and marked to prevent double counting of cells. For cell proliferation, 2-3 cross-sections of spinal cords per fish were imaged from n=3-5 zebrafish per timepoint. In these experiments, DAPI and EdU positive cells were counted within the ependymal zone (EZ) and subependymal zone (SEZ) per section. To analyze neuronal differentiation, 3 cross-sections

of spinal cords per fish (n=3-4) were imaged per timepoint. For both proliferation and differentiation experiments, the cell counts of all sections imaged were then averaged per zebrafish. Finally, each zebrafish per experimental group was averaged to result in a single averaged cell count that would be further used for analysis. In cases where adult and juvenile zebrafish were to be compared, the cell counts were normalized due to the difference in size of the central canal between adults and juveniles. To normalize EdU positive cells to the DAPI population, the absolute number of EdU cells were divided by DAPI cell counts and multiplied by 100 to get a proportion represented as a percent. This was similarly repeated when studying neuronal differentiation where EdU/HuC/D cells were divided by EdU cell counts and multiplied by 100 to normalize the cell population.

For macrophage and microglial staining, one section rostral and caudal of the injury site was imaged from n=3-4 zebrafish per timepoint in a sagittal orientation. Quantifications were done by counting through z-stacks taken at 40X magnification. Mpeg1 positive, 4C4 positive and mpeg1/4C4 co-labelled cells were counted within a 120 μm distance from the injury site. Rostral and caudal sections were separately averaged per timepoint and summed for a total cell count.

3.14 Reverse Transcriptase Quantitative Polymerase Chain Reaction (RT-qPCR)

To study the temporal expression of pro- and anti-inflammatory cytokines released through SCI, RT-qPCR was used. The pro-inflammatory cytokines used were IL-1β and IL-8, and the anti-inflammatory cytokines were TGF-β1a and TGF-β3. To extract and purify RNA from adult and juvenile zebrafish a 350 μL fresh lysis mix of lysis buffer and β-mercaptoethanol was prepared into a 1.5 ml DNase/RNase-free microcentrifuge tube. Approximately 1 cm length of spinal cord

for adults, and 0.5 cm length of spinal cord for juveniles caudal and rostral to the transection site was dissected and pooled across adult zebrafish (n=3 fish) and juvenile zebrafish (n=4 fish). Spinal cord tissue was then transferred into microcentrifuge tubes that contained 200 µL of lysis mix. Tissue was incubated for 1-minute, pipetted slowly to gently dissociate the tissue and avoid any air bubbles. The rest of the 150 µL lysis mix was added to the microcentrifuge tube that contained the dissociated spinal cord. The tissue was incubated again at RT for 2 minutes and pipetted gently to mix the lysate.

To isolate RNA, Illustra™ RNAspin Mini Isolation Kit (Cytiva cat# 25-0500-71) was used. The RNAspin Mini Filter was placed into a collection tube and then loaded with the 350 µL of homogenized lysate. This was centrifuged at 11,000 x g for 1-minute. The RNAspin Mini Filter was discarded and the filtrate within the collection tube was kept. The filtrate was transferred to a new RNAse-free microcentrifuge tube and 70% EtOH was added to the filtrate which was then vortexed twice for 5 seconds. The lysate that contained 70% EtOH was pipetted up and down and then loaded onto the RNAspin Mini Column seated on a collection tube. This was centrifuged at 8,000 x g for 30 seconds and the RNAspin Mini Column was transferred to a new collection tube and the flow through was discarded. Desalting buffer was added onto the RNAspin Mini Column and then centrifuged at 11,000 x g for 1-minute to dry the membrane column. The flow though was once again discarded and the RNAspin Mini Column was returned to the collection tube.

To rid the sample of contaminating DNA, a DNAse I reaction mixture was prepared which contained 10 µL reconstituted DNase I and 90 µL of DNase reaction buffer. The tube was flicked to mix the reaction and then added directly onto the membrane of the RNAspin Mini Column. The

column was incubated at RT for 15 minutes. Afterwards, wash buffer I was added to the column and centrifuged at 11,000 x g for 1-minute. The column was then transferred to a new collection tube.

The RNA was next washed of contaminating ethanol or salt and dried through the use of wash buffer II that was added to the RNAspin Mini Column and centrifuged at 11,000 x g for 1-minute. The flow through from this was discarded and the RNAspin Mini Column was placed back into the collection tube. More wash buffer II was added and centrifuged again to completely dry the column membrane. The RNAspin Mini Column was transferred to a nuclease-free microcentrifuge tube.

To elute the RNA, 40 μL of RNase-free H2O was added into the RNAspin Mini Column and centrifuged at 11,000 x g for 1-minute. This was repeated once more, and the RNA elute was placed on ice immediately afterwards to prevent potential degradation. The RNA concentration and purity were determined with the NanoVue™ Spectrophotometer such that the A260/A280 concentration should be between 1.8 and 2.2 for pure RNA.

To next convert the RNA to cDNA, an ezDNase Reaction Mix was prepared with 1 μL of 10X ezDNase buffer, 1 μL of ezDNase enzyme and the template RNA last such that the mix adds to 10uL in total. This mix was kept on ice except for the ezDNase enzyme which was stored at -20°C. After having been gently mixed, the microcentrifuge tube was transferred from ice to a heater block that was warmed to 37°C. After the mix was incubated for 2 minutes the microcentrifuge tube was centrifuged briefly and placed back on ice.

To setup the reaction, the 10 µL ezDNase Reaction Mix was transferred to the PCR strip on ice and the SuperScript™ IV VILO™ Master Mix was added with nuclease-free water for a RT reaction of 20 µL total. To ensure all gDNA has been digested as stated above, the ezDNase Reaction Mix was added to SuperScript™ IV VILO™ No reverse transcriptase control that added to 20 µL total. These were mixed gently and placed in the thermal cycler PCR machine to anneal primers at 25°C for 10 minutes, reverse transcribe RNA at 50°C for 10 minutes and inactivate enzymes at 85°C for 5 minutes. When the cycle was finished, the PCR strips were transferred to ice and the cDNA was stored at -20°C for up to one week or -80°C for long-term storage.

To run the RT-qPCR, a mix of 10 µL SYBR Master Mix, 0.5 µL each of forward and reverse primers, 7 µL nuclease-free water, and 2 µL cDNA were combined. The volumes of nuclease-free water and cDNA were calculated based on the RNA concentration the spectrophotometer gave such that each tube consisted of 20 µL total. Duplicates of each primer were prepared to average the relative mRNA expression per run, and relative mRNA expression levels were normalized to β-actin, a housekeeping gene used as an internal control. The specific zebrafish primer sequences are listed in the Appendix (**Supplementary Table S2**).

Once the reaction mix was ready to be run, the optical tubes were arranged on a BLUE MicroAmp™ 96-well tray (ThermoFisher™ cat# A30588). The tray was briefly spun down using a PCR mini-plate mini centrifuge (VWR, C2001) and the protocol was set up with QuantStudio™ 3 Real-Time PCR System to activate the enzyme at 95°C for 2 minutes, denature the enzyme at

95°C for 15 seconds and anneal/extend for 1-minute at 61°C. The instrument was then set to perform a default dissociation step and relative mRNA levels were determined.

3.15 RT-qPCR Analysis

Primers were first validated by running an endpoint PCR, analyzing the melting curves and plotting a standard curve. Primers were validated using endpoint PCR when a single clean band was produced (**Fig. S2A**). The melting curve was used to ensure one peak is visible so that the primers produce a single, specific product (**Fig. S2B-F**). To determine the efficiency, or how well the polymerase is able to amplify the target cDNA given the primer sequences, a qPCR reaction was run, and a standard curve was plotted template quantity vs cycle threshold (Ct) value. From this plot, the best fit line reflected the efficiency of the reaction which was always between 90-100% indicating that for every number of cycles, the PCR product is being doubled (**Fig. S3**).

To analyze the relative mRNA, the average ΔCt value was calculated by subtracting the average β-actin Ct, that was used as an internal control, from the average target cytokine Ct. The ΔΔCt was calculated by subtracting the control ΔCt from the experimental ΔCt. The relative quantity of mRNA was calculated as $2^{-(\Delta\Delta Ct)}$.

3.16 Statistical Analysis and Graphical Representation

GraphPad Prism 9 was used for all statistical analysis and graphs. Statistics were performed on the averaged cell counts derived from each zebrafish within an experimental group. Significance was accepted at $p < 0.05$. Pairs of means were compared using independent samples t-tests. Comparisons between greater than two experimental groups were completed using one-way

ANOVA and exact *p*-values are stated. In cases where significance was present between groups, Tukey's or Dunnett's multiple comparisons tests were performed, and the adjusted *p*-value was reported. In cases where two datasets were compared, a two-way ANOVA was used with Dunnett's or Bonferroni's multiple comparisons test. All statistical results, including exact *p*-values, are reported in results or the appendix and graphical data represent mean ± standard error of the mean (SEM).

Chapter 4.0 Results

4.1 Multiple Cell Populations Surround the Zebrafish Spinal Cord Central Canal

The adult zebrafish spinal cord is comprised of many cell populations and vessels that are located near the central canal, within the dorsal/ventral horns, and throughout the parenchyma (**Fig. 2A**). Surrounding the central canal are large populations of ependymoglia that sit in a single layer termed the EZ and the two layers of the SEZ (**Fig. 2A**). Upon injury, many of these cell populations are disrupted or undergo cell death (Cigliola et al., 2020). The dorsal and ventral horns can be seen in the glial fibrillary acidic protein (GFAP) reporter line, Tg(gfap:GFP), stained with the pan-neuronal marker HuC/D (**Fig. 2B**). In this image, the long radial processes of the ependymoglia can be seen contacting the periphery of the spinal cord and neurons can be seen residing in the single dorsal horn and two ventral horns. Staining for motor neurons using the HB9 antibody, similarly, shows these neuronal cells in the dorsal and ventral horns as seen in an overview of the spinal cord (**Fig. 2C**). At higher magnification, combining the reporter line for GFAP and staining with the Sox2 antibody, that marks for NSCs, shows the layers of ependymoglia sitting around the central canal (**Fig. 2D**). Co-labelled cells that are $GFAP^{+}/Sox2^{+}$ are shown with white arrows, indicating the presence of some parent stem cells. In the Tg(Olig2:eGFP) line, oligodendrocytes can also be seen largely surrounding the SEZ and few are shown to reside within it (**Fig. 2E**). Using the Tg(Fli1a:eGFP) line that marks for endothelial cells, the nearby presence of vasculature was also visible in the zebrafish spinal cord (**Fig. 2F**).

Figure 2

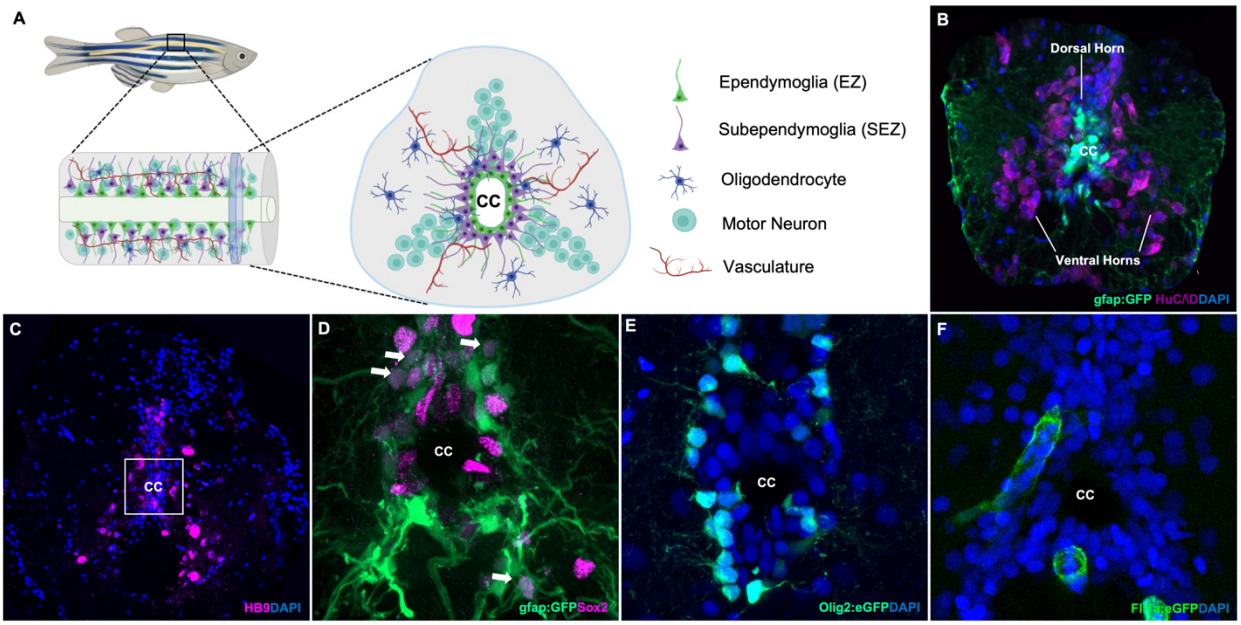

Figure 2. The uninjured spinal cord consists of many cell populations. (**A**) Schematic of an adult zebrafish displaying the different cell populations and vasculature in a sagittal and cross-section of a spinal cord. (**B**) Using the Tg(gfap:GFP) line, GFAP cells and their processes can be seen making contact with the periphery of the spinal cord and neurons are seen residing in the dorsal and ventral horns. (**C**) Motor neurons stained with the HB9 antibody in the dorsal and ventral horns. The white box centered around the central canal (CC) depicts the higher magnification images shown in **D-F**. (**D**) Neural stem cells can be seen around the central canal in the EZ and SEZ using the Tg(gfap:GFP) reporter line along with Sox2 antibody staining. Co-labelled cells are shown by the white arrows. (**E**) Oligodendrocytes are seen near the central canal using the Tg(Olig2:eGFP) line. (**F**) Using the reporter line Tg(Fli1a:eGFP) to mark for endothelial cells shows vasculature near the spinal cord central canal. (**B-C**) imaged at 20X; (**D-F**) imaged at 63X; 4′,6-diamidino-2-phenylindole (DAPI) counterstaining in blue. In all images, dorsal is up.

4.2 Validation of Adult and Juvenile Models of SCI show Swimming Activity Abolished Following Injury as a Result of Full Transection

To study SCI in zebrafish, I first established our adult and juvenile SCI models. Adult zebrafish SCI models already exist, but juveniles have never been used before in this context. Establishing a juvenile SCI model is advantageous to compare with adult SCI models to develop a quicker method to study SCI beyond larval stages. To validate our injury models, I tracked the behaviour of injured, sham and control zebrafish for 5 minutes using Ethovision tracking software. Zebrafish were acclimated for 30 minutes before recording and tracked for 5 minutes. SCI was performed in adult zebrafish under anesthetic using surgical scissors to cut through the skin and superficial layers of the muscle to reach the intact spinal cord, followed by complete transection (**Fig. 3A**). For sham injuries only the skin and muscles were cut leaving the spinal cord intact. As expected from previous adult SCI studies, the zebrafish to be either unable to swim or less active than control/sham groups after a full transection (Becker & Becker, 2006).

Representative heat maps (**Fig. 3B-D**) and tracking images of the total distance travelled (**Fig. 3E-G**) of a single zebrafish over the 5-minute duration for control, sham and SCI groups, clearly showed less movement and activity in the SCI group. The heat maps are indicative of the time spent in a given area of the arena, with the red indicating the most time spent and the blue indicating the least. To confirm that following SCI a full transection occurred, I tracked the behaviour of all three groups, and analyzed the total distance travelled using a one-way ANOVA test. Results showed that a significant between group effect was present ($p = 0.0027$, **Fig. 3H**). Moreover, as predicted, Tukey's post-hoc multiple comparisons tests showed a significant reduction in swimming between control and SCI groups ($p = 0.0036$) and between sham and SCI groups ($p =$

0.0085), while no significant change in swimming was observed between control and sham groups ($p > 0.05$, **Fig. 3H**). These results confirm that the impaired swimming seen was due to the full spinal cord transection itself.

Juvenile zebrafish require fewer cuts to reach the depth of the spinal cord as compared to adult zebrafish who have qualitatively thicker skin and more muscle surrounding the spinal cord. Despite this, the spinal cord sits at a similar depth as adults (**Fig. 3I**). Juvenile zebrafish showed similar heat maps and tracking behaviour to adult zebrafish (**Fig. 3J-O**). To determine if there was a difference between juvenile control, sham and SCI groups, total distance travelled was similarly analyzed using a one-way ANOVA test that resulted in a significant group effect ($p = 0.0003$, **Fig. 3P**). Furthermore, using Tukey's post-hoc multiple comparisons tests resulted in no significant difference between the total distance travelled of the control and sham groups ($p > 0.05$, **Fig. 3P**), indicating that injury to the muscle alone is not sufficient to abolish swimming behaviour. However, total distance travelled was significant comparing control to SCI groups ($p = 0.0006$, **Fig. 3P**), and sham to SCI groups ($p = 0.0006$, **Fig. 3P**). Collectively, these results validate that our adult and juvenile SCI models cause equal impairment in functional swimming behaviour.

Figure 3

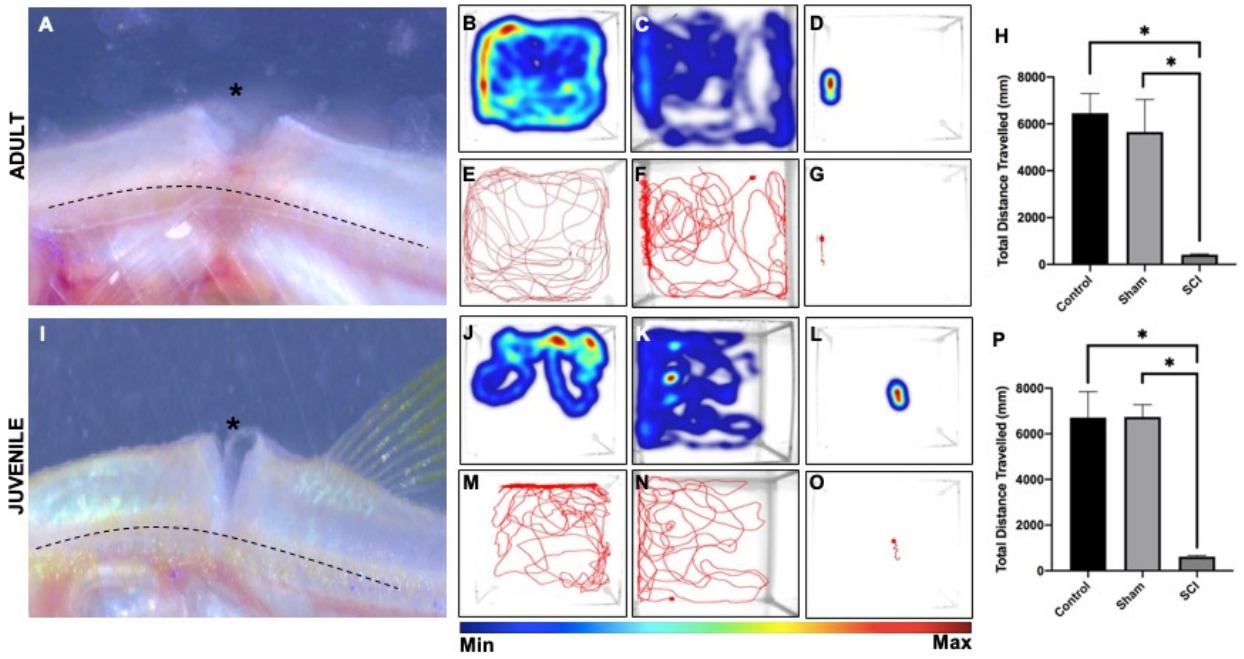

Figure 3. SCI abolishes swimming behaviour of adult and juvenile zebrafish. (**A**) Lateral view of a transected spinal cord in an adult zebrafish. Black dashed line demarcates the ventral border of the spinal cord and the asterisk shows the site of injury. (**B-G**) Heat map activity and tracking behaviour after 5-minute recording in adult control, sham and SCI groups. (**H**) Comparison of total distance travelled over a 5-minute recording between adult zebrafish groups. (**I**) Lateral view of a transected spinal cord in a juvenile zebrafish. The asterisk indicates the site of injury and the dashed line highlights the spinal cord. (**J-O**) Heat map activity and tracking behaviour in control, sham and SCI groups in juvenile zebrafish. (**P**) Comparison of total distance travelled over a 5-minute recording between juvenile zebrafish groups. One-way ANOVA with Tukey's multiple comparisons test; *$p < 0.05$; n=4 animals for each group; error bars indicate SEM. In **A** and **I**, dorsal is up

To next validate anatomically that a full transection of the spinal cord occurred, I used H&E staining on sagittal sections of the spinal cord at 1dpi and 7dpi to compare with uninjured control tissue. Spinal cord tissue for both adult and juvenile zebrafish was analyzed in the second segment of the spinal cord as indicated in the dorsal view of the intact adult zebrafish spinal cord (**Fig. 4A**). For H& E analysis, I examined tissue +/-0.5 mm from the injury site (**Fig. 4A**). Control spinal cord of adults and juveniles demonstrates the intact anatomy including the superficial muscle tissue dorsal to the spinal cord and the vertebrae located ventrally (**Fig. 4B**). At 1dpi and 7dpi, the injury is visible providing evidence of a full transection of the spinal cord (**Fig. 4C-D**). There appears no connection between rostral and caudal sides of the injury and the surrounding tissue appears to be disrupted as well. At 7dpi, this surrounding tissue of muscle fibers and vertebrae can be seen in the break of the spinal cord (**Fig. 4D**). These images suggest that anatomically the rostral and caudal segments of the spinal cord appear to remain disconnected over the first week post-SCI.

Figure 4

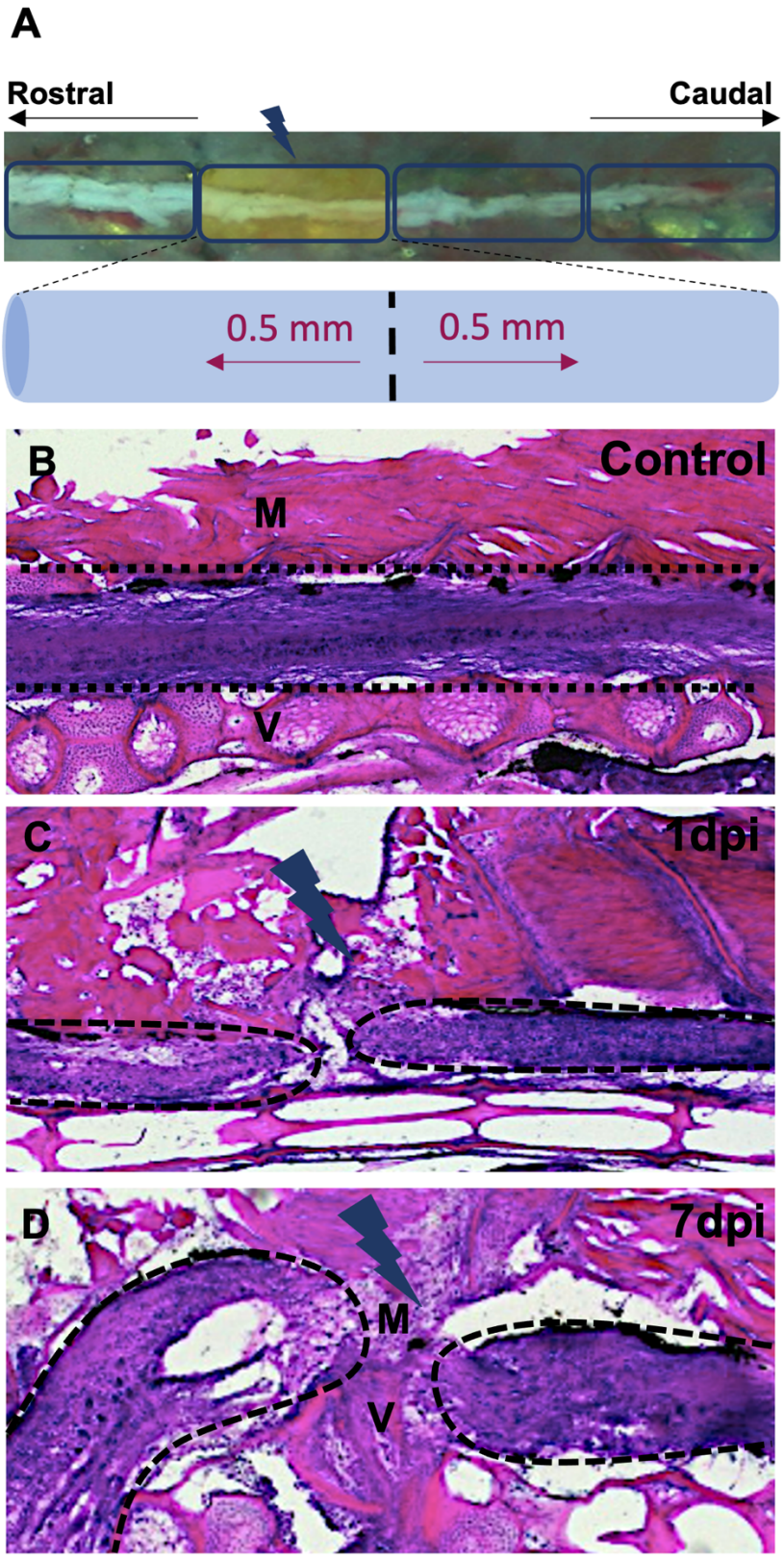

Figure 4. H&E staining confirms full transection following SCI. (**A**) Histological image of a dissected spinal cord. The solid blue outlines indicate the spinal cord segments where analysis took place in the second segment as shown in the schematic. Here tissue was analyzed +/- 0.5 mm from the injury site. (**B**) H&E staining shows an intact, uninjured spinal cord surrounded by muscle (M) and vertebrae (V). (**C-D**) At 1dpi and 7dpi the spinal cord appears broken as indicated by the asterisk at the injury site. At 7dpi the spinal cord still appears injured and severed with muscle fibers and vertebrae appearing in the break. All H&E staining was imaged at 5X; dorsal is up. In **B-D**, rostral is left.

4.3 Ependymoglial Proliferation Around the Central Canal Peaks Earlier in Juveniles than Adults After SCI

To investigate the proliferation of NSCs in the spinal cord, I investigated the temporal dynamics of ependymoglial cell division post-SCI. Adult zebrafish were bathed in a 10mM EdU solution for 12 hours prior to sacrifice and EdU staining was completed across multiple timepoints following injury (**Fig. 5A**). To first assess when the overall peak of ependymoglial proliferation was following SCI, I analyzed the total number of EdU^+ cells across both the EZ and SEZ. Few EdU^+ cells were labelled in control, sham (data not shown), 12hpi and 1dpi tissue (**Fig. 5B-D**). At 3dpi there was a slight increase, but most EdU^+ cells were detected at 7dpi and continued until 14dpi (**Fig. 5E-G**). Statistical analysis of total EdU^+ cell counts using a one-way ANOVA further confirmed a significant effect of time post-SCI on total number of EdU^+ cells ($p < 0.0001$). Notably, a significant difference ($p < 0.05$) was observed between 7dpi and 14dpi in comparison to all other timepoints, respectively (**Fig. 5H**, see **Supplemental Table S3** for Tukey's post-hoc multiple comparisons tests). Interestingly, a similar trend was seen among the expansion of the central canal following SCI. The diameters of the central canal in adult spinal cords showed a significant effect of time post-SCI ($p < 0.0001$) with significant differences ($p < 0.05$) between 7dpi and 14dpi to all other timepoints (**Fig. S4**, see **Supplemental Table S5** for Tukey's post-hoc multiple comparisons tests). This indicates that as the central canal expands due to injury, the proliferative response of ependymoglia surrounding the central canal increases as well.

After determining significant differences in total amounts of EdU^+ cells, I asked whether the majority of EdU^+ cells came from the EZ or SEZ. To determine this difference, I first analyzed the EZ using a one-way ANOVA which indicated a significant group effect ($p < 0.0001$, **Fig. 5I**). The

greatest increase in proliferation occurred at 7dpi and 14dpi ($p < 0.05$, **Fig. 5I**, see **Supplemental Table S3** for Tukey's post-hoc), similar to the trend observed following analysis of total EdU^+ cells. Statistical analysis of the SEZ using a one-way ANOVA also confirmed a significant effect of time on the population size of EdU^+ cells ($p = 0.0009$, **Fig. 5J**). Tukey's post-hoc multiple comparisons tests demonstrated significant differences between 7dpi and 14dpi to other time points except for 3dpi, respectively ($p < 0.05$, **Fig. 5J**, see **Supplemental Table S3** for Tukey's post-hoc). These results illustrate that proliferation post-SCI in adult zebrafish peaks at 7dpi across total, EZ and SEZ data.

Figure 5

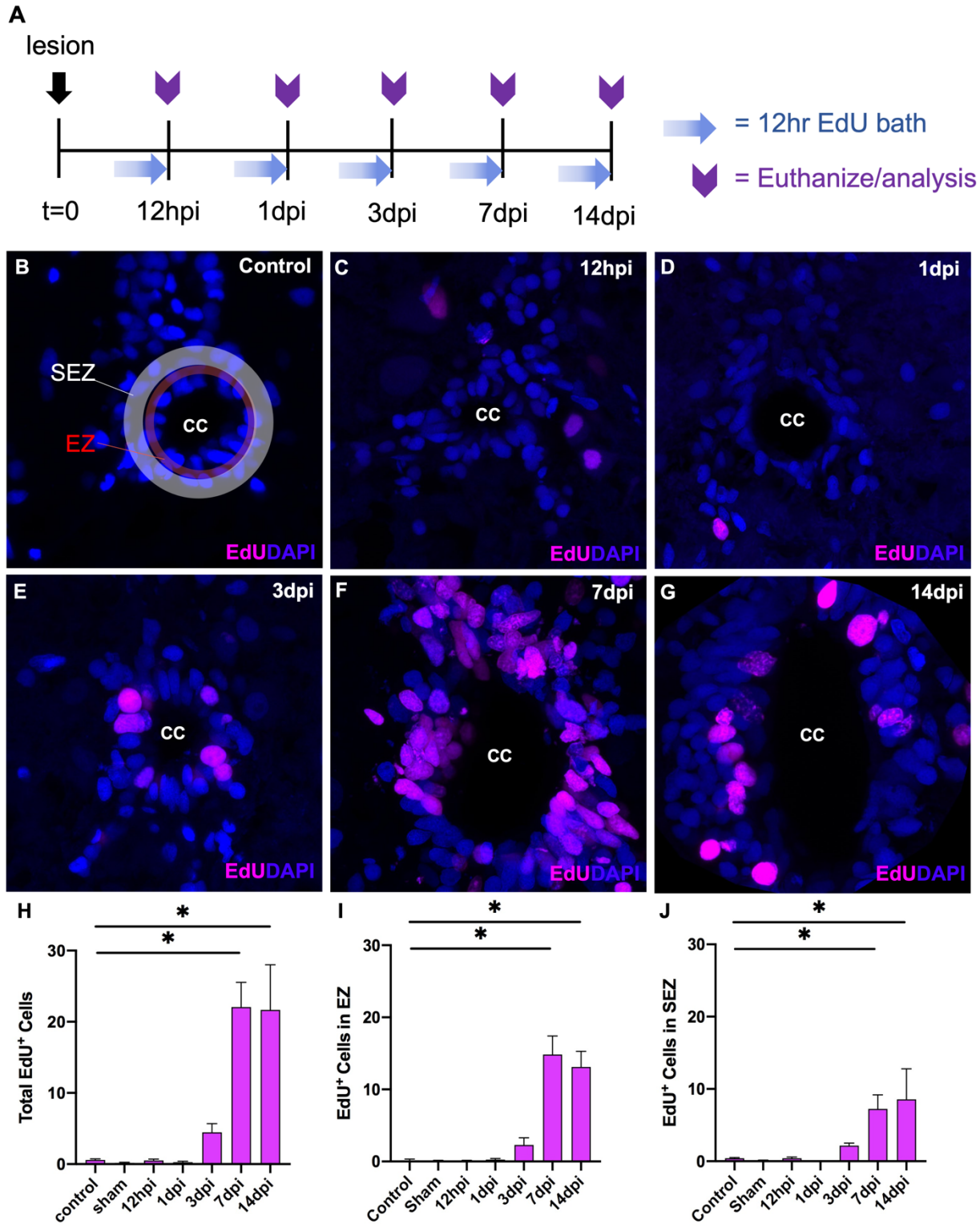
A
lesion
t=0
12hpi
1dpi
3dpi
7dpi
14dpi
= 12hr EdU bath
= Euthanize/analysis
B
Control
SEZ
EZ
cc
EdUDAPI
C
12hpi
D
1dpi
E
3dpi
F
7dpi
G
14dpi
H
Total EdU+ Cells
I
EdU+ Cells in EZ
J
EdU+ Cells in SEZ
control
sham
12hpi
1dpi
3dpi
7dpi
14dpi
Control
Sham

Figure 5. Proliferation of ependymoglia in the adult zebrafish spinal cord. (**A**) Timeline of SCI represents lesion timepoints, EdU treatments and tissue analysis. (**B-G**) Representative images for EdU^+ cells across experimental groups. Control image displays the EZ and SEZ around the central canal used for cell counting at all timepoints. (**H-J**) Quantification of total EdU^+ cells (EZ + SEZ) surrounding the adult central canal (CC, **H**), EdU^+ cells within the EZ (**I**), and EdU^+ cells within the SEZ (**J**). One-way ANOVA with Tukey's multiple comparisons test; $*p < 0.0001$; n=3-4 animals for each timepoint; DAPI counterstaining in blue; errors bars indicate SEM; all images are taken at 63X and displayed dorsal up.

This is the first study to establish juvenile zebrafish as a model of SCI. Thus, a fundamental question is whether their proliferative response to SCI mimics a similar time frame as adults or if it is more rapid in this younger model. To address this, juvenile zebrafish received the same EdU exposure paradigm as adults and were analyzed similarly for total EdU^+ population, and separately in the EZ and SEZ (**Fig. 6A**). Labelling demonstrated little to no EdU^+ cells in control, sham (data not shown), 12hpi and 1dpi groups (**Fig. 6B-D**). However, at 3dpi and 7dpi there appeared to be a greater increase in proliferation that began to decrease by 14dpi. (**Fig. 6E-G**). One-way ANOVA analysis of the total EdU^+ population across the EZ and SEZ confirmed a significant effect of time post-SCI ($p < 0.0001$, **Fig. 6H**). This was then examined used Tukey's multiple comparisons test where a significant difference ($p < 0.05$) was observed between 3dpi and 7dpi to all other timepoints, respectively (see **Supplemental Table S4** for Tukey's post-hoc). Similar to adults, I next separately analyzed the EZ and SEZ using a one-way ANOVA that showed a significant effect of time in each zone ($p < 0.0001$). Multiple comparisons tests for both the EZ and SEZ, respectfully, displayed a significant increase at 3dpi and 7dpi ($p < 0.05$, **Fig. 6I-J**, see **Supplemental Table S4** for Tukey's post-hoc). Examining the expansion of the central canal in juvenile zebrafish following SCI demonstrated a significant effect of time ($p = 0.0060$) with a significant increase at 7dpi (**Fig. S4**, see **Supplemental Table S5** for Tukey's post-hoc multiple comparisons tests). This suggested a correlation between the size of the central canal and an increase in proliferation. Collectively, these results indicate that proliferation of ependymoglia post-SCI in juvenile zebrafish peaks earlier at 3dpi than adults.

Figure 6

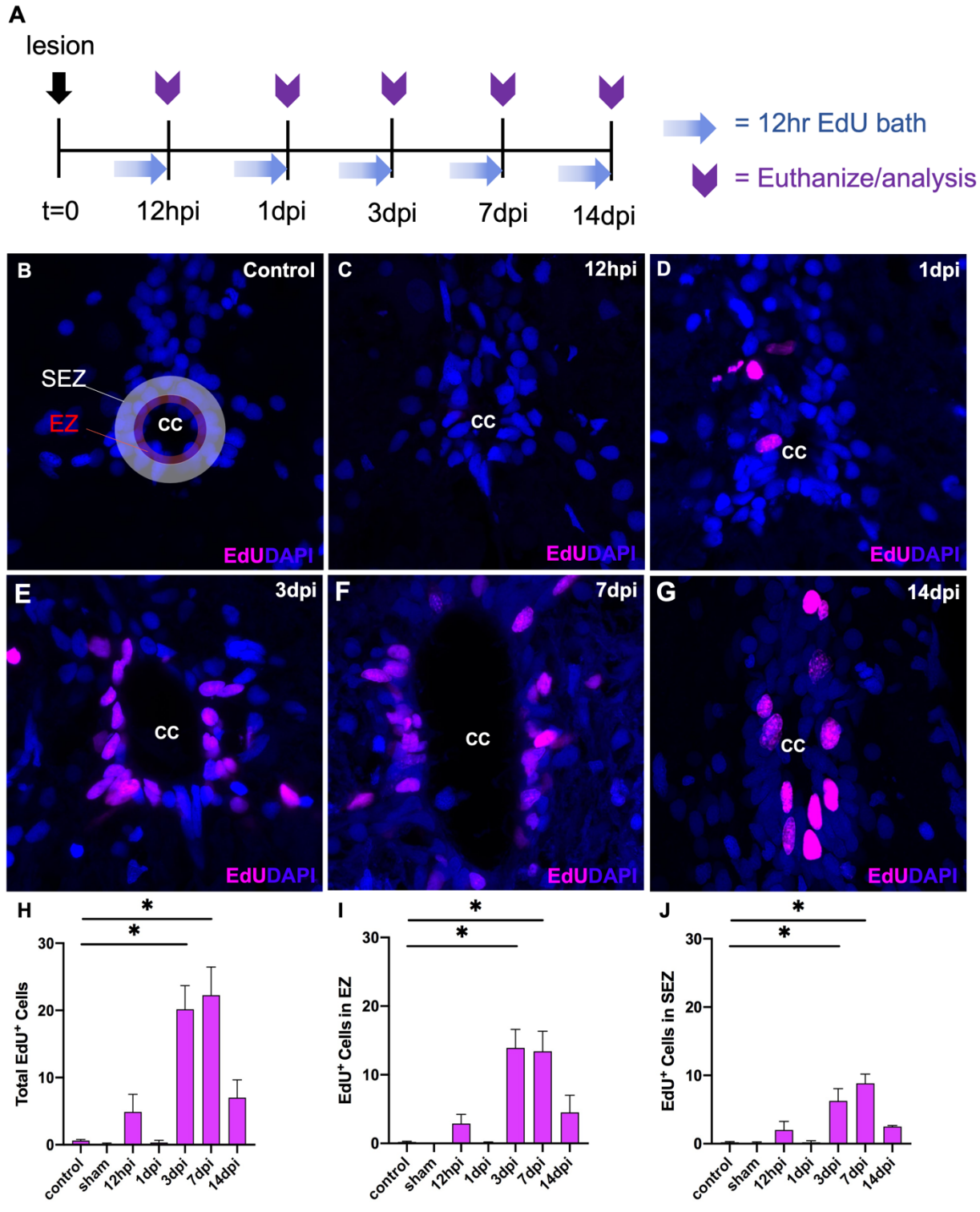
A
lesion
t=0
12hpi
1dpi
3dpi
7dpi
14dpi
= 12hr EdU bath
= Euthanize/analysis
B
Control
SEZ
EZ
cc
EdUDAPI
C
12hpi
cc
EdUDAPI
D
1dpi
cc
EdUDAPI
E
3dpi
cc
EdUDAPI
F
7dpi
cc
EdUDAPI
G
14dpi
cc
EdUDAPI
H
Total EdU+ Cells
I
EdU+ Cells in EZ
J
EdU+ Cells in SEZ
control
sham
12hpi
1dpi
3dpi
7dpi
14dpi

Figure 6. Proliferation of ependymoglia in juvenile zebrafish. (**A**) Timeline of SCI represents lesion timepoints, EdU treatments and tissue analysis. (**B-G**) Representative images for EdU^+ cells across experimental groups in the juvenile zebrafish spinal cord. (**H-J**) Quantification of total EdU^+ cells (EZ + SEZ) surrounding the juvenile central canal (CC, **H**), EdU^+ cells within the EZ (**I**), and EdU^+ cells within the SEZ (**J**). One-way ANOVA with Tukey's multiple comparisons test; $*p < 0.0001$; n=3-5 animals for each timepoint; DAPI counterstaining in blue; errors bars indicate SEM; all images are taken at 63X and displayed dorsal up.

I next asked if there were any differences in the population size of EdU^+ ependymoglia between juvenile and adult zebrafish following SCI. However, the absolute cell counts could not be directly compared between adult and juvenile zebrafish due to the variation in central canal sizes. A larger central canal would result in more EdU^+ cells around it, not allowing for proper comparisons to be completed. Thus, to properly compare these two developmental stages, EdU^+ cell counts (total, EZ, or SEZ) were normalized by dividing the EdU^+ cells by the total DAPI population, also cell counted in the EZ and SEZ, to obtain the proportions of EdU^+ cells. Once data was normalized unpaired t-tests were performed to compare both developmental stages. Adults and juveniles in each treatment group were first compared for total EdU^+ cells normalized to DAPI, resulting in a significant difference at 3dpi ($p = 0.0168$, unpaired t-test, **Fig. 7A**). Similarly, a significant difference was detected at 3dpi in the EZ ($p = 0.0081$, unpaired t-test, **Fig. 7B**), but within the SEZ no significant difference (unpaired t-test; $p > 0.05$) across treatment groups was observed (**Fig. 7C**). This data comparing the proliferative response of ependymoglia between adult and juvenile zebrafish, further supports my results that peak of proliferation following SCI in juveniles occurs at an earlier timepoint (3dpi) as compared to adults (7dpi).

Figure 7

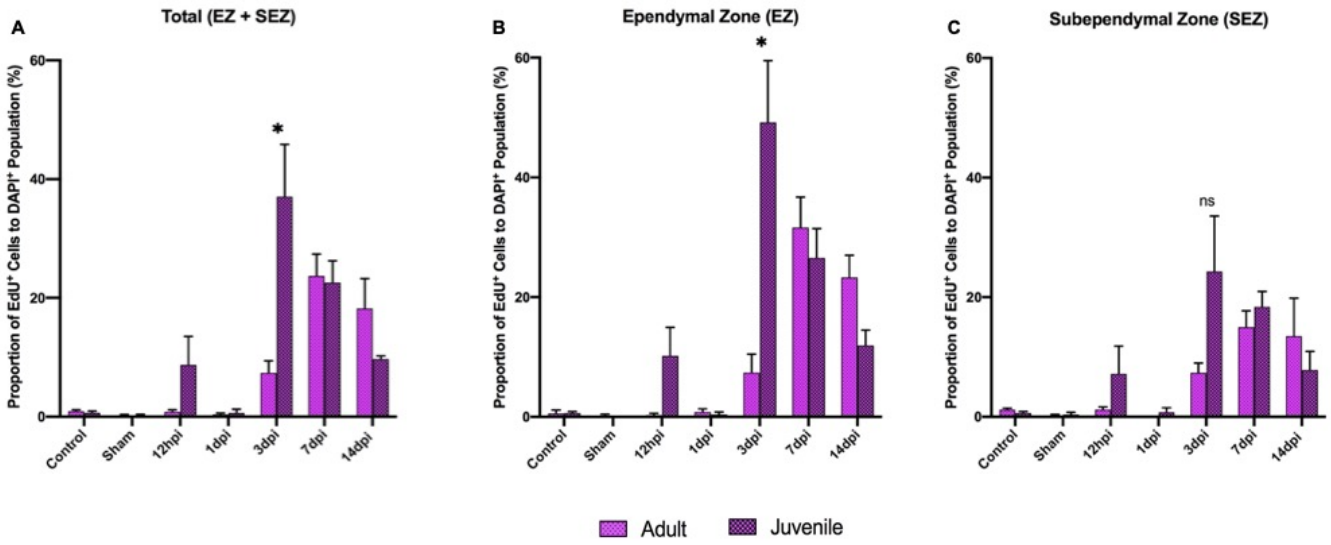

Figure 7. Comparison of EdU$^+$ ependymoglia proliferation between adult and juvenile zebrafish. EdU cell counts were normalized to DAPI population and the proportion is represented as a percent. (**A-B**) Proportion of cells across both total (**A**) and EZ (**B**) indicate significant difference between adult and juvenile zebrafish at 3dpi. (**C**) Proportion of cells within the SEZ. No significant difference was observed across timepoints. Unpaired t-test; *$p < 0.05$; statistical analyses were run for all timepoints except 14dpi due to small sample size (n=2); n=3-5 animals for each timepoint excluding 14dpi; errors bars indicate SEM.

4.4 Neuronal Differentiation after SCI in Adult and Juvenile Zebrafish Appears Similar

After injury, zebrafish are able to regenerate newborn neurons from ependymoglial cells, but it is unknown if this occurs at a similar rate between adult and juvenile zebrafish. Upon injury, many neuronal populations are disrupted or undergo cell death, so to study neuronal differentiation, EdU chase experiments were conducted on adult and juvenile spinal cords. Zebrafish underwent SCI before being bathed in 10mM EdU for 24 hours at the time of peak of proliferation as defined in **Figures 5-6** (7dpi for adults and 3dpi for juveniles). Following bath treatment, animals were removed and placed in fresh facility water and left until 7-days, 14-days or and 28-days post-EdU (**Fig. 8A**). This method allows for cells to divide and pass along EdU to progeny in order to gain information on proliferation over a longer period of time, in this case to determine newborn neurons arising from ependymoglia. Sections were then co-labelled with the proliferative marker EdU, the pan-neuronal marker HuC/D and DAPI, to study the generation of newborn neurons after different chase periods. The images shown are representative of both adults and juveniles as they displayed similar trends (**Fig. 8B-D**). In these images, many proliferating cells can be seen surrounding the central canal within the EZ and SEZ at all timepoints studied. Immunofluorescence staining confirmed that a subpopulation of these proliferating cells produced newly generated neurons post-SCI, as evidenced by EdU^+ nuclear staining and HuC/D^+ staining in the cytoplasm (**Fig. 8E-E'''**). An important aspect of spinal cord regeneration is the formation of new motor neurons. Co-labelling of EdU, HuC/D and HB9, further indicated the presence of newly differentiated motor neurons in adult and juvenile spinal cords at 14-days post-EdU (**Fig. 8F-F''''**).

Knowing that cells are born in the EZ and migrate away from the central canal overtime, I was interested in examining the difference in newly generated neurons between the EZ and SEZ. Within adult zebrafish, the EZ displayed lower numbers of co-labelled $EdU^+/HuC/D^+$ cells as compared to the SEZ across all chase periods (**Fig. 8G**). Rather, co-labelled $EdU^+/HuC/D^+$ cells in juvenile zebrafish remained consistently low across all timepoints in the EZ while in the SEZ steadily decreased from 7-days to 28-days post-EdU (**Fig. 8H**). To quantify the population size of co-labelled cells between the EZ and SEZ at each timepoint, I employed unpaired t-tests for statistical analyses in both adult and juvenile spinal cords. Comparing the EZ and SEZ within adults, demonstrated a significant difference in the 7-day ($p = 0.0197$, **Fig. 8G**) and the 28-day post-EdU timepoint ($p = 0.0070$, **Fig. 8G**). By contrast, the co-labelled cell counts within juvenile zebrafish displayed a significant difference at 7-day ($p = 0.0148$, **Fig. 8H**) and the 14-day post-EdU timepoints ($p = 0.0001$, **Fig. 8H**). These results indicate that the population of newly generated neurons is greater in the SEZ in both adult and juvenile zebrafish.

To next compare the number of newborn neurons regenerated post-SCI directly between adult and juvenile zebrafish, $EdU^+/HuC/D^+$ co-labelled cells were divided by EdU^+ cells to normalize the cell counts as the central canal sizes varied. Normalized data was represented as a percent and used to compare adults and juveniles in each treatment group. Between adults and juveniles there was no significant difference observed within the EZ across all timepoints (unpaired t-test; $p > 0.05$, **Fig. 8I**). This same finding was observed within the SEZ although a non-significant upward trend was present at 28-day post-EdU (unpaired t-test; $p = 0.0699$, **Fig. 8J**). These results reveal that despite the use of a younger developmental model, juveniles display similar rates of neuronal differentiation as adults following SCI.

Figure 8

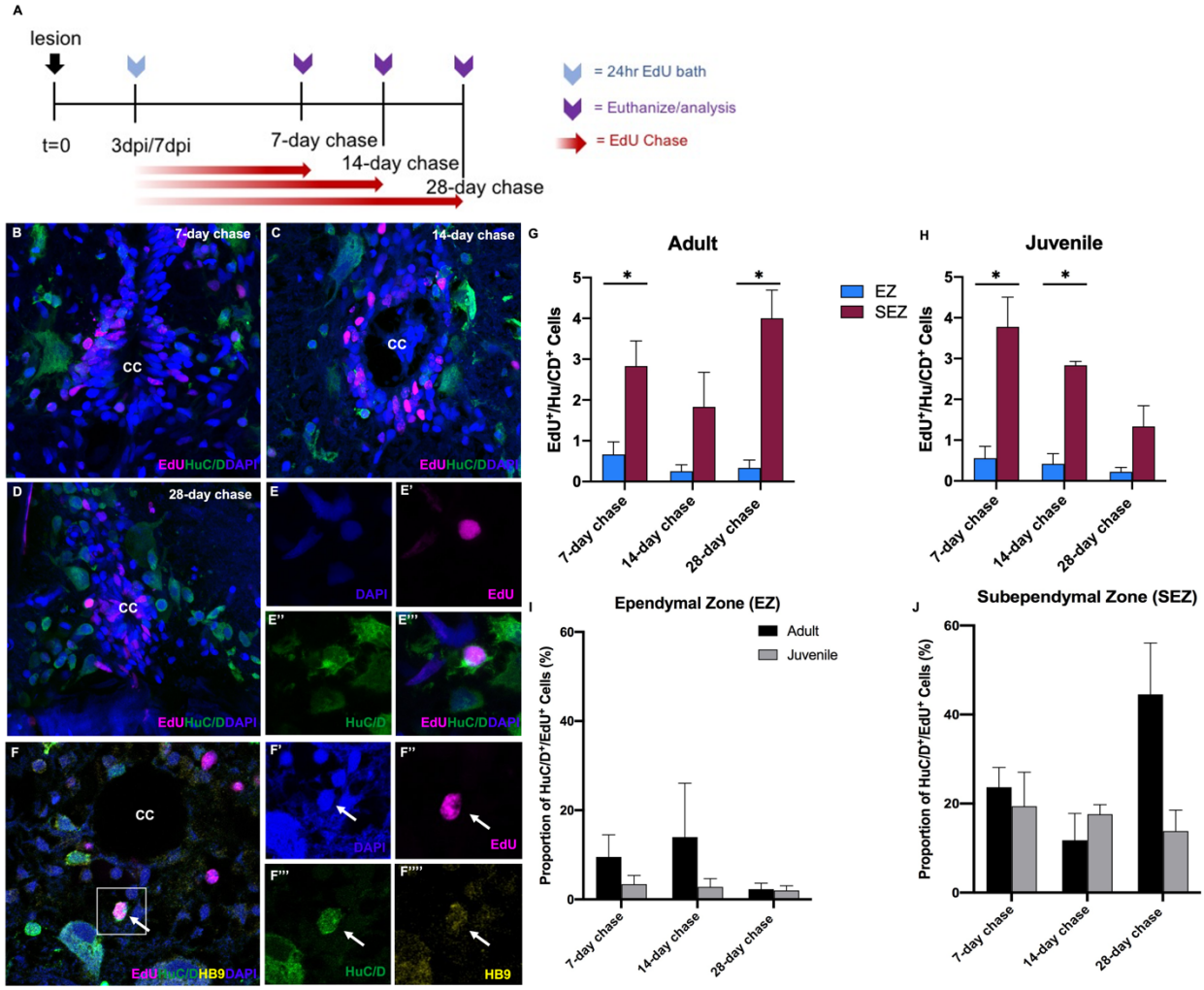
A
lesion
t=0
3dpi/7dpi
7-day chase
14-day chase
28-day chase
= 24hr EdU bath
= Euthanize/analysis
= EdU Chase
B
7-day chase
C
14-day chase
D
28-day chase
CC
EdUHuC/DDAPI
E
E'
E''
E'''
DAPI
EdU
HuC/D
F
F'
F''
F'''
F''''
HB9
G
Adult
H
Juvenile
EZ
SEZ
EdU+/Hu/CD+ Cells
I
Ependymal Zone (EZ)
J
Subependymal Zone (SEZ)
Adult
Juvenile
Proportion of HuC/D+/EdU+ Cells (%)

Figure 8. Adults and juveniles show no differences in neuronal differentiation after SCI. (**A**) Timeline of chase experiment represents day of lesion, 24-hour EdU baths at peak proliferation (adults 7dpi; juveniles 3dpi) and length of EdU chase until tissue analysis. For adults, 7-day chase groups were sacrificed at 14dpi, 14-day chase groups at 21dpi and 28-day chase groups at 35dpi. For juveniles, 7-day chase groups were sacrificed at 10dpi, 14-day chase groups at 17dpi and 28-day chase groups at 31dpi. (**B-D**) Representative images of adults and juveniles after 7-day, 14-day and 28-day chase periods centered around the central canal. (**E-E'''**) Example of a co-labelled newly formed neuron shown in single channels and merged. (**F-F''''**) Representative image displaying a newly formed motor neuron indicated by the white box and displayed at higher magnification in single channels stained with DAPI, EdU, HuC/D and HB9. (**G-H**) $EdU^+/HuC/D^+$ co-labelled cells in adult (**G**) and juvenile (**H**) zebrafish were greater in the SEZ as compared to the EZ. (**I-J**) No significant difference was seen between adults and juveniles in either the EZ or the SEZ. All images are taken at 40X and co-labelled images are cropped and enlarged for better visualization. Unpaired t-tests; $*p < 0.05$; n=3-4 animals for each timepoint; errors bars indicate SEM. In all images dorsal is up.

4.5 Microglial Populations Increase Following SCI in Adult and Juvenile Zebrafish

To next determine when microglia and macrophages infiltrate the spinal cord following injury, I took advantage of the reporter line Tg(mpeg1:eGFP) that labels all tissue macrophages and microglia. In addition, to further distinguish between local spinal cord microglia and peripheral macrophages, I used the 4C4 antibody, marking specifically for microglia. This method results in different marker combinations that would indicate macrophages ($mpeg1^{+}/4C4^{-}$) and microglia ($mpeg1^{+}/4C4^{+}$, $mpeg1^{-}/4C4^{+}$). Immunofluorescence staining of 4C4 on Tg(mpeg1:eGFP) tissue confirmed detection of the $mpeg1^{+}/4C4^{+}$ microglial phenotype (**Fig. 9A-C**). The separate $mpeg1^{+}/4C4^{-}$ and $mpeg1^{-}/4C4^{+}$ populations can be distinctly seen in a higher magnification image of the spinal cord (**Fig. 9D**).

To study the infiltration of macrophages and microglia, tissue at 12hpi, 1dpi and 7dpi in adult animals, or 12hpi, 1dpi, and 3dpi in juveniles was stained and compared to the uninjured control spinal cord (**Fig. 9E**). The different timepoints used for adults and juveniles was a result of availability of animals at the time of experiment. Using a one-way ANOVA, I first examined changes in macrophage and microglial populations at different time points, respectively. In rare instances, uninjured control spinal cord tissue unexpectedly displayed a small number of macrophages labelled with $mpeg1^{+}/4C4^{-}$ (**Fig. 9F-G**). In both adults and juveniles, the macrophage population showed no significant difference when compared to uninjured control tissue ($p > 0.05$, **Fig. 9F-G**). However, the microglial populations showed a significant effect of time post-SCI in both adults and juveniles (Adults: $p = 0.0232$, Juveniles: $p = 0.0097$, **Fig. 9F-G**). Tukey's post-hoc multiple comparisons test was used to compare the changes in microglial populations to uninjured control tissue. This analysis determined a significant increase in adult populations at

1dpi ($p = 0.0320$) and 7dpi ($p = 0.0296$) and in juvenile zebrafish at 12hpi ($p = 0.0056$). Next, the two immune cell populations were compared between adult and juvenile zebrafish in overlapping groups, including control, 12hpi and 1dpi (**Fig. 9H-I**). Unpaired t-tests revealed no significant difference in either cell population ($p > 0.05$). These results indicate that both adult and juvenile zebrafish show a similar increase in the microglial response following SCI, with little change in the population size of infiltrating macrophages.

Figure 9

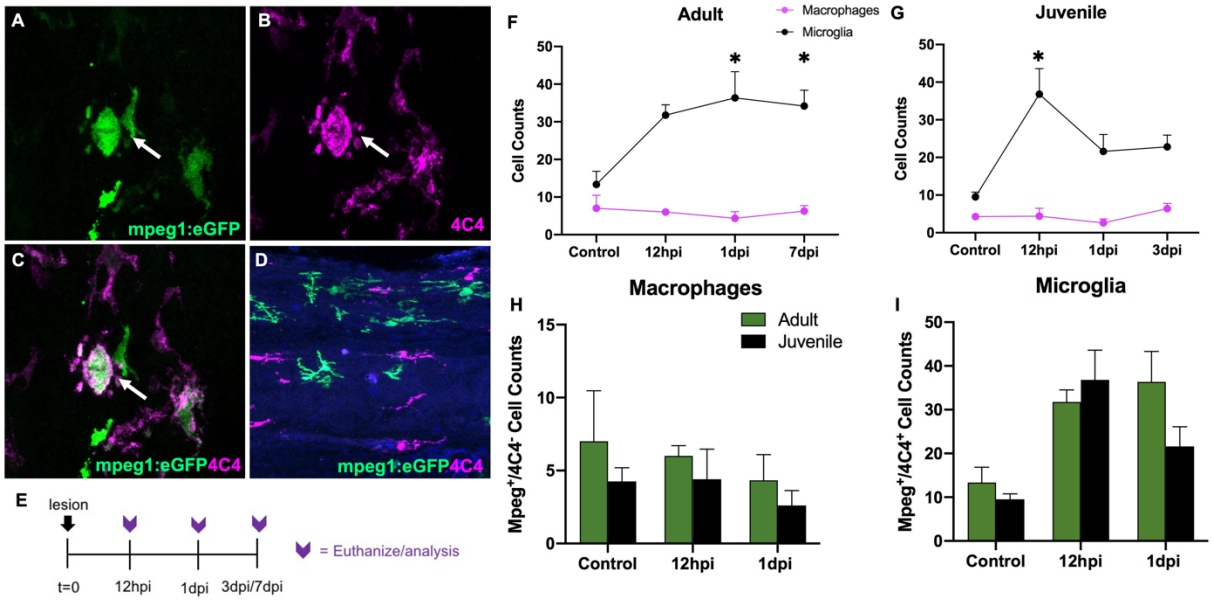

Figure 9. Microglial populations increase after SCI within adult and juvenile zebrafish. (**A-C**) A representative image of a co-labelled mpeg1^{+}/4C4^{+} microglia displayed in single channels and merged. (**D**) A sagittal spinal cord showing both mpeg1^{-}/4C4^{+} microglia and mpeg1^{+}/4C4^{-} macrophage populations. (**E**) Timeline of SCI represents lesion timepoints and tissue analysis until 3dpi in juveniles and 7dpi in adults. (**F**) Microglia showed a significant increase at 1dpi and 7dpi compared to control adult levels, while no difference in macrophages was seen. (**G**) Similarly, there was no significance among the population of macrophages in juveniles. The juvenile microglial population displayed a significant increase at 12hpi compared to control levels, but no change in the macrophage population. (**H-I**) Comparing timepoints in adult and juvenile zebrafish in both cell populations displayed no significant difference between developmental stages. One-way ANOVA with Tukey's multiple comparisons test (**F-G**); Unpaired t-tests (**H-I**); *$p < 0.05$; n=3-5 animals for each timepoint; errors bars indicate SEM. Images taken at 40X (**A-C**) and at 20X (**D**); all images are dorsal up and in a sagittal orientation.

After observing a significant response in only the microglial populations of adult and juvenile zebrafish, I was interested in whether the rostral and caudal response occurred differently which may indicate a difference in infiltration of microglia. To this end, I separately compared the total number of adult and juvenile mpeg1^{+}/4C4^{+} and mpeg1^{-}/4C4^{+} cells per timepoint within rostral and caudal zones of analysis. I first performed a one-way ANOVA to separately analyze changes in rostral and caudal microglial populations post-SCI in adult and juvenile zebrafish. Here, a significant group effect was observed in the rostral sections of adult spinal cord tissue ($p = 0.0263$) and both rostral and caudal sections among juvenile zebrafish (Rostral: $p = 0.0229$, Caudal: $p = 0.0183$, **Fig. 10A-B**). Tukey's post-hoc multiple comparisons test confirmed a significant increase in the rostral number of microglia of adults at 1dpi ($p = 0.0222$) as compared to control. Among juvenile zebrafish, when comparing timepoints to the control population, a significant increase was seen at 12hpi in both rostral ($p = 0.0181$) and caudal ($p = 0.0148$) sections. Similarly, to the total macrophage population, rostral and caudal sections did not demonstrate a significant difference between the two, and across multiple timepoints remained consistent in cell counts (**Fig. S5A-B**). These results indicate that the microglial population in juveniles appears to peak sooner than adults, similar to the proliferative data in **Figures 5-6**.

Rather than only separately analyze the rostral and caudal zones, I further compared individual timepoints between rostral and caudal tissue by using unpaired t-tests that resulted in no significant difference ($p > 0.05$, **Fig. 10A-B**). These results indicated that only differences among timepoints compared to control are observed within rostral and caudal zones and the microglial populations on either side of the injury site are activated at a similar level. In representative images of rostral and caudal uninjured control tissue, an example of a microglia, co-labelled with mpeg1 and 4C4

can be seen (**Fig. 10C-D, white arrow**). Comparing these images to an example of macrophages and microglia at 1dpi, there is a clear increase in the number of macrophages and microglia as observed by the mpeg1^{+}/4C4^{-} and mpeg1^{-}/4C4^{+} populations (**Fig. 10E-F**). This corresponds to the increase in microglia seen in both adult and juvenile zebrafish. Collectively, these results suggest that among adult and juvenile zebrafish only the total population of microglia around the injury site show an increase following SCI.

Figure 10

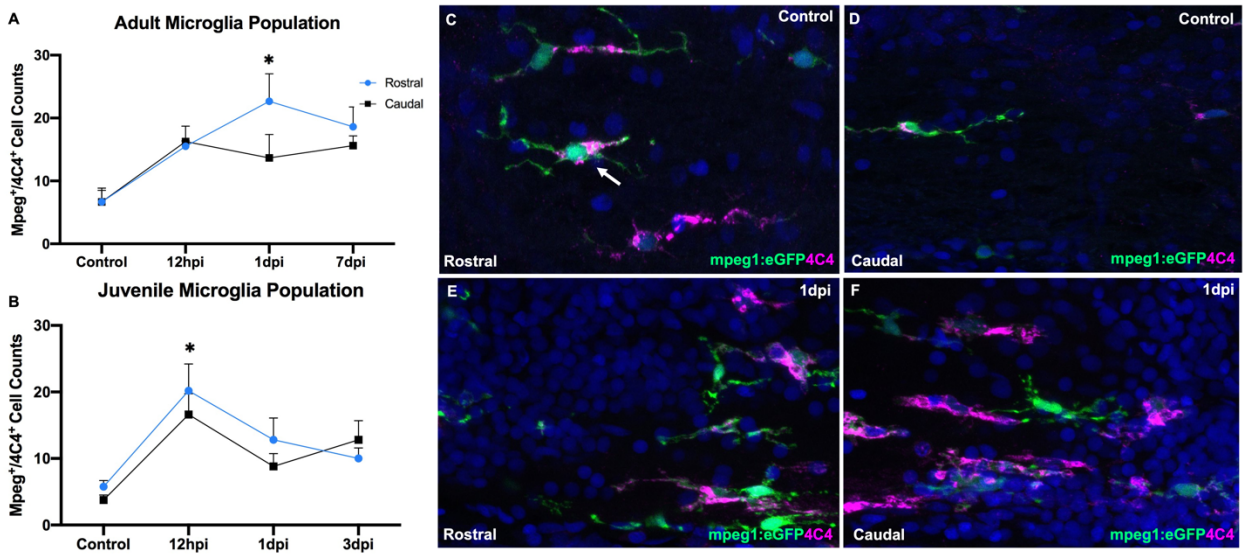

Figure 10. Rostral and caudal zones display a significant difference in the microglial population to control. (**A**) Microglial populations among adults show a significant increase from control levels at 1dpi in the rostral zone, but not in the caudal zone. (**B**) In both the rostral and caudal zones of the juvenile spinal cord, a significant difference is seen at 12hpi from control. (**C-D**) Representative images of uninjured control spinal cords in adult and juvenile zebrafish. A co-labelled microglial cell is highlighted by a white arrow in **C**. (**E-F**) An example of an injured spinal cord at 1dpi displays populations of mpeg1^{+}/4C4^{-} and mpeg1^{-}/4C4^{+} cells in both the rostral and caudal zones. Unpaired t-test; *$p < 0.05$; n=3-5 animals for each timepoint; errors bars indicate SEM. All images taken at 40X in a sagittal orientation; dorsal is up.

4.6 A Pro-Inflammatory Response Appears to be Involved in Adult and Juvenile Zebrafish SCI

The inflammatory response following SCI in juveniles has not been documented and few adult zebrafish studies have focused on inflammatory cytokine expression post-SCI. Therefore, to gain a better understanding of the temporal dynamics of cytokine release after SCI, the relative mRNA expression of pro-inflammatory cytokines IL-1β and IL-8, and anti-inflammatory cytokines TGF-β1α and TGF-β3 were examined using RT-qPCR. In these experiments, each cytokine transcript level was examined across five timepoints and the mean Ct values represented were used to compare adult and juvenile trends (Livak & Schmittgen, 2001). The uninjured control levels analyzed were all normalized to 1 as indicated on each graph. The pro-inflammatory cytokine IL-1β in adult zebrafish appeared to be highly expressed at 4hpi and 12hpi before decreasing towards control levels (**Fig. 11A**). In comparison, juvenile zebrafish revealed a greater, and sustained, increase from 12hpi to 1dpi, before decreasing to control levels at 3dpi (**Fig. 11A**). This indicates that juveniles seem to sustain mRNA expression of IL-1β longer and at greater levels as compared to adults (**Fig. 11A**). Examination of the pro-inflammatory cytokine IL-8 transcript level further showed adult mRNA expression increased at 12hpi, whereas juvenile IL-8 mRNA expression had the greatest increase at 1dpi (**Fig. 11B**). Additionally, in both adults and juveniles, IL-8 had higher mRNA expression as compared to IL-1β. These pro-inflammatory trends align closely with previous results in my study that display an increase in peak proliferation levels at 3dpi in juveniles and 7dpi in adults, when mRNA expression is lowest or nearing control levels.

Compared to the similar pattern observed post-SCI in pro-inflammatory cytokine expression, the anti-inflammatory cytokine TGF-β1a showed an opposing trend between adult and juvenile

zebrafish. Among adult timepoints, mRNA expression is upregulated from 4hpi to 12hpi, before beginning to drop at 1dpi until reaching control levels at 3dpi (**Fig. 11C**). Juvenile expression showed the opposite trend. The mRNA expression first dropped below control levels at 4hpi, and then increased and stabilized over 12hpi to 3dpi, before decreasing (**Fig. 11C**). Comparing the TGF-β3 mRNA expression levels, the trends between adults and juveniles appeared more consistent. Both trends begin with low expression below control levels at 4hpi before increasing and stabilizing, except for a reduction at 3dpi in adults and 1dpi in juveniles (**Fig. 11D**). While the trends follow a similar pattern, adult expression remains below control levels across the period of analysis. Importantly, cytokine expression levels driven by pro-inflammatory cytokines had levels greatly exceeding the anti-inflammatory cytokines. Statistical analyses on all RT-qPCR results were not performed on these data sets since only two replicates were run. The small deviations from control levels of both anti-inflammatory cytokines studied here in adult and juvenile zebrafish implies they may play a minor role in shaping the injured microenvironment following SCI and regulating ependymoglial activity.

Figure 11

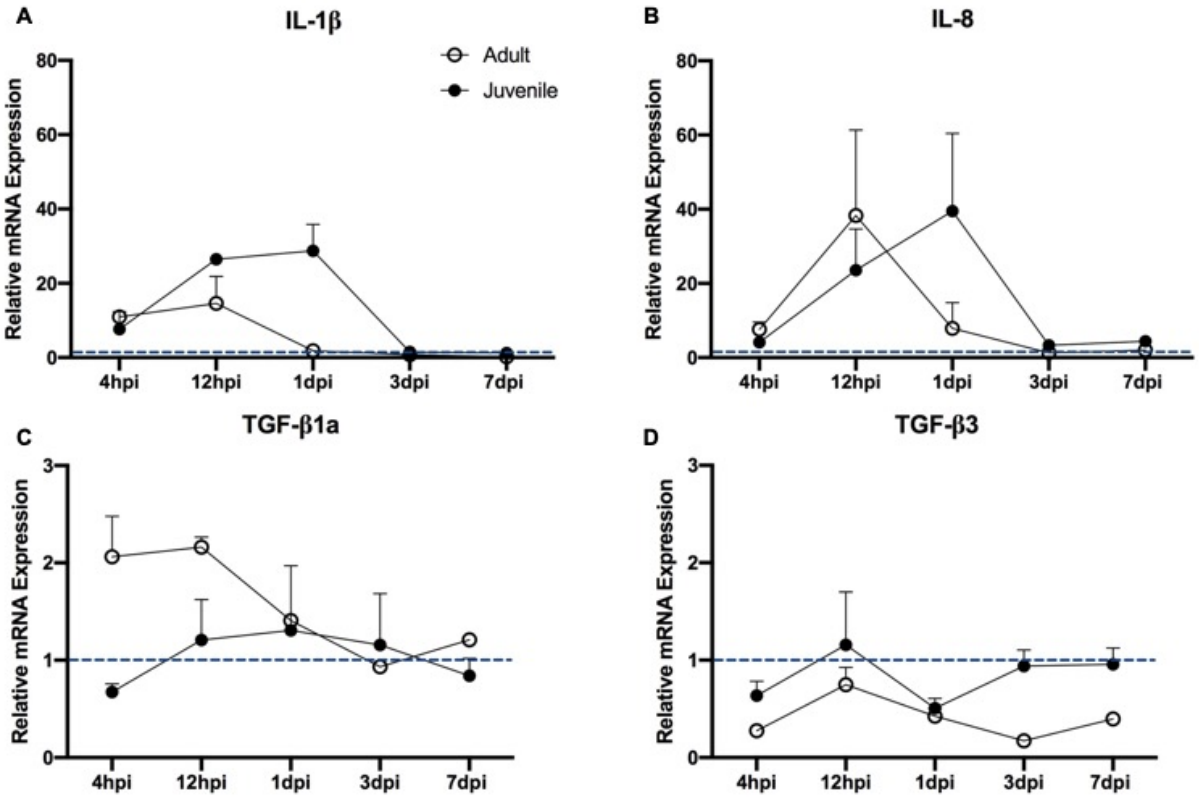

Figure 11. Pro-inflammatory response in adults and juveniles appears to be involved early after injury. (**A-B**) Expression of the mRNA levels of pro-inflammatory cytokines IL-1β and IL-8 in adults and juveniles is increased at earlier timepoints before dropping to near control levels. (**C**) Anti-inflammatory cytokine TGF-β1a is increased earlier in adults, with a steep drop below control levels, but in juveniles appears to peak at 1dpi. (**D**) Expression of anti-inflammatory cytokine TGF-β3 generally remains below control levels in both adults and juveniles. All mRNA levels are compared to control which is indicated by the blue dashed line at 1. No statistical analyses were run as only 2 replicates were completed; error bars indicate SEM of 2 replicates.

4.7 Functional Swimming is Restored to Control Levels in Adult and Juvenile Zebrafish

Functional recovery post-SCI has been shown to occur at 6 weeks in adult zebrafish (Becker & Becker, 2006), but this has not been previously studied in juveniles nor compared to the timeline of adult recovery (Becker & Becker, 2006). To examine this, I tracked the behaviour of adult and juvenile zebrafish every 2-3 days beginning on the day of SCI, until 28dpi (week 4; **Fig. 12A**). Full recovery post-SCI is considered to have been achieved when swimming behaviour is no longer significantly different from control levels, indicating that injured zebrafish travel the same distance as uninjured control zebrafish. Here, a two-way ANOVA was performed to study the effect of developmental age, timeline of functional swimming recovery, and the interaction effect between the above two factors. Statistical results showed a significant effect of the timepoints post-SCI ($p < 0.0001$), adult and juvenile development stages ($p = 0.0003$), and an interaction effect between timepoints post-injury and developmental stage ($p < 0.0001$). To first study the effect of time post-SCI on swimming recovery for adult and for juvenile animals, Dunnett's multiple comparisons test was used. These comparisons determined a significant decrease in total distance travelled within the first week compared to control levels in both adults (D0-D5) and juveniles (D0-D7; $p < 0.05$, **Fig. 12B**, see **Supplemental Table S6** for Dunnett's multiple comparisons test). Following the first week of injury (D9-D28), adults began to show swimming recovery as illustrated by the absence of a significant difference, similarly seen in juveniles ($p > 0.05$).

To next directly compare the rate of functional swimming recovery between adult and juvenile zebrafish (interaction effect) to determine if juvenile zebrafish might recover earlier, Bonferroni multiple comparison tests were completed. Immediately following injury until day 18, adult and juvenile zebrafish show no significant difference in swimming ability ($p > 0.05$). At later

timepoints from day 20 until day 28 (week 4), a significant difference was detected with greater distance travelled among juvenile zebrafish ($p < 0.05$, see **Supplemental Table S7** for Bonferroni's multiple comparisons test). However, over week 4, both adult and juvenile zebrafish demonstrate consistent functional swimming recovery. These results indicate that adults and juveniles display recovery swimming after the first week of SCI, but in week 4 of recording (D20-D28) juveniles appeared to be more active than adults.

Figure 12

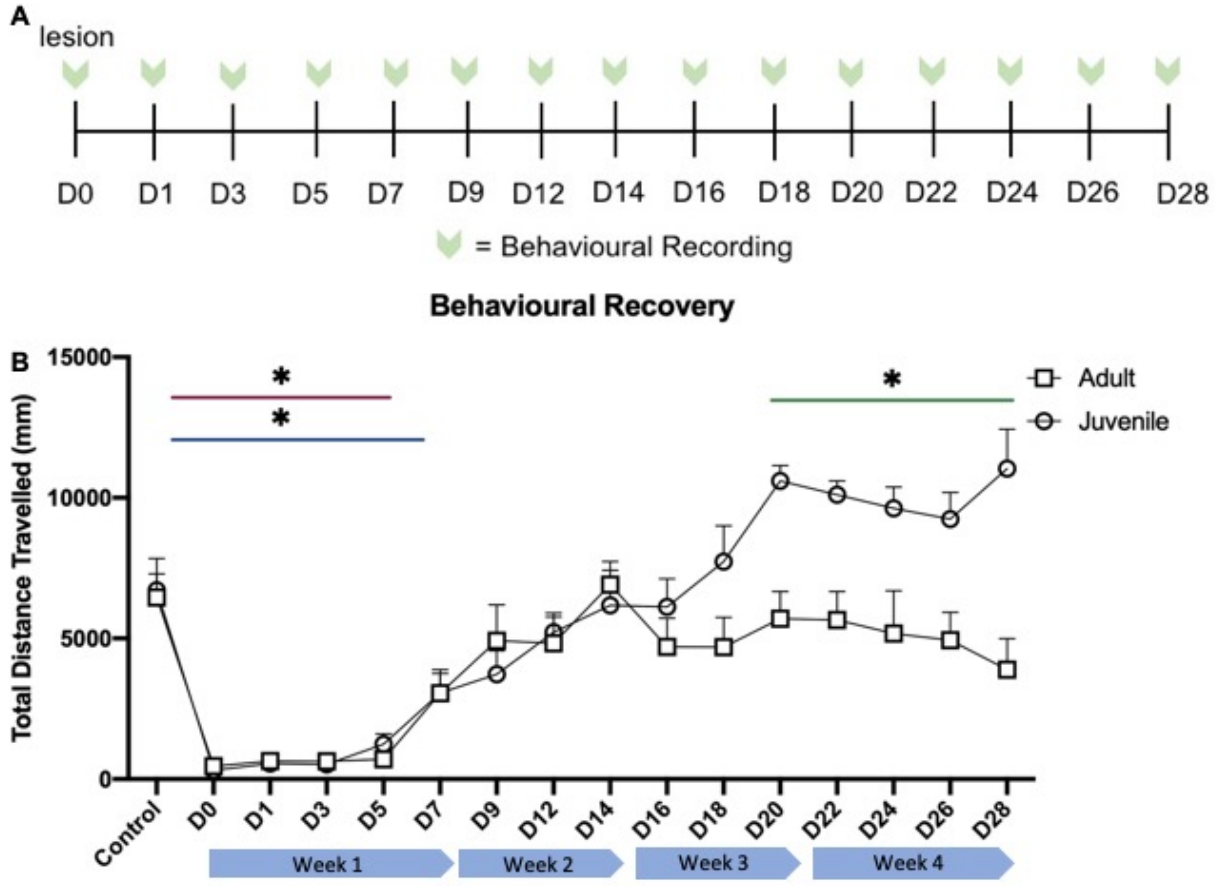

Figure 12. Behavioural tracking of functional swimming recovery in adult and juvenile zebrafish. (**A**) Timeline of behavioural recording across adult and juvenile zebrafish, beginning on day of SCI and every 2-3 day until day 28. (**B**) Comparing total distance travelled of control zebrafish to all injured timepoints indicated a significant difference within the first week in adults (D0-D5; purple line) and juveniles (D0-D7; blue line). Following this period of time, there was no significant difference seen in adult and juvenile zebrafish, indicating recovered swimming. Comparing between adults and juveniles demonstrated a significant difference at day 20 to day 28 post-SCI (green line). Two-way ANOVA with Dunnett's multiple comparisons test and Bonferroni's multiple comparisons test; *$p < 0.05$; n=4-10 animals per timepoint; error bars indicate SEM.

Chapter 5.0 Discussion

5.1 Project Summary

The overall goal of my project was to shed light on the role of macrophages and microglial following SCI and the activity of ependymoglial cells to allow for functional regeneration to occur in post-larval zebrafish. In order to study targets in mammals that cannot recover post-SCI, more knowledge on the relation between immune cells and NSCs is required to understand the permissive microenvironment seen in zebrafish. There currently exists only a small body of literature on the immune response within larval zebrafish post-SCI, but this knowledge is completely lacking in older developmental stages that would be more representative for future translational studies in mammals. In addition, older life stages, such as the juvenile zebrafish (~1-3 months), has not been utilized to study SCI but would offer a much more representative model to mammals than larvae. For this reason, in my study I employed both adult and juvenile zebrafish to test the hypothesis that for functional recovery to occur following SCI, the pro-inflammatory response must be activated ahead of ependymoglial proliferation.

In my project I have established a new model of SCI through the use of juvenile zebrafish and compared this to adults that have been more broadly studied in the context of spinal cord regeneration. My work comparing adult and juvenile models of SCI has led to five major findings (summarized in **Fig. 13**). *First*, the proliferative response of ependymoglia in adults peaked at 7dpi and in juveniles appeared to peak earlier at 3dpi. *Second*, the recruitment of microglia in adult spinal cords increased from control zebrafish until 1dpi and the levels remained elevated until 7dpi. Rather, in juveniles there was a peak in microglial increase at 12hpi that dropped afterwards, but still remained above control levels. These results indicated that microglia infiltrate well before the peak of proliferation is observed. *Third*, the mRNA expression of pro-inflammatory cytokines was

increased at 12hpi in adults and 1dpi in juveniles, similar to the infiltration of microglia that can release these cytokines. *Fourth*, the number of newborn neurons was the greatest in the SEZ of both adults and juveniles, but trends slightly differed. In adult zebrafish there was an increase at 7-day post-EdU and then again at 28 day-post EdU, but juvenile zebrafish displayed an increase at 7-day post-EdU that steadily decreased. *Finally*, both adults and juveniles showed behavioural recovery over similar timepoints post-SCI, but interestingly juvenile zebrafish revealed greater swimming activity in week 4 compared to adults.

Overall, these results support my hypothesis as a result of the decrease in inflammation that occurred prior to the peak in ependymoglial proliferation in both models of SCI. Moreover, since the trends in the macrophage and microglial response, ependymoglial activity, and functional swimming recovery are similar across adults and juveniles, these findings also lend support to establishing the juvenile zebrafish as a more rapid model to study SCI moving forward. Having a better understanding of the mechanisms regulating successful zebrafish spinal cord regeneration, and establishing a younger regenerative model, may aid in future research that targets mammalian SCI.

Figure 13

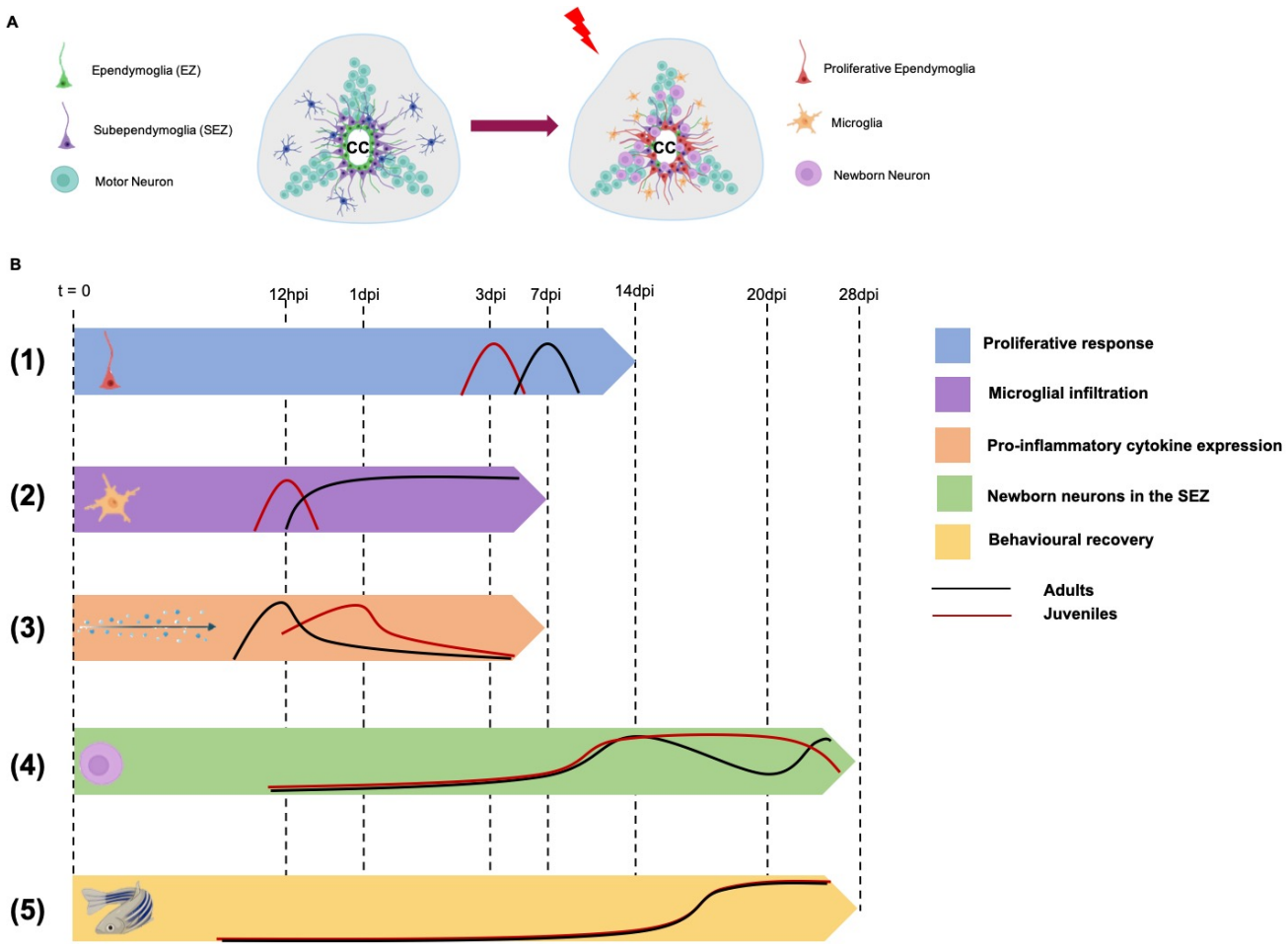
A
Ependymoglia (EZ)
Subependymoglia (SEZ)
Motor Neuron
CC
CC
Proliferative Ependymoglia
Microglia
Newborn Neuron
B
t = 0
12hpi
1dpi
3dpi
7dpi
14dpi
20dpi
28dpi
(1)
(2)
(3)
(4)
(5)
Proliferative response
Microglial infiltration
Pro-inflammatory cytokine expression
Newborn neurons in the SEZ
Behavioural recovery
Adults
Juveniles

Figure 13. Summary model comparing the major study findings between adult and juvenile zebrafish models of SCI. (**A**) Schematic of an uninjured zebrafish spinal cord in a cross-section depicts the population of ependymoglia located in the EZ and SEZ, and neurons residing in the dorsal and ventral horns. A similar schematic of an injured spinal cord (red lightning bolt) displays proliferating ependymoglia in both the EZ and SEZ, activated microglia scattered throughout the spinal cord, and newborn neurons seen both around the central canal and within the horns. (**B**) Timeline summarizing major findings and trends. (*1*) Proliferation of ependymoglial cells showed that adult zebrafish had a peak at 7dpi and juveniles at 3dpi. (*2*) Infiltration of microglia in adult spinal cords occurred at 1dpi and remained stable until 7dpi. Juvenile zebrafish exhibited an increase of microglia at 12hpi. (*3*) Pro-inflammatory cytokines are increased at 12hpi in adults and 1dpi in juveniles. (*4*) The number of newborn neurons in the SEZ occurred in adults near 14dpi before dropping and increasing again around 28dpi. Juvenile zebrafish displayed an increase at 14dpi until approximately 28dpi when the numbers began to decrease. (*5*) Adults and juveniles showed differences in recovery near 20dpi where juveniles exhibited more activity in comparison to adult swimming behaviour. In 1-5, adults are denoted by a black line and juveniles in red.

5.2 Juvenile Model of SCI Displays Similar Characteristics to Adult Model

Across existing literature, adult zebrafish used to study SCI are most commonly between the ages of 6 months to 1 year, whereas the newer juvenile model is between 1-3 months. Across these two models, the uninjured spinal cord contains a variety of cell populations that become disrupted following injury. In my project I showed examples of these populations with the use of transgenic lines and antibodies, similar to other observations of motor neurons, ependymoglia, oligodendrocytes and vasculature seen in adult and larval models of SCI (Reimer et al., 2008; Reimer et al., 2009; Goldshmit et al., 2012; Ohnmacht et al., 2016; Nelson et al., 2019). The impairment that is seen post-SCI has been characterized in my project within both models, behaviourally and anatomically. First, few studies demonstrate sham injuries to compare uninjured and injured zebrafish, but here I showed that sham and control groups displayed similar activity, indicating that physical impairment occurs when the spinal cord is severed (**Fig. 3H-P**). Second, my data shows that the same degree of behavioural impairment is observed in both adult and juvenile zebrafish following SCI, demonstrating consistency between models.

This impairment was also validated through H&E staining of sagittal spinal cords, proving a transection occurs and the tissue analyzed is adjacent to the injury site (**Fig. 4**). The spinal cords in both adults and juveniles appeared injured at 1dpi that persisted until 7dpi in contrast to larvae who display near complete functional locomotor recovery within 48hpi (Dehnisch Ellström et al., 2019). Previous studies using transected adult zebrafish also showed anatomical impairment at early and late timepoints, similar to my results (Goldshmit et al., 2012). In addition, a study that used a crush injury on adult zebrafish observed similar timepoints at 1dpi and 7dpi that resulted in similar physical impairment (Hui et al., 2010). Therefore, since both adult and juvenile zebrafish

show a comparable degree of behavioural and anatomical impairment, juveniles can be used as a more efficient and younger model to study behavioural recovery after SCI.

5.3 The Proliferative Response of Ependymoglia Correlates with a Decrease in Inflammation

To examine regeneration in adult and juvenile zebrafish I studied their proliferative and immune response following SCI. By first quantifying the amount of proliferation surrounding the central canal, I detected more EdU^+ cells within the EZ than the SEZ in both adult and juvenile zebrafish (**Fig. 5I & 6I**). Similar findings have been seen in murine models of SCI where active NSCs are directly located in the EZ rather than the SEZ (Cusimano et al., 2018). This may suggest that the NSCs sitting directly adjacent the central canal are entering the cell cycle at a faster rate possibly due to the upregulation of signaling pathways found throughout development. There exists some controversy on whether the CSF acts to increase the yield of NSCs or contains inhibitory components (Ren et al., 2018). Therefore, it is also possible that post-SCI, the CSF may be providing cues to ependymoglia, instructing them to proliferate. In addition, my results demonstrated that juvenile zebrafish had an earlier peak in proliferation as compared to adults (**Fig. 7A-B**). The peaks in proliferation were noticed at 3dpi in juveniles and 7dpi in adults. Previous work has shown similar trends in adult zebrafish following SCI where increases in proliferation were detected at 7dpi and 14dpi (Reimer et al., 2008). These increases were similar to my work, however, the researchers utilized PCNA to stain for proliferation which is expressed across all cell cycle phases except G0, accounting for their greater number of dividing cells. Studies have also shown that signaling pathways necessary for proper spinal cord development are upregulated following SCI in larval and adult zebrafish, and rats (Cardozo et al., 2017). Some of these pathways required for regenerative neurogenesis, gliogenesis, and locomotor activity include

Notch, Shh, BMP, Wnt, FGF, and RA (Cardozo et al., 2017). The distance in which signaling gradients need to be established during adult regeneration have larger distances due to the expansion of the central canal and as such have been thought to take longer in promoting proliferation (Cardozo et al., 2017). Thus, it would be predicted that using a juvenile model would provide an intermediate for this gradient to occur. Additionally, studying Wnt expression was seen as early as 1dpi following SCI in larvae until regeneration occurred around 7dpi (Briona et al., 2015). Research focusing on motor neurons in adults following SCI demonstrated that signaling pathways upregulated in the embryo are recapitulated again during motor neuron regeneration (Reimer et al., 2009). Therefore, it is not unreasonable to predict juveniles might exhibit similar early upregulation in signaling pathways following SCI.

Interestingly, in my study, pro-inflammatory cytokines, IL-1β and IL-8, decreased to control mRNA levels in advance of the increased proliferation seen in both adult and juvenile life stages (**Fig. 11A-B**). This may indicate that for regeneration to occur through proliferation of ependymoglia, the pro-inflammatory response must be attenuated. These pro-inflammatory responses show a drastic contrast to the prolonged and detrimental pro-inflammatory response seen in mammals post-SCI. Additionally, it would be expected for the levels of anti-inflammatory cytokines to be elevated, however, I observed that these cytokines remained low across multiple timepoints implying that the permissive environment seen in zebrafish following SCI may be independent of the anti-inflammatory response and more of a product of the short pro-inflammatory response. The small changes seen within TGF-β1a and TGF-β3 could have meaningful results and further clarified by examining the mRNA expression of other anti-inflammatory cytokines or by examining more timepoints, particularly early after injury.

It has also been previously shown in larval zebrafish models of SCI that macrophages/microglia express both pro- and anti-inflammatory cytokines, but mutants lacking macrophages/microglia displayed higher uncontrolled levels of pro-inflammatory cytokines (Tsarouchas et al., 2018). In this study the authors concluded that anti-inflammatory cytokines, TGF-β1a and TGF-β3, could be responsible for reducing pro-inflammatory phenotypes and as such reducing inflammation after SCI (Tsarouchas et al., 2018). Accordingly, my findings showed that TGF-β1a was above control levels in adult and juvenile zebrafish at the same timepoints as the increased activity of microglia (**Fig. 10A-B, Fig. 11C**). Outside of the spinal cord, anti-inflammatory cytokines have been the focus of research regarding liver exposure to toxins, gill homeostasis, and retinal injury (Zhang et al., 2019; Bottiglione et al., 2020; Iribarne & Hyde, 2021). Following retinal injury, TGF-β1 showed similar levels to the control samples throughout all timepoints evaluated in larval zebrafish, similar to my results shown (**Fig. 11C**) (Iribarne & Hyde, 2021). Beyond these results, there is limited research that has examined the contribution of anti-inflammatory cytokines in SCI using a zebrafish model.

While my data showed that microglia numbers increased following injury, peripherally infiltrating macrophages showed little change following SCI. Since immune cells aid in controlling inflammation, mutants lacking macrophages/microglia fail to regenerate due to the abnormally high levels of IL-1β seen in larval zebrafish (Tsarouchas et al., 2018). This was confirmed using Dexamethasone to attenuate the immune response by decreasing levels of immune cells. With reduced levels of microglia, macrophages and neutrophils, larvae exhibited a great reduction in axonal bridging. By contrast, in this same study bacterial lipopolysaccharides were used to increase

levels of immune cells resulting in greater axonal regeneration, supporting the notion that the immune cell response is necessary for regeneration (Tsarouchas et al., 2018). Unlike work in larvae following SCI, I showed stable levels of macrophages across multiple timepoints in adult and juvenile zebrafish in addition to low levels of IL-1β. In the adult zebrafish brain, IL-8 levels appeared to peak within the first 24hpi, similar to my findings in the adult spinal cord. However, to date there is little information on IL-8 following SCI. Therefore, my findings indicate that peripheral macrophage recruitment does not appear to be required, or if so to only a minor extent, in the pro-regenerative environment seen within zebrafish as compared to microglia that displayed an early peak post-SCI.

5.4 Adult and Juvenile Zebrafish Display Differences in Locomotor Activity at Late Stages of Functional Recovery but Show Similar Trends in Neuronal Differentiation after SCI

SCI results in the loss of neuronal populations and for functional recovery to occur, these lost populations need to be replenished. This had led to the study of NSC differentiation capacity and motor activity. Using markers to stain for differentiation of neurons at multiple timepoints after EdU exposure (7-day, 14-day, 28-day chase periods), adult and juvenile zebrafish showed little differences in the number of newborn neurons (**Fig. 8G-J**). Adult zebrafish displayed a greater number of newborn neurons in the SEZ within the 7-day and 28-day chase periods (**Fig. 8G**). This revealed that at the two timepoints, neurons had migrated from the EZ surrounding the central canal, towards the SEZ where more mature neurons resided (**Fig. 8G**). Juveniles revealed a greater number of newborn neurons in the SEZ beginning at the 7-day chase period until the 14-day chase period (**Fig. 8H**). The earlier, 7-day timepoint correlates with 10dpi which is closely associated with the behavioural recovery seen within the first week post SCI. While motor neurons were only

qualitatively studied, I showed evidence of the presence of new motor neuron differentiation through co-labelling of HuC/D/EdU/HB9. This indicates that a subpopulation of newborn neurons after SCI indeed differentiate into motor neurons and express relevant markers (**Fig. 8F**).

Comparing neural differentiation post-SCI to motor recovery studied until 28dpi (4-weeks), my data suggests that juvenile zebrafish recover to a greater extent. Soon after SCI, both adults and juveniles show the same amount of swimming impairment until the first week following injury (**Fig. 12B**). However, near 20dpi juvenile zebrafish exhibit significantly increased movement relative to adults as demonstrated by the total distance travelled. This trend persisted until 28dpi. When comparing between adult and juvenile co-labelled HuC/D^{+} and EdU^{+} cells, adult zebrafish had a larger population of newborn neurons in the SEZ following the 28-day chase (**Fig. 8J**). This may imply that to maintain functional recovery, there must be a continuous production of newborn neurons, possibly acting in a positive feedback loop. On the other hand, it appears that despite there being fewer newborn neurons produced in juvenile zebrafish following the 28-day chase (**Fig. 8H**), neuronal differentiation may not be necessary for overall functional recovery as seen by the greater motor activity. This greater motor activity may be a result of greater axonal regeneration that has been studied in larval zebrafish but less so in older developmental stages like adults. Since juveniles are still developing, they may be more primed to respond to SCI by bridging the gap of a transection site or they have a more permissive environment as compared to the adult model that has reached maturity and is no longer developing.

5.5 Limitations and Future Directions

My study has contributed many new findings in the new juvenile model of SCI and the older adult model. Despite this, there are still limitations to be considered. Below, I will discuss some of these limitations including the lack of information on proliferating subpopulations around the central canal post-SCI, how macrophages and microglia were analyzed, the RNA extractions and RT-qPCR runs, and lack of information on motor neuron generation following SCI.

5.5.1 Proliferation of Ependymoglial Cells

In analyzing ependymoglial proliferation post-SCI in adult and juvenile zebrafish, one shortcoming of my study was that EdU labeling alone did not permit identification of subpopulations around the central canal or cell lineage relationships. In future experiments it would be valuable to co-label the EdU^+ cells with NSC or glial markers in order to distinguish these different proliferating cell populations and gain further insight into lineage relationships. For example, Foxj1a could be used to distinguish cells in the EZ and SEZ since it has been shown to mark all cells maintaining contact with the central canal in the EZ of the zebrafish model (Ribeiro et al., 2017). Additionally, this marker has been shown to be expressed in new ependymoglia that are formed in response to zebrafish SCI (Ribeiro et al., 2017). To further determine progenitors from parent NSCs, a marker such as tbr2 or nestin could be used since ependymoglial cells that express high levels of nestin are characteristic of progenitor features and tbr2 has been shown to mark intermediate progenitors (Goldshmit et al., 2012; Hall & Tropepe et al., 2018). Parent NSCs could further be revealed using the stem cell marker, Sox2 which I showed **Figure 2**, but further quantification is needed (Johnson et al., 2016). More advanced techniques such as, Zebrabrow, or Zebrafish Brainbow, is a technique that relies on Cre-*loxP* recombination to manipulate gene

expression and is used to create combinations of different fluorescent colours in adjacent cells that are then inherited by daughter cells (Pan et al., 2013). This technique could allow for lineage tracing of the ependymoglia surrounding the central canal to obtain direct evidence of the trajectory from the parent NSC to the daughter progenitor cells that differentiate into newborn neurons post-SCI.

In addition, different markers or transgenic lines for signaling pathways could be used to determine if pathways arise earlier in juveniles and if the upregulation is closely associated with a peak in proliferation of adults and juveniles. A few used in previous work include Tg(shha:gfp) to label Shh activity and Tg(7xTCFXla.siam:mCherry) to monitor Wnt/β-catenin (Reimer et al., 2009; Briona et al., 2015; Strand et al., 2016). In our lab we have the BMP4 antibody to study the role of BMP signaling, βcat to mark for Wnt/βcat activity and the transgenic line Tg(Her4.1:mCherry) that labels for Notch signaling. Combining NSC and progenitor markers with these signaling pathway markers/transgenic lines could provide more resolution on the role of signaling pathways in spinal cord regeneration.

5.5.2 Analysis of Macrophages and Microglia

To study the infiltration of macrophages and microglia, I took advantage of the Tg(mpeg1:eGFP) line that marks for all infiltrating macrophages and resident microglia (Ellet et al., 2011). To further distinguish between these two immune populations, the 4C4 antibody was used such that $mpeg^{+}4C4^{+}$ cells were classified as microglia. From staining across multiple timepoints in both adult and juvenile zebrafish tissue, I expected to clearly see $mpeg^{+}/4C4^{-}$ (macrophages) and $mpeg^{+}/4C4^{+}$ (microglia) cells. While this expectation proved to be true in most cases, I also saw

many cells that were mpeg^{-}/4C4^{+}. Previous research employing the same hybridoma derived 4C4 antibody did not state whether they observed similar cell populations (Ma et al., 2014; Tsarouchas et al., 2018). This was curious as prior to commencing staining experiments I ran controls to ensure that the 4C4 staining seen was not due to the secondary antibody or the serum used to culture 4C4 from the original hybridoma cell population (**Fig. S1**). Given both results showed no evidence of 4C4 staining, this provided confidence in utilizing this marker to specifically distinguish local microglia from peripheral macrophages. Therefore, during my analysis it was considered that these cells were also microglia even though they were not co-labelling with the transgenic macrophage line. It is possible that this assumption may have led to some degree of inaccuracy in cell counts of these cells.

Related to my labeling analysis of microglial and macrophage populations, another observation I found was that control tissue showed the presence of a small number of macrophages. Since macrophages infiltrate from the periphery and into the spinal cord after injury, it was unexpected that I found macrophages in the uninjured control spinal cords across adults and juveniles. While this result was not anticipated, previous research has shown macrophage populations in an uninjured adult brain (Kanagaraj et al., 2020). Beyond this, few researchers have shown control results when staining for macrophages and microglia in a similar fashion. Despite the unexpected presence of macrophages in control tissue, these cells were still counted as normal, but this could have led to inaccurate statistical comparisons when analyzing injury timepoints to control cell counts.

In my current study, I analyzed cell counts 120 μm on either side of the injury site, however, this method may limit cell counts due to the infiltration of immune cells towards the site of injury. Future studies on immune cells could have a more focused analysis by examining a larger area on either side of the injury site, rather than the tissue directly adjacent as this will allow for a better understanding of the migration pattern. Cell counting individual macrophages and microglial cells was also difficult at times due to their irregular morphology, including elongated cell bodies that had numerous, often times, overlapping ramified processes. Moving forward, it may be interesting to examine such morphology to determine the proportion of these cells in an activated state, that could be stained with proliferative markers, rather than a resting state. In addition, perhaps a better approach for analysis would be calculating the percent coverage of macrophages and microglia within a specific surface area for more accurate results.

5.5.3 Cytokine Response

To study the response of pro- and anti-inflammatory cytokines following injury in adult and juvenile animals, sufficient spinal cord tissue had to be dissected to obtain enough extracted RNA for analysis. In these experiments, I dissected spinal cords from n=3 adults and n=4 juveniles. However, when performing dissections, 1 cm length of spinal cord for adults, and 0.5 cm length of spinal cord for juveniles on either side of the injury site was removed. Expression levels may have been affected by using tissue more distal from the injury where changes in cytokine expression would be expected to show little change. Specifically, the mRNA levels may have been diluted because of the small portion of injured tissue adjacent the injury site that was combined with a longer segment of uninjured spinal cord. However, in previous research performing RT-qPCR experiments, there was variation in how much tissue researchers extracted, and the number

of zebrafish used. In some studies, researchers used n=50-60 adult zebrafish taking 1 mm rostral and caudal from the injury site and others used 4 adult zebrafish taking only 4 mm caudal to the injury site (Lin et al., 2012; Hui et al., 2014). If a similar approach was used here to extract out only tissue adjacent to the injury site, a larger number of zebrafish would have been needed that were not available at the time of dissections. In addition, dissecting more zebrafish would have taken longer to perform, in which case the RNA would have begun to degrade. Here, my results only represent the relative mRNA expression averaged over two RT-qPCR runs, as the third run displaying Ct levels that considerably varied. Moving forward more replicates are required across cytokines of interest to perform statistical analyses. Furthermore, by adding in later timepoints, cytokine results could be more accurately compared with previous experiments.

5.5.4 Regenerative Neurogenesis & Behavioural Recovery

In studying regenerative neurogenesis post-SCI, I used the pan-neuronal marker HuC/D and EdU to mark for newly generated neurons. However, these markers do not answer the question of what types of neurons are being generated. In future experiments I would utilize the HB9 antibody or transgenic line Tg(hb9:eGFP) that marks for motor neurons to determine the process of motor neuron differentiation in relation to motor activity. These results would likely be better compared to the behavioural recovery data obtained in my study. Likewise, using BrdU instead of EdU to stain dividing cells in the Tg(hb9:eGFP) line may conserve the endogenous fluorescence, that often times is quenched in our transgenic lines, and specifically stain newly generated motor neurons.

Finally, while the behavioural data showed for the most part displays similar trends between adult and juvenile zebrafish, several timepoints in the behavioural recovery data had variation in sample

sizes. For instance, early recovery timepoints (D1-D16) had around n=10 zebrafish in both adults and juveniles, but the later timepoints (D18-D28) were limited to only n=4 juvenile zebrafish and n=6 adult zebrafish. Thus, it would be optimal in the future to fill in sample sizes to have a consistent set of n=10 for all timepoints measured to ensure the accuracy of trends in functional recovery.

5.6 Conclusion

My present findings have importantly established a new juvenile model of SCI. Using this model, along with the traditional adult zebrafish model of SCI, my data contributes novel information regarding the relationship between the temporospatial dynamics of macrophages and microglia with phases of neuroregeneration. This greatly increases our understanding of how resident microglia and central canal ependymoglial cells interact over the timeline of functional spinal cord regeneration beyond post-larval stages. My work shows that proliferation of ependymoglial cells in juvenile zebrafish is increased earlier than that in adults, and there appears to be an abundance of microglia in the adult and juvenile injured spinal cord. This new juvenile model of SCI will now provide an earlier and more efficient model to study SCI due to the similar responses and trends to adult zebrafish. Additionally, the pro-inflammatory response appeared to be decreased prior to proliferation, indicating that this response is critical for a permissive environment in order for regeneration to occur. This directly contrasts the prolonged pro-inflammatory response seen in mammalian models of SCI who lack the capacity for functional recovery. Understanding how inflammation regulates the process of successful neuroregeneration in the zebrafish spinal cord will provide much needed insight into the relationship between immune cells and NSCs to improve therapeutic strategies to treat mammalian SCI.

Chapter 6.0 References

Ahuja, C.S., Mothe, A., Khazaei, M., Badhiwala, J.H., Gilbert, E.A., Kooy, D., Morshead, C.M., Tator, C., Fehlings, M.G., 2020. The leading edge: Emerging neuroprotective and neuroregenerative cell-based therapies for spinal cord injury. STEM CELLS Transl Med 9, 1509–1530. https://doi.org/10.1002/sctm.19-0135

Ahuja, C.S., Wilson, J.R., Nori, S., Kotter, M.R.N., Druschel, C., Curt, A., Fehlings, M.G., 2017. Traumatic spinal cord injury. Nat Rev Dis Primers 3, 17018. https://doi.org/10.1038/nrdp.2017.18

Alizadeh, A., Dyck, S.M., Karimi-Abdolrezaee, S., 2019. Traumatic Spinal Cord Injury: An Overview of Pathophysiology, Models and Acute Injury Mechanisms. Front Neurol 10, 282. https://doi.org/10.3389/fneur.2019.00282

All, A.H., Gharibani, P., Gupta, S., Bazley, F.A., Pashai, N., Chou, B.-K., Shah, S., Resar, L.M., Cheng, L., Gearhart, J.D., Kerr, C.L., 2015. Early Intervention for Spinal Cord Injury with Human Induced Pluripotent Stem Cells Oligodendrocyte Progenitors. PLoS ONE 10, e0116933. https://doi.org/10.1371/journal.pone.0116933

Al-Sammarraie, N., Ray, S.K., 2020. Bone morphogenic protein signaling in spinal cord injury. NN 2020. https://doi.org/10.20517/2347-8659.2020.34

Amarante-Mendes, G.P., Adjemian, S., Branco, L.M., Zanetti, L.C., Weinlich, R., Bortoluci, K.R., 2018. Pattern Recognition Receptors and the Host Cell Death Molecular Machinery. Front. Immunol. 9, 2379. https://doi.org/10.3389/fimmu.2018.02379

Ankeny, D.P., McTigue, D.M., Jakeman, L.B., 2004. Bone marrow transplants provide tissue protection and directional guidance for axons after contusive spinal cord injury in rats. Exp Neurol 190, 17–31. https://doi.org/10.1016/j.expneurol.2004.05.045

Arkhipova, V., Wendik, B., Devos, N., Ek, O., Peers, B., Meyer, D., 2012. Characterization and regulation of the hb9/mnx1 beta-cell progenitor specific enhancer in zebrafish. Developmental Biology 365, 290–302. https://doi.org/10.1016/j.ydbio.2012.03.001

Assinck, P., Duncan, G.J., Hilton, B.J., Plemel, J.R., Tetzlaff, W., 2017. Cell transplantation therapy for spinal cord injury. Nat Neurosci 20, 637–647. https://doi.org/10.1038/nn.4541

Babin, P.J., Goizet, C., Raldúa, D., 2014. Zebrafish models of human motor neuron diseases: Advantages and limitations. Progress in Neurobiology 118, 36–58. https://doi.org/10.1016/j.pneurobio.2014.03.001

Barnabé-Heider, F., Göritz, C., Sabelström, H., Takebayashi, H., Pfrieger, F.W., Meletis, K., Frisén, J., 2010. Origin of new glial cells in intact and injured adult spinal cord. Cell Stem Cell 7, 470–482. https://doi.org/10.1016/j.stem.2010.07.014

Becker, C.G., Becker, T., 2006. Model Organisms in Spinal Cord Regeneration, 1st ed. Wiley. https://doi.org/10.1002/9783527610365

Becker, C.G., Becker, T., 2008. Adult zebrafish as a model for successful central nervous system regeneration. Restor Neurol Neurosci 26, 71–80.

Becker, T., Wullimann, M.F., Becker, C.G., Bernhardt, R.R., Schachner, M., 1997. Axonal regrowth after spinal cord transection in adult zebrafish. J Comp Neurol 377, 577–595. https://doi.org/10.1002/(sici)1096-9861(19970127)377:4<577::aid-cne8>3.0.co;2-#

Becker, T., Becker, C.G., 2001. Regenerating descending axons preferentially reroute to the gray matter in the presence of a general macrophage/microglial reaction caudal to a spinal transection in adult zebrafish. J. Comp. Neurol. 433, 131–147. https://doi.org/10.1002/cne.1131

Bernardos, R.L., Raymond, P.A., 2006. GFAP transgenic zebrafish. Gene Expression Patterns 6, 1007–1013. https://doi.org/10.1016/j.modgep.2006.04.006

Björnfors, E.R., El Manira, A., 2016. Functional diversity of excitatory commissural interneurons in adult zebrafish. eLife 5, e18579. https://doi.org/10.7554/eLife.18579

Boato, F., Rosenberger, K., Nelissen, S., Geboes, L., Peters, E.M., Nitsch, R., Hendrix, S., 2013. Absence of IL-1β positively affects neurological outcome, lesion development and axonal plasticity after spinal cord injury. J Neuroinflammation 10, 792. https://doi.org/10.1186/1742-2094-10-6

Bottiglione, F., Dee, C.T., Lea, R., Zeef, L.A.H., Badrock, A.P., Wane, M., Bugeon, L., Dallman, M.J., Allen, J.E., Hurlstone, A.F.L., 2020. Zebrafish IL-4–like Cytokines and IL-10 Suppress Inflammation but Only IL-10 Is Essential for Gill Homeostasis. J.I. 205, 994–1008. https://doi.org/10.4049/jimmunol.2000372

Bradbury, E.J., Burnside, E.R., 2019. Moving beyond the glial scar for spinal cord repair. Nat Commun 10, 3879. https://doi.org/10.1038/s41467-019-11707-7

Briona, L.K., Dorsky, R.I., 2014a. Spinal cord transection in the larval zebrafish. J Vis Exp. https://doi.org/10.3791/51479

Briona, L.K., Dorsky, R.I., 2014b. Radial glial progenitors repair the zebrafish spinal cord following transection. Exp Neurol 256, 81–92. https://doi.org/10.1016/j.expneurol.2014.03.017

Briona, L.K., Poulain, F.E., Mosimann, C., Dorsky, R.I., 2015. Wnt/ß-catenin signaling is required for radial glial neurogenesis following spinal cord injury. Dev Biol 403, 15–21. https://doi.org/10.1016/j.ydbio.2015.03.025

Brown, W., Liu, J., Tsang, M., Deiters, A., 2018. Cell-Lineage Tracing in Zebrafish Embryos with an Expanded Genetic Code. Chembiochem 19, 1244–1249. https://doi.org/10.1002/cbic.201800040

Bruni, J.E., 1998. Ependymal development, proliferation, and functions: a review. Microsc Res Tech 41, 2–13. https://doi.org/10.1002/(SICI)1097-0029(19980401)41:1<2::AID-JEMT2>3.0.CO;2-Z

Buss, A., Pech, K., Kakulas, B.A., Martin, D., Schoenen, J., Noth, J., Brook, G.A., 2008. TGF-β1 and TGF-β2 expression after traumatic human spinal cord injury. Spinal Cord 46, 364–371. https://doi.org/10.1038/sj.sc.3102148

Cardozo, Marcos Julian, Karolina S. Mysiak, Thomas Becker, and Catherina G. Becker. Reduce, Reuse, Recycle – Developmental Signals in Spinal Cord Regeneration. Developmental Biology 432, 53–62. https://doi.org/10.1016/j.ydbio.2017.05.011.

Carmeliet, P., 2003. Blood vessels and nerves: common signals, pathways and diseases. Nat Rev Genet 4, 710–720. https://doi.org/10.1038/nrg1158

Chen, J., Poskanzer, K.E., Freeman, M.R., Monk, K.R., 2020. Live-imaging of astrocyte morphogenesis and function in zebrafish neural circuits. Nat Neurosci 23, 1297–1306. https://doi.org/10.1038/s41593-020-0703-x

Chen, L., Deng, H., Cui, H., Fang, J., Zuo, Z., Deng, J., Li, Y., Wang, X., Zhao, L., 2018. Inflammatory responses and inflammation-associated diseases in organs. Oncotarget 9, 7204–7218. https://doi.org/10.18632/oncotarget.23208

Chen, Y., He, Y., DeVivo, M.J., 2016. Changing Demographics and Injury Profile of New Traumatic Spinal Cord Injuries in the United States, 1972-2014. Arch Phys Med Rehabil 97, 1610–1619. https://doi.org/10.1016/j.apmr.2016.03.017

Cheriyan, T., Ryan, D.J., Weinreb, J.H., Cheriyan, J., Paul, J.C., Lafage, V., Kirsch, T., Errico, T.J., 2014. Spinal cord injury models: a review. Spinal Cord 52, 588–595. https://doi.org/10.1038/sc.2014.91

Cho, T.A., 2015. Spinal Cord Functional Anatomy: CONTINUUM: Lifelong Learning in Neurology 21, 13–35. https://doi.org/10.1212/01.CON.0000461082.25876.4a

Cigliola, V., Becker, C.J., Poss, K.D., 2020. Building bridges, not walls: spinal cord regeneration in zebrafish. Disease Models & Mechanisms 13, dmm044131. https://doi.org/10.1242/dmm.044131

Clark, E.M., Nonarath, H.J.T., Bostrom, J.R., Link, B.A., 2020. Establishment and validation of an endoplasmic reticulum stress reporter to monitor zebrafish ATF6 activity in development and disease. Dis Model Mech 13, dmm041426. https://doi.org/10.1242/dmm.041426

Cooney, D.S., Wimmers, E.G., Ibrahim, Z., Grahammer, J., Christensen, J.M., Brat, G.A., Wu, L.W., Sarhane, K.A., Lopez, J., Wallner, C., Furtmüller, G.J., Yuan, N., Pang, J., Sarkar, K., Lee, W.P.A., Brandacher, G., 2016. Mesenchymal Stem Cells Enhance Nerve Regeneration in a Rat Sciatic Nerve Repair and Hindlimb Transplant Model. Sci Rep 6, 31306. https://doi.org/10.1038/srep31306

Coutts, M., Keirstead, H.S., 2008. Stem cells for the treatment of spinal cord injury. Exp Neurol 209, 368–377. https://doi.org/10.1016/j.expneurol.2007.09.002

Crane, A.M., Bhattacharya, S.K., 2013. The Use of Bromodeoxyuridine Incorporation Assays to Assess Corneal Stem Cell Proliferation, in: Wright, B., Connon, C.J. (Eds.), Corneal Regenerative Medicine: Methods and Protocols. Humana Press, Totowa, NJ, pp. 65–70. https://doi.org/10.1007/978-1-62703-432-6_4

Cusimano, M., Brambilla, E., Capotondo, A., De Feo, D., Tomasso, A., Comi, G., D'Adamo, P., Muzio, L., Martino, G., 2018. Selective killing of spinal cord neural stem cells impairs locomotor recovery in a mouse model of spinal cord injury. J Neuroinflammation 15, 58. https://doi.org/10.1186/s12974-018-1085-9

Dasgupta, K., Jeong, J., 2019. Developmental biology of the meninges. Genesis 57, e23288. https://doi.org/10.1002/dvg.23288

Dehnisch Ellström, I., Spulber, S., Hultin, S., Norlin, N., Ceccatelli, S., Hultling, C., Uhlén, P., 2019. Spinal cord injury in zebrafish induced by near-infrared femtosecond laser pulses. Journal of Neuroscience Methods 311, 259–266. https://doi.org/10.1016/j.jneumeth.2018.10.035

del Corral, R.D., Storey, K.G., 2004. Opposing FGF and retinoid pathways: a signalling switch that controls differentiation and patterning onset in the extending vertebrate body axis. Bioessays 26, 857–869. https://doi.org/10.1002/bies.20080

Dias, T.B., Yang, Y.-J., Ogai, K., Becker, T., Becker, C.G., 2012. Notch Signaling Controls Generation of Motor Neurons in the Lesioned Spinal Cord of Adult Zebrafish. Journal of Neuroscience 32, 3245–3252. https://doi.org/10.1523/JNEUROSCI.6398-11.2012

Diep, C.Q., Ma, D., Deo, R.C., Holm, T.M., Naylor, R.W., Arora, N., Wingert, R.A., Bollig, F., Djordjevic, G., Lichman, B., Zhu, H., Ikenaga, T., Ono, F., Englert, C., Cowan, C.A., Hukriede, N.A., Handin, R.I., Davidson, A.J., 2011. Identification of adult nephron progenitors capable of kidney regeneration in zebrafish. Nature 470, 95–100. https://doi.org/10.1038/nature09669

Dyck, S.M., Karimi-Abdolrezaee, S., 2015. Chondroitin sulfate proteoglycans: Key modulators in the developing and pathologic central nervous system. Exp Neurol 269, 169–187. https://doi.org/10.1016/j.expneurol.2015.04.006

Ellett, F., Pase, L., Hayman, J.W., Andrianopoulos, A., Lieschke, G.J., 2011. mpeg1 promoter transgenes direct macrophage-lineage expression in zebrafish. Blood 117, e49–e56. https://doi.org/10.1182/blood-2010-10-314120

Fang, P., Lin, J.-F., Pan, H.-C., Shen, Y.-Q., Schachner, M., 2012. A Surgery Protocol for Adult Zebrafish Spinal Cord Injury. Journal of Genetics and Genomics 39, 481–487. https://doi.org/10.1016/j.jgg.2012.07.010

Fang, W., Bonaffini, S., Zou, J., Wang, X., Zhang, C., Tsujimura, T., Kawamura, S., Wei, X., 2013. Characterization of transgenic zebrafish lines that express GFP in the retina, pineal gland, olfactory bulb, hatching gland, and optic tectum. Gene Expression Patterns 13, 150–159. https://doi.org/10.1016/j.gep.2013.02.006

Feldman, D.S., McCauley, J.F., 2018. Mesenchymal Stem Cells and Transforming Growth Factor-β3 (TGF-β3) to Enhance the Regenerative Ability of an Albumin Scaffold in Full Thickness Wound Healing. J Funct Biomater 9, E65. https://doi.org/10.3390/jfb9040065

Fernández-Arjona, M. del M., Grondona, J.M., Granados-Durán, P., Fernández-Llebrez, P., López-Ávalos, M.D., 2017. Microglia Morphological Categorization in a Rat Model of Neuroinflammation by Hierarchical Cluster and Principal Components Analysis. Front. Cell. Neurosci. 11, 235. https://doi.org/10.3389/fncel.2017.00235

Flanagan-Steet, H., Fox, M.A., Meyer, D., Sanes, J.R., 2005. Neuromuscular synapses can form in vivo by incorporation of initially aneural postsynaptic specializations. Development 132, 4471–4481. https://doi.org/10.1242/dev.02044

Gadani, S.P., Walsh, J.T., Lukens, J.R., Kipnis, J., 2015. Dealing with Danger in the CNS: The Response of the Immune System to Injury. Neuron 87, 47–62. https://doi.org/10.1016/j.neuron.2015.05.019

Gao, L., Peng, Y., Xu, W., He, P., Li, T., Lu, X., Chen, G., 2020. Progress in Stem Cell Therapy for Spinal Cord Injury. Stem Cells Int 2020, 2853650. https://doi.org/10.1155/2020/2853650

Garcia, E., Aguilar-Cevallos, J., Silva-Garcia, R., Ibarra, A., 2016. Cytokine and Growth Factor Activation In Vivo and In Vitro after Spinal Cord Injury. Mediators of Inflammation 2016, 1–21. https://doi.org/10.1155/2016/9476020

Gensel, J.C., Zhang, B., 2015. Macrophage activation and its role in repair and pathology after spinal cord injury. Brain Research 1619, 1–11. https://doi.org/10.1016/j.brainres.2014.12.045

Gepstein, L., 2002. Derivation and Potential Applications of Human Embryonic Stem Cells. Circulation Research 91, 866–876. https://doi.org/10.1161/01.RES.0000041435.95082.84

Ghosh, S., Hui, S.P., 2016. Regeneration of Zebrafish CNS: Adult Neurogenesis. Neural Plast 2016, 5815439. https://doi.org/10.1155/2016/5815439

Godwin, J.W., Pinto, A.R., Rosenthal, N.A., 2013. Macrophages are required for adult salamander limb regeneration. Proc Natl Acad Sci U S A 110, 9415–9420. https://doi.org/10.1073/pnas.1300290110

Goldshmit, Y., Sztal, T.E., Jusuf, P.R., Hall, T.E., Nguyen-Chi, M., Currie, P.D., 2012. Fgf-dependent glial cell bridges facilitate spinal cord regeneration in zebrafish. J Neurosci 32, 7477–7492. https://doi.org/10.1523/JNEUROSCI.0758-12.2012

Gordon, D., Pavlovska, G., Uney, J.B., Wraith, D.C., Scolding, N.J., 2010. Human mesenchymal stem cells infiltrate the spinal cord, reduce demyelination, and localize to white matter lesions in experimental autoimmune encephalomyelitis. J Neuropathol Exp Neurol 69, 1087–1095. https://doi.org/10.1097/NEN.0b013e3181f97392

Gottipati, M.K., D'Amato, A.R., Ziemba, A.M., Popovich, P.G., Gilbert, R.J., 2020. TGFβ3 is neuroprotective and alleviates the neurotoxic response induced by aligned poly-l-lactic acid fibers on naïve and activated primary astrocytes. Acta Biomater 117, 273–282. https://doi.org/10.1016/j.actbio.2020.09.057

Goulão, M., C. Lepore, A., 2016. iPS Cell Transplantation for Traumatic Spinal Cord Injury. CSCR 11, 321–328. https://doi.org/10.2174/1574888X10666150723150059

Grupp, L., Wolburg, H., Mack, A.F., 2010. Astroglial structures in the zebrafish brain. J. Comp. Neurol. 518, 4277–4287. https://doi.org/10.1002/cne.22481

Hachem, L.D., Mothe, A.J., Tator, C.H., 2015. Effect of BDNF and Other Potential Survival Factors in Models of *In Vitro* Oxidative Stress on Adult Spinal Cord–Derived Neural Stem/Progenitor Cells. BioResearch Open Access 4, 146–159. https://doi.org/10.1089/biores.2014.0058

Hachem, L.D., Mothe, A.J., Tator, C.H., 2020. Unlocking the paradoxical endogenous stem cell response after spinal cord injury. Stem Cells 38, 187–194. https://doi.org/10.1002/stem.3107

Haggerty, A.E., Marlow, M.M., Oudega, M., 2017. Extracellular matrix components as therapeutics for spinal cord injury. Neuroscience Letters 652, 50–55. https://doi.org/10.1016/j.neulet.2016.09.053

Hale, M.E., Ritter, D.A., Fetcho, J.R., 2001. A confocal study of spinal interneurons in living larval zebrafish: Spinal Interneurons in Zebrafish. J. Comp. Neurol. 437, 1–16. https://doi.org/10.1002/cne.1266

Hall, Z.J., Tropepe, V., 2018. Movement maintains forebrain neurogenesis via peripheral neural feedback in larval zebrafish. Elife 7, e31045. https://doi.org/10.7554/eLife.31045

Hamilton, L.K., Truong, M.K.V., Bednarczyk, M.R., Aumont, A., Fernandes, K.J.L., 2009. Cellular organization of the central canal ependymal zone, a niche of latent neural stem cells in the adult

mammalian spinal cord. Neuroscience 164, 1044–1056. https://doi.org/10.1016/j.neuroscience.2009.09.006

Hawryluk, G.W.J., Mothe, A., Wang, J., Wang, S., Tator, C., Fehlings, M.G., 2012. An in vivo characterization of trophic factor production following neural precursor cell or bone marrow stromal cell transplantation for spinal cord injury. Stem Cells Dev 21, 2222–2238. https://doi.org/10.1089/scd.2011.0596

Hellenbrand, D.J., Quinn, C.M., Piper, Z.J., Morehouse, C.N., Fixel, J.A., Hanna, A.S., 2021. Inflammation after spinal cord injury: a review of the critical timeline of signaling cues and cellular infiltration. J Neuroinflammation 18, 284. https://doi.org/10.1186/s12974-021-02337-2

Henderson, K.W., Menelaou, E., Hale, M.E., 2019. Sensory neurons in the spinal cord of zebrafish and their local connectivity. Current Opinion in Physiology 8, 136–140. https://doi.org/10.1016/j.cophys.2019.01.008

Hess, M.J., Hough, S., 2012. Impact of spinal cord injury on sexuality: broad-based clinical practice intervention and practical application. J Spinal Cord Med 35, 211–218. https://doi.org/10.1179/2045772312Y.0000000025

Hetz, C., Chevet, E., Oakes, S.A., 2015. Proteostasis control by the unfolded protein response. Nat Cell Biol 17, 829–838. https://doi.org/10.1038/ncb3184

Hines, D.J., Hines, R.M., Mulligan, S.J., Macvicar, B.A., 2009. Microglia processes block the spread of damage in the brain and require functional chloride channels. Glia 57, 1610–1618. https://doi.org/10.1002/glia.20874

Howe, K., Clark, M.D., Torroja, C.F., Torrance, J., Berthelot, C., Muffato, M., Collins, J.E., Humphray, S., McLaren, K., Matthews, L., McLaren, S., Sealy, I., Caccamo, M., Churcher, C., Scott, C., Barrett, J.C., Koch, R., Rauch, G.-J., White, S., Chow, W., Kilian, B., Quintais, L.T., Guerra-Assunção, J.A., Zhou, Y., Gu, Y., Yen, J., Vogel, J.-H., Eyre, T., Redmond, S., Banerjee, R., Chi, J., Fu, B., Langley, E., Maguire, S.F., Laird, G.K., Lloyd, D., Kenyon, E., Donaldson, S., Sehra, H., Almeida-King, J., Loveland, J., Trevanion, S., Jones, M., Quail, M., Willey, D., Hunt, A., Burton, J., Sims, S., McLay, K., Plumb, B., Davis, J., Clee, C., Oliver, K., Clark, R., Riddle, C., Elliot, D., Eliott, D., Threadgold, G., Harden, G., Ware, D., Begum, S., Mortimore, B., Mortimer, B., Kerry, G., Heath, P., Phillimore, B., Tracey, A., Corby, N., Dunn, M., Johnson, C., Wood, J., Clark, S., Pelan, S., Griffiths, G., Smith, M., Glithero, R., Howden, P., Barker, N., Lloyd, C., Stevens, C., Harley, J., Holt, K., Panagiotidis, G., Lovell, J., Beasley, H., Henderson, C., Gordon, D., Auger, K., Wright, D., Collins, J., Raisen, C., Dyer, L., Leung, K., Robertson, L., Ambridge, K., Leongamornlert, D., McGuire, S., Gilderthorp, R., Griffiths, C., Manthravadi, D., Nichol, S., Barker, G., Whitehead, S., Kay, M., Brown, J., Murnane, C., Gray, E., Humphries, M., Sycamore, N., Barker, D., Saunders, D., Wallis, J., Babbage, A., Hammond, S., Mashreghi-Mohammadi, M., Barr, L., Martin, S., Wray, P., Ellington, A., Matthews, N., Ellwood, M., Woodmansey, R., Clark, G., Cooper, J.D., Cooper, J., Tromans, A., Grafham, D., Skuce, C., Pandian, R., Andrews, R., Harrison, E., Kimberley, A., Garnett, J., Fosker, N., Hall, R., Garner, P., Kelly, D., Bird, C., Palmer, S., Gehring, I., Berger, A., Dooley, C.M., Ersan-Ürün, Z., Eser,

C., Geiger, H., Geisler, M., Karotki, L., Kirn, A., Konantz, J., Konantz, M., Oberländer, M., Rudolph-Geiger, S., Teucke, M., Lanz, C., Raddatz, G., Osoegawa, K., Zhu, B., Rapp, A., Widaa, S., Langford, C., Yang, F., Schuster, S.C., Carter, N.P., Harrow, J., Ning, Z., Herrero, J., Searle, S.M.J., Enright, A., Geisler, R., Plasterk, R.H.A., Lee, C., Westerfield, M., de Jong, P.J., Zon, L.I., Postlethwait, J.H., Nüsslein-Volhard, C., Hubbard, T.J.P., Roest Crollius, H., Rogers, J., Stemple, D.L., 2013. The zebrafish reference genome sequence and its relationship to the human genome. Nature 496, 498–503. https://doi.org/10.1038/nature12111

Huang, L., Fu, C., Xiong, F., He, C., Wei, Q., 2021. Stem Cell Therapy for Spinal Cord Injury. Cell Transplant 30, 963689721989266. https://doi.org/10.1177/0963689721989266

Huemer, K., Squirrell, J.M., Swader, R., Pelkey, K., LeBert, D.C., Huttenlocher, A., Eliceiri, K.W., 2017. Long-term Live Imaging Device for Improved Experimental Manipulation of Zebrafish Larvae. J Vis Exp. https://doi.org/10.3791/56340

Hui, S.P., Dutta, A., Ghosh, S., 2010. Cellular response after crush injury in adult zebrafish spinal cord. Dev. Dyn. 239, 2962–2979. https://doi.org/10.1002/dvdy.22438

Hui, S.P., Nag, T.C., Ghosh, S., 2015. Characterization of Proliferating Neural Progenitors after Spinal Cord Injury in Adult Zebrafish. PLoS One 10, e0143595. https://doi.org/10.1371/journal.pone.0143595

Hui, S.P., Sengupta, D., Lee, S.G.P., Sen, T., Kundu, S., Mathavan, S., Ghosh, S., 2014. Genome Wide Expression Profiling during Spinal Cord Regeneration Identifies Comprehensive Cellular Responses in Zebrafish. PLoS ONE 9, e84212. https://doi.org/10.1371/journal.pone.0084212

Huie, J.R., Baumbauer, K.M., Lee, K.H., Bresnahan, J.C., Beattie, M.S., Ferguson, A.R., Grau, J.W., 2012. Glial Tumor Necrosis Factor Alpha (TNFα) Generates Metaplastic Inhibition of Spinal Learning. PLoS ONE 7, e39751. https://doi.org/10.1371/journal.pone.0039751

Iribarne, M., Hyde, D.R., 2021. Inflammation modulates regeneration in the acute or chronically damaged zebrafish retina (preprint). Neuroscience. https://doi.org/10.1101/2021.10.06.463331

Iwai, H., Nori, S., Nishimura, S., Yasuda, A., Takano, M., Tsuji, O., Fujiyoshi, K., Toyama, Y., Okano, H., Nakamura, M., 2014. Transplantation of Neural Stem/Progenitor Cells at Different Locations in Mice with Spinal Cord Injury. Cell Transplant 23, 1451–1464. https://doi.org/10.3727/096368913X670967

Jin, X., Lin, T., Xu, Y., 2016. Stem Cell Therapy and Immunological Rejection in Animal Models. CMP 9, 284–288. https://doi.org/10.2174/1874467208666150928153511

Johnson, K., Barragan, J., Bashiruddin, S., Smith, C.J., Tyrrell, C., Parsons, M.J., Doris, R., Kucenas, S., Downes, G.B., Velez, C.M., Schneider, C., Sakai, C., Pathak, N., Anderson, K., Stein, R., Devoto, S.H., Mumm, J.S., Barresi, M.J.F., 2016. Gfap-positive radial glial cells are an essential

progenitor population for later-born neurons and glia in the zebrafish spinal cord. Glia 64, 1170–1189. https://doi.org/10.1002/glia.22990

Kabashi, E., Brustein, E., Champagne, N., Drapeau, P., 2011. Zebrafish models for the functional genomics of neurogenetic disorders. Biochim Biophys Acta 1812, 335–345. https://doi.org/10.1016/j.bbadis.2010.09.011

Kalueff, A.V., Gebhardt, M., Stewart, A.M., Cachat, J.M., Brimmer, M., Chawla, J.S., Craddock, C., Kyzar, E.J., Roth, A., Landsman, S., Gaikwad, S., Robinson, K., Baatrup, E., Tierney, K., Shamchuk, A., Norton, W., Miller, N., Nicolson, T., Braubach, O., Gilman, C.P., Pittman, J., Rosemberg, D.B., Gerlai, R., Echevarria, D., Lamb, E., Neuhauss, S.C.F., Weng, W., Bally-Cuif, L., Schneider, H., Zebrafish Neuroscience Research Consortium, 2013. Towards a comprehensive catalog of zebrafish behavior 1.0 and beyond. Zebrafish 10, 70–86. https://doi.org/10.1089/zeb.2012.0861

Kanagaraj, P., Chen, J.Y., Skaggs, K., Qadeer, Y., Conner, M., Cutler, N., Richmond, J., Kommidi, V., Poles, A., Affrunti, D., Powell, C., Goldman, D., Parent, J., 2020. Microglia Stimulate Zebrafish Brain Repair Via a Specific Inflammatory Cascade (preprint). Neuroscience. https://doi.org/10.1101/2020.10.08.330662

Karimi-Abdolrezaee, S., Schut, D., Wang, J., Fehlings, M.G., 2012. Chondroitinase and growth factors enhance activation and oligodendrocyte differentiation of endogenous neural precursor cells after spinal cord injury. PLoS One 7, e37589. https://doi.org/10.1371/journal.pone.0037589

Katoh, H., Yokota, K., Fehlings, M.G., 2019. Regeneration of Spinal Cord Connectivity Through Stem Cell Transplantation and Biomaterial Scaffolds. Front Cell Neurosci 13, 248. https://doi.org/10.3389/fncel.2019.00248

Kaur, P., Sharma, S., 2018. Recent Advances in Pathophysiology of Traumatic Brain Injury. Curr Neuropharmacol 16, 1224–1238. https://doi.org/10.2174/1570159X15666170613083606

Keatinge, M., Tsarouchas, T.M., Munir, T., Porter, N.J., Larraz, J., Gianni, D., Tsai, H.-H., Becker, C.G., Lyons, D.A., Becker, T., 2021. CRISPR gRNA phenotypic screening in zebrafish reveals pro-regenerative genes in spinal cord injury. PLoS Genet 17, e1009515. https://doi.org/10.1371/journal.pgen.1009515

Khan, Y.S., Lui, F., 2021. Neuroanatomy, Spinal Cord, in: StatPearls. StatPearls Publishing, Treasure Island (FL).

Khazaei, M., Ahuja, C.S., Fehlings, M.G., 2016. Induced Pluripotent Stem Cells for Traumatic Spinal Cord Injury. Front Cell Dev Biol 4, 152. https://doi.org/10.3389/fcell.2016.00152

Kigerl, K.A., Gensel, J.C., Ankeny, D.P., Alexander, J.K., Donnelly, D.J., Popovich, P.G., 2009. Identification of Two Distinct Macrophage Subsets with Divergent Effects Causing either Neurotoxicity or Regeneration in the Injured Mouse Spinal Cord. Journal of Neuroscience 29, 13435–13444. https://doi.org/10.1523/JNEUROSCI.3257-09.2009

Kim, E., Tae, G., 2016. Direct reprogramming and biomaterials for controlling cell fate. Biomater Res 20, 39. https://doi.org/10.1186/s40824-016-0086-y

Kojima, A., Tator, C.H., 2000. Epidermal Growth Factor and Fibroblast Growth Factor 2 Cause Proliferation of Ependymal Precursor Cells in the Adult Rat Spinal Cord In Vivo. J Neuropathol Exp Neurol 59, 687–697. https://doi.org/10.1093/jnen/59.8.687

Kong, X., Gao, J., 2017. Macrophage polarization: a key event in the secondary phase of acute spinal cord injury. J Cell Mol Med 21, 941–954. https://doi.org/10.1111/jcmm.13034

Kriegstein, A., Alvarez-Buylla, A., 2009. The glial nature of embryonic and adult neural stem cells. Annu Rev Neurosci 32, 149–184. https://doi.org/10.1146/annurev.neuro.051508.135600

Kroner, A., Rosas Almanza, J., 2019. Role of microglia in spinal cord injury. Neuroscience Letters 709, 134370. https://doi.org/10.1016/j.neulet.2019.134370

Kyritsis, N., Kizil, C., Zocher, S., Kroehne, V., Kaslin, J., Freudenreich, D., Iltzsche, A., Brand, M., 2012. Acute Inflammation Initiates the Regenerative Response in the Adult Zebrafish Brain. Science 338, 1353–1356. https://doi.org/10.1126/science.1228773

Lawson, N.D., Weinstein, B.M., 2002. In Vivo Imaging of Embryonic Vascular Development Using Transgenic Zebrafish. Developmental Biology 248, 307–318. https://doi.org/10.1006/dbio.2002.0711

Lee, B.B., Cripps, R.A., Fitzharris, M., Wing, P.C., 2014. The global map for traumatic spinal cord injury epidemiology: update 2011, global incidence rate. Spinal Cord 52, 110–116. https://doi.org/10.1038/sc.2012.158

Lee, Y.-H., Kawakami, K., HuangFu, W.-C., Liu, I.-H., 2020. Chondroitin sulfate proteoglycan 4 regulates zebrafish body axis organization via Wnt/planar cell polarity pathway. PLoS One 15, e0230943. https://doi.org/10.1371/journal.pone.0230943

Lee-Liu, D., Edwards-Faret, G., Tapia, V.S., Larraín, J., 2013. Spinal cord regeneration: lessons for mammals from non-mammalian vertebrates. Genesis 51, 529–544. https://doi.org/10.1002/dvg.22406

Leung, B., Shimeld, S.M., 2019. Evolution of vertebrate spinal cord patterning. Developmental Dynamics 248, 1028–1043. https://doi.org/10.1002/dvdy.77

Lewis, K.E., Eisen, J.S., 2003. From cells to circuits: development of the zebrafish spinal cord. Prog Neurobiol 69, 419–449. https://doi.org/10.1016/s0301-0082(03)00052-2

Li, J., Lepski, G., 2013. Cell transplantation for spinal cord injury: a systematic review. Biomed Res Int 2013, 786475. https://doi.org/10.1155/2013/786475

Liau, L.L., Looi, Q.H., Chia, W.C., Subramaniam, T., Ng, M.H., Law, J.X., 2020. Treatment of spinal cord injury with mesenchymal stem cells. Cell Biosci 10, 112. https://doi.org/10.1186/s13578-020-00475-3

Lin, J.-F., Pan, H.-C., Ma, L.-P., Shen, Y.-Q., Schachner, M., 2012. The Cell Neural Adhesion Molecule Contactin-2 (TAG-1) Is Beneficial for Functional Recovery after Spinal Cord Injury in Adult Zebrafish. PLoS ONE 7, e52376. https://doi.org/10.1371/journal.pone.0052376

Lindsey, B.W., Douek, A.M., Loosli, F., Kaslin, J., 2018a. A Whole Brain Staining, Embedding, and Clearing Pipeline for Adult Zebrafish to Visualize Cell Proliferation and Morphology in 3-Dimensions. Front. Neurosci. 11, 750. https://doi.org/10.3389/fnins.2017.00750

Lindsey, B.W., Hall, Z.J., Heuzé, A., Joly, J.-S., Tropepe, V., Kaslin, J., 2018b. The role of neuro-epithelial-like and radial-glial stem and progenitor cells in development, plasticity, and repair. Prog Neurobiol 170, 99–114. https://doi.org/10.1016/j.pneurobio.2018.06.004

Liu, C.-J., Xie, L., Cui, C., Chu, M., Zhao, H.-D., Yao, L., Li, Y.-H., Schachner, M., Shen, Y.-Q., 2016. Beneficial roles of melanoma cell adhesion molecule in spinal cord transection recovery in adult zebrafish. J. Neurochem. 139, 187–196. https://doi.org/10.1111/jnc.13707

Liu, S., Chen, Z., 2019. Employing Endogenous NSCs to Promote Recovery of Spinal Cord Injury. Stem Cells International 2019, 1–10. https://doi.org/10.1155/2019/1958631

Liu, S., Xiao, Z., Li, X., Zhao, Y., Wu, X., Han, J., Chen, B., Li, J., Fan, C., Xu, B., Xue, X., Xue, W., Yang, Y., Dai, J., 2019. Vascular endothelial growth factor activates neural stem cells through epidermal growth factor receptor signal after spinal cord injury. CNS Neurosci Ther 25, 375–385. https://doi.org/10.1111/cns.13056

Liu, Y.-C., Zou, X.-B., Chai, Y.-F., Yao, Y.-M., 2014. Macrophage Polarization in Inflammatory Diseases. Int. J. Biol. Sci. 10, 520–529. https://doi.org/10.7150/ijbs.8879

Livak, K.J., Schmittgen, T.D., 2001. Analysis of Relative Gene Expression Data Using Real-Time Quantitative PCR and the 2−ΔΔCT Method. Methods 25, 402–408. https://doi.org/10.1006/meth.2001.1262

Ma, L., Shen, Y.-Q., Khatri, H.P., Schachner, M., 2014. The Asparaginyl Endopeptidase Legumain Is Essential for Functional Recovery after Spinal Cord Injury in Adult Zebrafish. PLoS ONE 9, e95098. https://doi.org/10.1371/journal.pone.0095098

Mariano, E.D., Teixeira, M.J., Marie, S.K.N., Lepski, G., 2015. Adult stem cells in neural repair: Current options, limitations and perspectives. World J Stem Cells 7, 477–482. https://doi.org/10.4252/wjsc.v7.i2.477

Matsuyama, D., Watanabe, M., Suyama, K., Kuroiwa, M., Mochida, J., 2014. Endoplasmic reticulum stress response in the rat contusive spinal cord injury model-susceptibility in specific cell types. Spinal Cord 52, 9–16. https://doi.org/10.1038/sc.2013.118

Mautes, A.E., Weinzierl, M.R., Donovan, F., Noble, L.J., 2000. Vascular events after spinal cord injury: contribution to secondary pathogenesis. Phys Ther 80, 673–687.

McDonough, A., Martínez-Cerdeño, V., 2012. Endogenous proliferation after spinal cord injury in animal models. Stem Cells Int 2012, 387513. https://doi.org/10.1155/2012/387513

McKillop, W.M., Dragan, M., Schedl, A., Brown, A., 2013. Conditional Sox9 ablation reduces chondroitin sulfate proteoglycan levels and improves motor function following spinal cord injury. Glia 61, 164–177. https://doi.org/10.1002/glia.22424

McKinley, W.O., Seel, R.T., Hardman, J.T., 1999. Nontraumatic spinal cord injury: Incidence, epidemiology, and functional outcome. Archives of Physical Medicine and Rehabilitation 80, 619–623. https://doi.org/10.1016/S0003-9993(99)90162-4

Medvedev, S.P., Grigor'eva, E.V., Shevchenko, A.I., Malakhova, A.A., Dementyeva, E.V., Shilov, A.A., Pokushalov, E.A., Zaidman, A.M., Aleksandrova, M.A., Plotnikov, E.Y., Sukhikh, G.T., Zakian, S.M., 2011. Human induced pluripotent stem cells derived from fetal neural stem cells successfully undergo directed differentiation into cartilage. Stem Cells Dev 20, 1099–1112. https://doi.org/10.1089/scd.2010.0249

Medzhitov, R., 2008. Origin and physiological roles of inflammation. Nature 454, 428–435. https://doi.org/10.1038/nature07201

Meletis, K., Barnabé-Heider, F., Carlén, M., Evergren, E., Tomilin, N., Shupliakov, O., Frisén, J., 2008. Spinal Cord Injury Reveals Multilineage Differentiation of Ependymal Cells. PLoS Biol 6, e182. https://doi.org/10.1371/journal.pbio.0060182

Mokalled, M.H., Patra, C., Dickson, A.L., Endo, T., Stainier, D.Y.R., Poss, K.D., 2016. Injury-induced ctgfa directs glial bridging and spinal cord regeneration in zebrafish. Science 354, 630–634. https://doi.org/10.1126/science.aaf2679

Möllmert, S., Kharlamova, M.A., Hoche, T., Taubenberger, A.V., Abuhattum, S., Kuscha, V., Kurth, T., Brand, M., Guck, J., 2020. Zebrafish Spinal Cord Repair Is Accompanied by Transient Tissue Stiffening. Biophysical Journal 118, 448–463. https://doi.org/10.1016/j.bpj.2019.10.044

Morganti-Kossman, M.C., Lenzlinger, P.M., Hans, V., Stahel, P., Csuka, E., Ammann, E., Stocker, R., Trentz, O., Kossmann, T., 1997. Production of cytokines following brain injury: beneficial and deleterious for the damaged tissue. Mol Psychiatry 2, 133–136. https://doi.org/10.1038/sj.mp.4000227

Nakajima, H., Uchida, K., Guerrero, A.R., Watanabe, S., Sugita, D., Takeura, N., Yoshida, A., Long, G., Wright, K.T., Johnson, W.E.B., Baba, H., 2012. Transplantation of Mesenchymal Stem Cells

Promotes an Alternative Pathway of Macrophage Activation and Functional Recovery after Spinal Cord Injury. Journal of Neurotrauma 29, 1614–1625. https://doi.org/10.1089/neu.2011.2109

Nandoe Tewarie, R.S., Hurtado, A., Bartels, R.H., Grotenhuis, A., Oudega, M., 2009. Stem cell-based therapies for spinal cord injury. J Spinal Cord Med 32, 105–114. https://doi.org/10.1080/10790268.2009.11760761

Nelson, C.M., Lennon, V.A., Lee, H., Krug, R.G., Kamalova, A., Madigan, N.N., Clark, K.J., Windebank, A.J., Henley, J.R., 2019. Glucocorticoids Target Ependymal Glia and Inhibit Repair of the Injured Spinal Cord. Front. Cell Dev. Biol. 7, 56. https://doi.org/10.3389/fcell.2019.00056

Noonan, V.K., Fingas, M., Farry, A., Baxter, D., Singh, A., Fehlings, M.G., Dvorak, M.F., 2012. Incidence and prevalence of spinal cord injury in Canada: a national perspective. Neuroepidemiology 38, 219–226. https://doi.org/10.1159/000336014

Nussbaum, J., Minami, E., Laflamme, M.A., Virag, J.A.I., Ware, C.B., Masino, A., Muskheli, V., Pabon, L., Reinecke, H., Murry, C.E., 2007. Transplantation of undifferentiated murine embryonic stem cells in the heart: teratoma formation and immune response. FASEB J 21, 1345–1357. https://doi.org/10.1096/fj.06-6769com

Ohnmacht, J., Yang, Y., Maurer, G.W., Barreiro-Iglesias, A., Tsarouchas, T.M., Wehner, D., Sieger, D., Becker, C.G., Becker, T., 2016. Spinal motor neurons are regenerated after mechanical lesion

and genetic ablation in larval zebrafish. Development dev.129155. https://doi.org/10.1242/dev.129155

Ohri, S.S., Hetman, M., Whittemore, S.R., 2013. Restoring endoplasmic reticulum homeostasis improves functional recovery after spinal cord injury. Neurobiology of Disease 58, 29–37. https://doi.org/10.1016/j.nbd.2013.04.021

Ohri, S.S., Maddie, M.A., Zhao, Y., Qiu, M.S., Hetman, M., Whittemore, S.R., 2011. Attenuating the endoplasmic reticulum stress response improves functional recovery after spinal cord injury. Glia 59, 1489–1502. https://doi.org/10.1002/glia.21191

Orekhov, A.N., Orekhova, V.A., Nikiforov, N.G., Myasoedova, V.A., Grechko, A.V., Romanenko, E.B., Zhang, D., Chistiakov, D.A., 2019. Monocyte differentiation and macrophage polarization. VP 2019. https://doi.org/10.20517/2574-1209.2019.04

Osuka, A., Ogura, H., Ueyama, M., Shimazu, T., Lederer, J.A., 2014. Immune response to traumatic injury: harmony and discordance of immune system homeostasis. Acute Med Surg 1, 63–69. https://doi.org/10.1002/ams2.17

Oudega, M., 2012. Molecular and cellular mechanisms underlying the role of blood vessels in spinal cord injury and repair. Cell Tissue Res 349, 269–288. https://doi.org/10.1007/s00441-012-1440-6

Ousman, S.S., Kubes, P., 2012. Immune surveillance in the central nervous system. Nat Neurosci 15, 1096–1101. https://doi.org/10.1038/nn.3161

Oyinbo, C.A., 2011. Secondary injury mechanisms in traumatic spinal cord injury: a nugget of this multiply cascade. Acta Neurobiol Exp (Wars) 71, 281–299.

Pan, Y.A., Freundlich, T., Weissman, T.A., Schoppik, D., Wang, X.C., Zimmerman, S., Ciruna, B., Sanes, J.R., Lichtman, J.W., Schier, A.F., 2013. Zebrabow: multispectral cell labeling for cell tracing and lineage analysis in zebrafish. Development 140, 2835–2846. https://doi.org/10.1242/dev.094631

Paridaen, J.T.M.L., Huttner, W.B., 2014. Neurogenesis during development of the vertebrate central nervous system. EMBO Rep 15, 351–364. https://doi.org/10.1002/embr.201438447

Piltti, K.M., Funes, G.M., Avakian, S.N., Salibian, A.A., Huang, K.I., Carta, K., Kamei, N., Flanagan, L.A., Monuki, E.S., Uchida, N., Cummings, B.J., Anderson, A.J., 2017. Increasing Human Neural Stem Cell Transplantation Dose Alters Oligodendroglial and Neuronal Differentiation after Spinal Cord Injury. Stem Cell Reports 8, 1534–1548. https://doi.org/10.1016/j.stemcr.2017.04.009

Pineau, I., Lacroix, S., 2007. Proinflammatory cytokine synthesis in the injured mouse spinal cord: Multiphasic expression pattern and identification of the cell types involved. J. Comp. Neurol. 500, 267–285. https://doi.org/10.1002/cne.21149

Pinho, A.G., Cibrão, J.R., Silva, N.A., Monteiro, S., Salgado, A.J., 2020. Cell Secretome: Basic Insights and Therapeutic Opportunities for CNS Disorders. Pharmaceuticals (Basel) 13, E31. https://doi.org/10.3390/ph13020031

Poss, K.D., Keating, M.T., Nechiporuk, A., 2003. Tales of regeneration in zebrafish. Dev. Dyn. 226, 202–210. https://doi.org/10.1002/dvdy.10220

Poss, K.D., Wilson, L.G., Keating, M.T., 2002. Heart Regeneration in Zebrafish. Science 298, 2188–2190. https://doi.org/10.1126/science.1077857

Rehermann, M.I., Marichal, N., Russo, R.E., Trujillo-Cenóz, O., 2009. Neural reconnection in the transected spinal cord of the freshwater turtle *Trachemys dorbignyi*. J. Comp. Neurol. 515, 197–214. https://doi.org/10.1002/cne.22061

Reimer, M.M., Kuscha, V., Wyatt, C., Sörensen, I., Frank, R.E., Knüwer, M., Becker, T., Becker, C.G., 2009. Sonic hedgehog is a polarized signal for motor neuron regeneration in adult zebrafish. J Neurosci 29, 15073–15082. https://doi.org/10.1523/JNEUROSCI.4748-09.2009

Reimer, M.M., Sorensen, I., Kuscha, V., Frank, R.E., Liu, C., Becker, C.G., Becker, T., 2008. Motor Neuron Regeneration in Adult Zebrafish. Journal of Neuroscience 28, 8510–8516. https://doi.org/10.1523/JNEUROSCI.1189-08.2008

Ren, C., Yin, P., Ren, N., Wang, Z., Wang, J., Zhang, C., Ge, W., Geng, D., Wang, X., 2018. Cerebrospinal fluid-stem cell interactions may pave the path for cell-based therapy in neurological diseases. Stem Cell Res Ther 9, 66. https://doi.org/10.1186/s13287-018-0807-3

Ren, H., Chen, X., Tian, M., Zhou, J., Ouyang, H., Zhang, Z., 2018. Regulation of Inflammatory Cytokines for Spinal Cord Injury Repair Through Local Delivery of Therapeutic Agents. Adv. Sci. 5, 1800529. https://doi.org/10.1002/advs.201800529

Ren, Y., Young, W., 2013. Managing Inflammation after Spinal Cord Injury through Manipulation of Macrophage Function. Neural Plasticity 2013, 1–9. https://doi.org/10.1155/2013/945034

Ribeiro, A., Monteiro, J.F., Certal, A.C., Cristovão, A.M., Saúde, L., 2017. Foxj1a is expressed in ependymal precursors, controls central canal position and is activated in new ependymal cells during regeneration in zebrafish. Open Biol 7, 170139. https://doi.org/10.1098/rsob.170139

Roberts, T.T., Leonard, G.R., Cepela, D.J., 2017. Classifications In Brief: American Spinal Injury Association (ASIA) Impairment Scale. Clin Orthop Relat Res 475, 1499–1504. https://doi.org/10.1007/s11999-016-5133-4

Rong, Z., Wang, M., Hu, Z., Stradner, M., Zhu, S., Kong, H., Yi, H., Goldrath, A., Yang, Y.-G., Xu, Y., Fu, X., 2014. An effective approach to prevent immune rejection of human ESC-derived allografts. Cell Stem Cell 14, 121–130. https://doi.org/10.1016/j.stem.2013.11.014

Sabelström, H., Stenudd, M., Frisén, J., 2014. Neural stem cells in the adult spinal cord. Exp Neurol 260, 44–49. https://doi.org/10.1016/j.expneurol.2013.01.026

Sabin, K., Santos-Ferreira, T., Essig, J., Rudasill, S., Echeverri, K., 2015. Dynamic membrane depolarization is an early regulator of ependymoglial cell response to spinal cord injury in axolotl. Developmental Biology 408, 14–25. https://doi.org/10.1016/j.ydbio.2015.10.012

Sahu, S., Li, R., Loers, G., Schachner, M., 2019. Knockdown of chondroitin-4-sulfotransferase-1, but not of dermatan-4-sulfotransferase-1, accelerates regeneration of zebrafish after spinal cord injury. FASEB j. 33, 2252–2262. https://doi.org/10.1096/fj.201800852RR

Saker, E., Henry, B.M., Tomaszewski, K.A., Loukas, M., Iwanaga, J., Oskouian, R.J., Tubbs, R.S., 2016. The Human Central Canal of the Spinal Cord: A Comprehensive Review of its Anatomy, Embryology, Molecular Development, Variants, and Pathology. Cureus 8, e927. https://doi.org/10.7759/cureus.927

Salic, A., Mitchison, T.J., 2008. A chemical method for fast and sensitive detection of DNA synthesis in vivo. Proceedings of the National Academy of Sciences 105, 2415–2420. https://doi.org/10.1073/pnas.0712168105

Sances, S., Bruijn, L.I., Chandran, S., Eggan, K., Ho, R., Klim, J.R., Livesey, M.R., Lowry, E., Macklis, J.D., Rushton, D., Sadegh, C., Sareen, D., Wichterle, H., Zhang, S.-C., Svendsen, C.N.,

2016. Modeling ALS with motor neurons derived from human induced pluripotent stem cells. Nat Neurosci 19, 542–553. https://doi.org/10.1038/nn.4273

Sasagawa, S., Nishimura, Y., Hayakawa, Y., Murakami, S., Ashikawa, Y., Yuge, M., Okabe, S., Kawaguchi, K., Kawase, R., Tanaka, T., 2016. E2F4 Promotes Neuronal Regeneration and Functional Recovery after Spinal Cord Injury in Zebrafish. Front Pharmacol 7, 119. https://doi.org/10.3389/fphar.2016.00119

Schrage, K., Koopmans, G., Joosten, E.A.J., Mey, J., 2006. Macrophages and neurons are targets of retinoic acid signaling after spinal cord contusion injury: Retinoid receptors after spinal cord injury. European Journal of Neuroscience 23, 285–295. https://doi.org/10.1111/j.1460-9568.2005.04534.x

Sehgal, I., M Das, J., 2021. Anatomy, Back, Spinal Meninges, in: StatPearls. StatPearls Publishing, Treasure Island (FL).

Shiao, R., Lee-Kubli, C.A., 2018. Neuropathic Pain After Spinal Cord Injury: Challenges and Research Perspectives. Neurotherapeutics 15, 635–653. https://doi.org/10.1007/s13311-018-0633-4

Shin, J., Park, H.-C., Topczewska, J.M., Mawdsley, D.J., Appel, B., 2003. Neural cell fate analysis in zebrafish using olig2 BAC transgenics. Methods Cell Sci 25, 7–14. https://doi.org/10.1023/B:MICS.0000006847.09037.3a

Shiras, A., Chettiar, S.T., Shepal, V., Rajendran, G., Prasad, G.R., Shastry, P., 2007. Spontaneous transformation of human adult nontumorigenic stem cells to cancer stem cells is driven by genomic instability in a human model of glioblastoma. Stem Cells 25, 1478–1489. https://doi.org/10.1634/stemcells.2006-0585

Singleman, C., Holtzman, N.G., 2014. Growth and maturation in the zebrafish, Danio rerio: a staging tool for teaching and research. Zebrafish 11, 396–406. https://doi.org/10.1089/zeb.2014.0976

Sofroniew, M.V., 2015. Astrocyte barriers to neurotoxic inflammation. Nat Rev Neurosci 16, 249–263. https://doi.org/10.1038/nrn3898

Stirling, D.P., Liu, S., Kubes, P., Yong, V.W., 2009. Depletion of Ly6G/Gr-1 leukocytes after spinal cord injury in mice alters wound healing and worsens neurological outcome. J Neurosci 29, 753–764. https://doi.org/10.1523/JNEUROSCI.4918-08.2009

Strand, N.S., Hoi, K.K., Phan, T.M.T., Ray, C.A., Berndt, J.D., Moon, R.T., 2016. Wnt/β-catenin signaling promotes regeneration after adult zebrafish spinal cord injury. Biochemical and Biophysical Research Communications 477, 952–956. https://doi.org/10.1016/j.bbrc.2016.07.006

Subramanian, L., Bershteyn, M., Paredes, M.F., Kriegstein, A.R., 2017. Dynamic behaviour of human neuroepithelial cells in the developing forebrain. Nat Commun 8, 14167. https://doi.org/10.1038/ncomms14167

Takahashi, K., Yamanaka, S., 2006. Induction of Pluripotent Stem Cells from Mouse Embryonic and Adult Fibroblast Cultures by Defined Factors. Cell 126, 663–676. https://doi.org/10.1016/j.cell.2006.07.024

Tazaki, A., Tanaka, E.M., Fei, J.-F., 2017. Salamander spinal cord regeneration: The ultimate positive control in vertebrate spinal cord regeneration. Dev Biol 432, 63–71. https://doi.org/10.1016/j.ydbio.2017.09.034

Than-Trong, E., Bally-Cuif, L., 2015. Radial glia and neural progenitors in the adult zebrafish central nervous system. Glia 63, 1406–1428. https://doi.org/10.1002/glia.22856

Trawczynski, M., Liu, G., David, B.T., Fessler, R.G., 2019. Restoring Motor Neurons in Spinal Cord Injury With Induced Pluripotent Stem Cells. Front. Cell. Neurosci. 13, 369. https://doi.org/10.3389/fncel.2019.00369

Tsarouchas, T.M., Wehner, D., Cavone, L., Munir, T., Keatinge, M., Lambertus, M., Underhill, A., Barrett, T., Kassapis, E., Ogryzko, N., Feng, Y., van Ham, T.J., Becker, T., Becker, C.G., 2018. Dynamic control of proinflammatory cytokines Il-1β and Tnf-α by macrophages in zebrafish spinal cord regeneration. Nat Commun 9, 4670. https://doi.org/10.1038/s41467-018-07036-w

Urbán, N., Blomfield, I.M., Guillemot, F., 2019. Quiescence of Adult Mammalian Neural Stem Cells: A Highly Regulated Rest. Neuron 104, 834–848. https://doi.org/10.1016/j.neuron.2019.09.026

Vajn, K., Plunkett, J.A., Tapanes-Castillo, A., Oudega, M., 2013. Axonal regeneration after spinal cord injury in zebrafish and mammals: differences, similarities, translation. Neurosci Bull 29, 402–410. https://doi.org/10.1007/s12264-013-1361-8

Vandestadt, C., Vanwalleghem, G.C., Castillo, H.A., Li, M., Schulze, K., Khabooshan, M., Don, E., Anko, M.-L., Scott, E.K., Kaslin, J., 2019. Early migration of precursor neurons initiates cellular and functional regeneration after spinal cord injury in zebrafish (preprint). Neuroscience. https://doi.org/10.1101/539940

Veldman, M.B., Lin, S., 2008. Zebrafish as a Developmental Model Organism for Pediatric Research. Pediatr Res 64, 470–476. https://doi.org/10.1203/PDR.0b013e318186e609

Vihtelic, T.S., Hyde, D.R., 2000. Light-induced rod and cone cell death and regeneration in the adult albino zebrafish (Danio rerio) retina. J Neurobiol 44, 289–307. https://doi.org/10.1002/1097-4695(20000905)44:3<289::aid-neu1>3.0.co;2-h

Wang, H., Wang, Y., Li, D., Liu, Z., Zhao, Z., Han, D., Yuan, Y., Bi, J., Mei, X., 2015. VEGF inhibits the inflammation in spinal cord injury through activation of autophagy. Biochemical and

Biophysical Research Communications 464, 453–458. https://doi.org/10.1016/j.bbrc.2015.06.146

Wang, Y.-C., Feng, G.-Y., Xia, Q.-J., Hu, Y., Xu, Y., Xiong, L., Chen, Z., Wang, H.-P., Wang, T.-H., Zhou, X., 2016. Knockdown of α-synuclein in cerebral cortex improves neural behavior associated with apoptotic inhibition and neurotrophin expression in spinal cord transected rats. Apoptosis 21, 404–420. https://doi.org/10.1007/s10495-016-1218-5

Watanabe, S., Uchida, K., Nakajima, H., Matsuo, H., Sugita, D., Yoshida, A., Honjoh, K., Johnson, W.E.B., Baba, H., 2015. Early Transplantation of Mesenchymal Stem Cells After Spinal Cord Injury Relieves Pain Hypersensitivity Through Suppression of Pain-Related Signaling Cascades and Reduced Inflammatory Cell Recruitment. Stem Cells 33, 1902–1914. https://doi.org/10.1002/stem.2006

Watanabe, T., Nagai, A., Sheikh, A.Md., Mitaki, S., Wakabayashi, K., Kim, S.U., Kobayashi, S., Yamaguchi, S., 2016. A human neural stem cell line provides neuroprotection and improves neurological performance by early intervention of neuroinflammatory system. Brain Research 1631, 194–203. https://doi.org/10.1016/j.brainres.2015.11.031

Wehner, D., Tsarouchas, T.M., Michael, A., Haase, C., Weidinger, G., Reimer, M.M., Becker, T., Becker, C.G., 2017. Wnt signaling controls pro-regenerative Collagen XII in functional spinal cord regeneration in zebrafish. Nat Commun 8, 126. https://doi.org/10.1038/s41467-017-00143-0

Wilson, L., Gale, E., Chambers, D., Maden, M., 2004. Retinoic acid and the control of dorsoventral patterning in the avian spinal cord. Dev Biol 269, 433–446. https://doi.org/10.1016/j.ydbio.2004.01.034

Wright, L.S., Prowse, K.R., Wallace, K., Linskens, M.H.K., Svendsen, C.N., 2006. Human progenitor cells isolated from the developing cortex undergo decreased neurogenesis and eventual senescence following expansion in vitro. Experimental Cell Research 312, 2107–2120. https://doi.org/10.1016/j.yexcr.2006.03.012

Xu, Y., Chen, M., Hu, Bingbing, Huang, R., Hu, Bing, 2017. In vivo Imaging of Mitochondrial Transport in Single-Axon Regeneration of Zebrafish Mauthner Cells. Front. Cell. Neurosci. 11. https://doi.org/10.3389/fncel.2017.00004

Yang, J., Shen, M., Wen, H., Luo, Y., Huang, R., Rong, L., Xie, J., 2020. Recent advance in delivery system and tissue engineering applications of chondroitin sulfate. Carbohydr Polym 230, 115650. https://doi.org/10.1016/j.carbpol.2019.115650

Yeo, S.-Y., Chitnis, A.B., 2007. Jagged-mediated Notch signaling maintains proliferating neural progenitors and regulates cell diversity in the ventral spinal cord. Proceedings of the National Academy of Sciences 104, 5913–5918. https://doi.org/10.1073/pnas.0607062104

Yu, B., Yao, C., Wang, Yongjun, Mao, S., Wang, Yaxian, Wu, R., Feng, W., Chen, Y., Yang, J., Xue, C., Liu, D., Ding, F., Gu, X., 2019. The Landscape of Gene Expression and Molecular

Regulation Following Spinal Cord Hemisection in Rats. Front. Mol. Neurosci. 12, 287. https://doi.org/10.3389/fnmol.2019.00287

Zambusi, A., Ninkovic, J., 2020. Regeneration of the central nervous system-principles from brain regeneration in adult zebrafish. World J Stem Cells 12, 8–24. https://doi.org/10.4252/wjsc.v12.i1.8

Zhang, D., Tang, J., Zhang, J., Zhang, D.L., Hu, C.X., 2019. Responses of pro- and anti-inflammatory cytokines in zebrafish liver exposed to sublethal doses of Aphanizomenon flosaquae DC-1 aphantoxins. Aquatic Toxicology 215, 105269. https://doi.org/10.1016/j.aquatox.2019.105269

Zhang, J.-M., An, J., 2007. Cytokines, Inflammation, and Pain. International Anesthesiology Clinics 45, 27–37. https://doi.org/10.1097/AIA.0b013e318034194e

Zhou, X., He, X., Ren, Y., 2014. Function of microglia and macrophages in secondary damage after spinal cord injury. Neural Regen Res 9, 1787–1795. https://doi.org/10.4103/1673-5374.143423

Zhou, X., Wahane, S., Friedl, M.-S., Kluge, M., Friedel, C.C., Avrampou, K., Zachariou, V., Guo, L., Zhang, B., He, X., Friedel, R.H., Zou, H., 2020. Microglia and macrophages promote corralling, wound compaction and recovery after spinal cord injury via Plexin-B2. Nat Neurosci 23, 337–350. https://doi.org/10.1038/s41593-020-0597-7

Chapter 7.0 Appendix

Figure S1

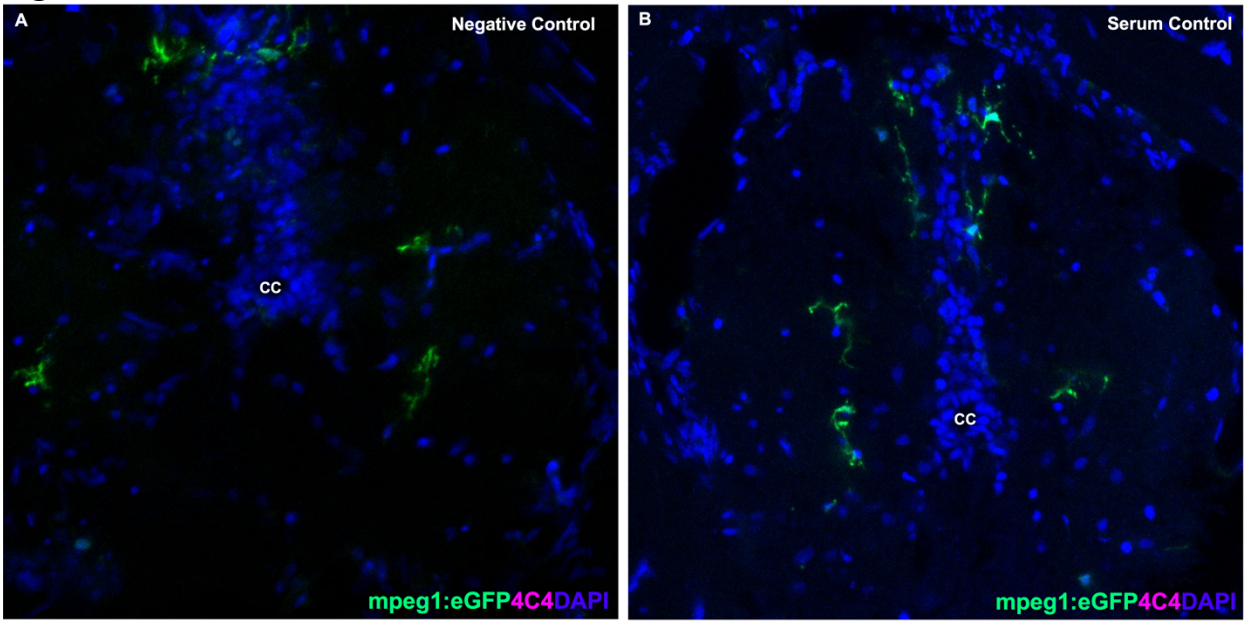

Figure S1. Negative and serum control confirm specific staining of the 4C4 antibody.

(**A**) Negative control in the Tg(mpeg1:eGFP) line by omitting the 4C4 antibody, showed no 4C4 microglial staining. (**B**) A serum was used to culture the hybridoma line and harvest the 4C4 antibody. Here a serum control was used to ensure the staining seen with 4C4 was not a result of the serum. No 4C4 positive labelling was observed on the Tg(mpeg1:eGFP). DAPI counterstaining was performed on each slide. All images taken at 20X. In all images dorsal is up.

Figure S2

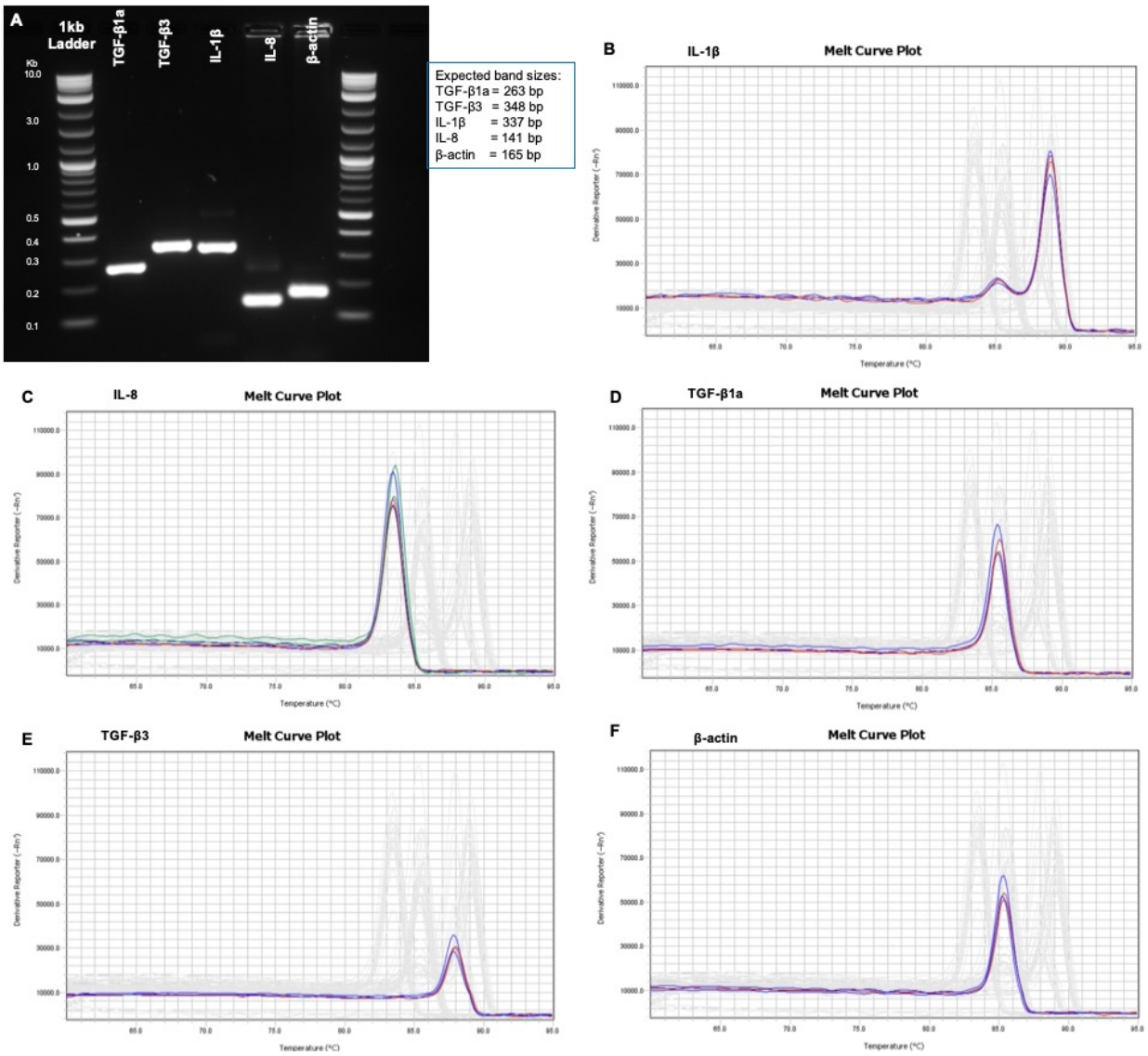

Figure S2. Endpoint PCR gel and melting curve plots for all primers used. (**A**) Running endpoint PCR displayed one band for all primers and the expected band sizes. (**B-F**) Melting curves for all primers used show that, with the exception of IL-1β, only a single peak was visible. The two peaks displayed by IL-1β may indicate two PCR products, but a single product was confirmed by the gel.

Figure S3

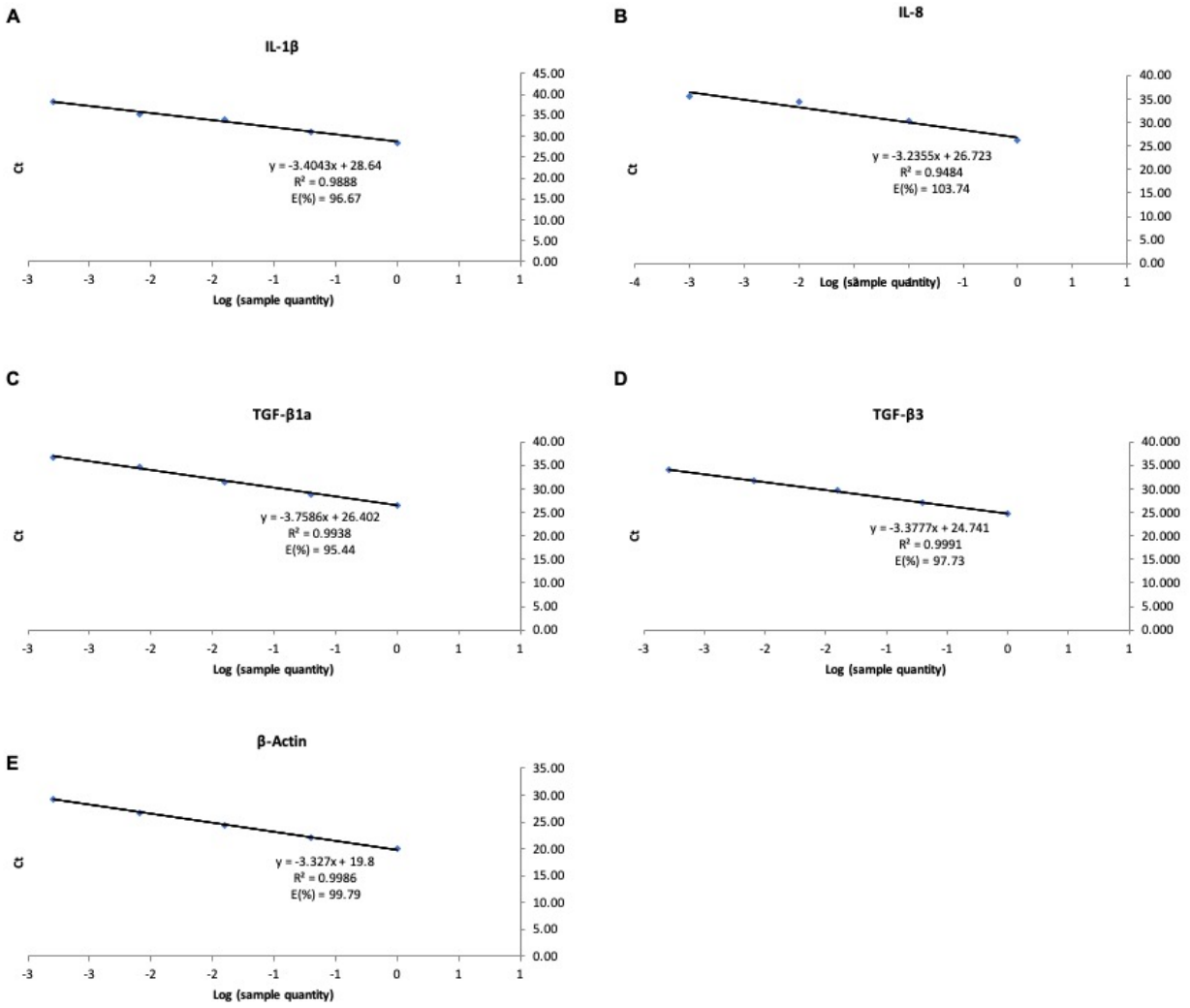

Figure S3. Efficiency curves for primers. (**A-E**) For all primers, the efficiency of the reaction was between 95-99% which is well within the target range of 90-110%. Equation used to calculate R^2 was y = mx+b and to get the efficiency $E = -1+10^{(-1/slope)}$ was used.

Figure S4

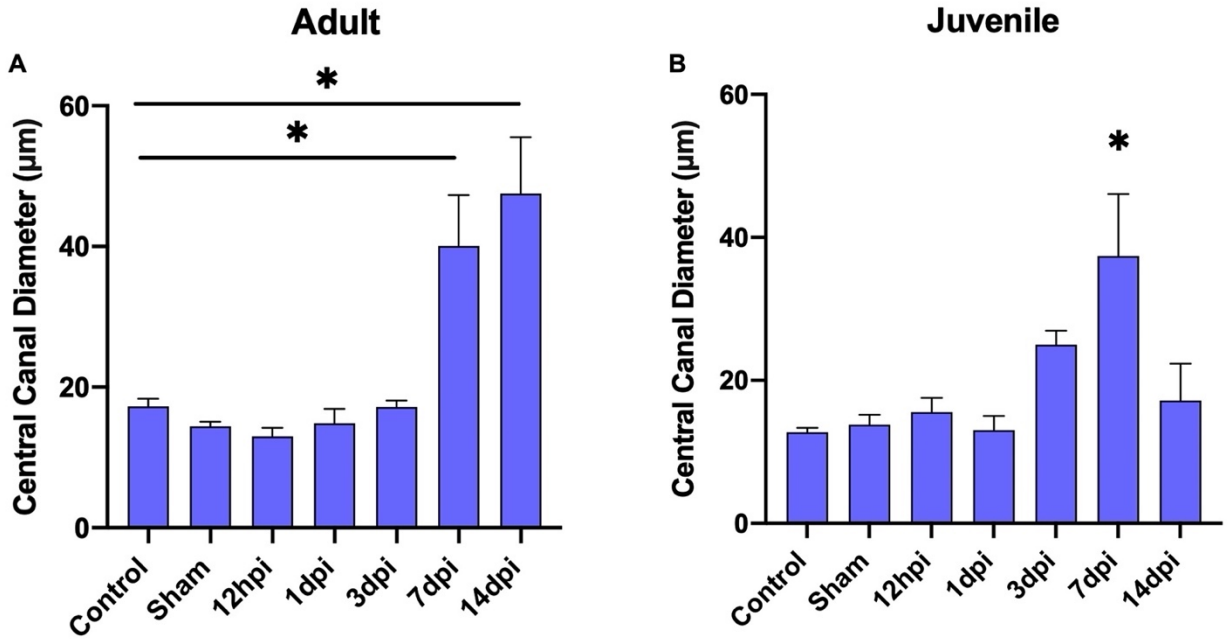

Figure S4. Diameters of central canals in adult and juvenile zebrafish. (**A**) Quantification of central canal diameters in adult zebrafish. (**B**) Quantification of central canal diameters in juvenile zebrafish. One-way ANOVA with Tukey's multiple comparisons test; *$p < 0.0001$; n=3-5 animals for each timepoint.

Figure S5

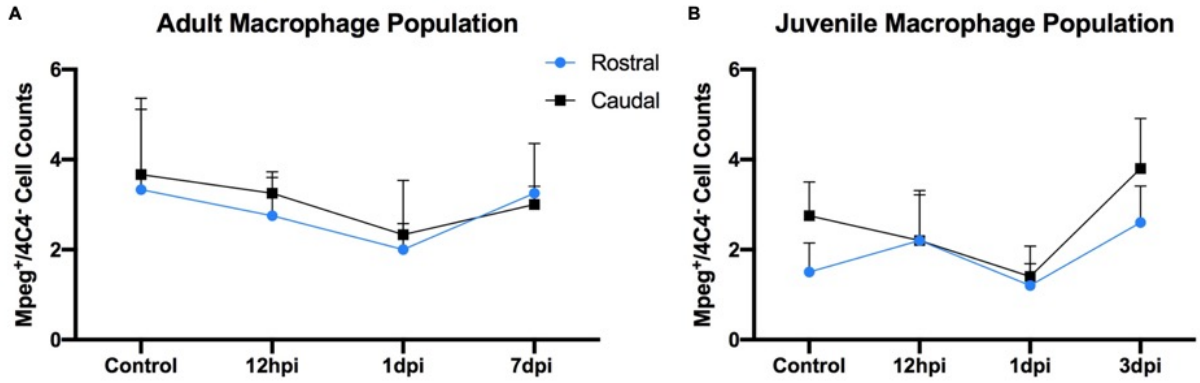

Figure S5. Populations of macrophages remain stable across adults and juveniles after SCI. (**A**) No significant difference was observed between control and SCI groups in populations of adult macrophages. In addition, comparison of rostral and caudal zones of the injury site at each timepoint yielded no significant difference. (**B**) Juvenile zebrafish show similar results as adults with a small population of macrophages in uninjured control groups and no significant difference at other timepoints. Rostral and caudal zones also showed no significant difference. One-way ANOVA with Tukey's multiple comparisons test was used to compared across timepoints; Unpaired t-tests were used to compared rostral and caudal macrophages at each timepoint; $*p < 0.05$; n=3-5 animals for each timepoint; errors bars indicate SEM.

Table S1. Antibody dilutions.

Antibody	**Host Animal**	**Source**	**Dilution**
HuC/D	Mouse	Life Technologies	1:400
HB9	Rabbit	Abcam	1:750
Sox2	Rabbit	Abcam	1:500
4C4	Mouse	Millipore Sigma	1:100

Table S2. RT-qPCR primer sequences.

β-actin	Forward	5'-CTCTTCCAGCCTTCCTTCCT-3'
	Reverse	5'-CTTCTGCATACGGTCAGCAA-3'
IL-1β	Forward	5'-ATGGCGAACGTCATCCAAGA-3'
	Reverse	5'-GAGACCCGCTGATCTCCTTG-3'
IL-8	Forward	5'-GTCGCTGCATTGAAACAGAA-3'
	Reverse	5'-AGGGGTCCAGACAGATCTCC-3'
TGF-β1a	Forward	5'-GCTGTATGCGCAAGCTTTACA-3'
	Reverse	5'-GGACAATTGCTCCACCTTGTG-3'
TGF-β3	Forward	5'-AAAACGCCAGCAACCTGTTC-3'
	Reverse	5'-CCTCAACGTCCATCCCTCTG-3'

Table S3. Tukey's post-hoc multiple comparisons test for significant timepoints in the EZ, SEZ and total cell counts in adult zebrafish.

Timepoint	**Total (EZ + SEZ)**	**EZ**	**SEZ**
14dpi vs. 3dpi	$p = 0.011$	$p = 0.0002$	_____
14dpi vs. 1dpi	$p < 0.0001$	$p < 0.0001$	$p = 0.0096$
14dpi vs. 12hpi	$p < 0.0001$	$p < 0.0001$	$p = 0.0148$
14dpi vs. sham	$p < 0.0001$	$p < 0.0001$	$p = 0.0105$
14dpi vs. control	$p < 0.0001$	$p < 0.0001$	$p = 0.0148$
7dpi vs. 3dpi	$p = 0.0004$	$p < 0.0001$	_____
7dpi vs. 1dpi	$p < 0.0001$	$p < 0.0001$	$p = 0.0203$
7dpi vs. 12hpi	$p < 0.0001$	$p < 0.0001$	$p = 0.0320$
7dpi vs. sham	$p < 0.0001$	$p < 0.0001$	$p = 0.0222$
7dpi vs. control	$p < 0.0001$	$p < 0.0001$	$p = 0.0319$

Table S4. Tukey's post-hoc multiple comparisons test for significant timepoints in the EZ, SEZ and total cell counts in juvenile zebrafish.

Timepoints	**Total (EZ +SEZ)**	**EZ**	**SEZ**
7dpi vs. 1dpi	$p = 0.0001$	$p = 0.0008$	$p = 0.0002$
7dpi vs. 12hpi	$p = 0.0018$	$p = 0.0088$	$p = 0.0029$
7dpi vs. sham	$p < 0.0001$	$p = 0.0002$	$p < 0.0001$
7dpi vs. control	$p < 0.0001$	$p = 0.0002$	$p < 0.0001$
3dpi vs. 1dpi	$p = 0.0004$	$p = 0.0006$	$p = 0.0094$
3dpi vs. 12hpi	$p = 0.0064$	$p = 0.0058$	_____
3dpi vs. sham	$p < 0.0001$	$p = 0.0001$	$p = 0.0024$
3dpi vs. control	$p < 0.0001$	$p = 0.0001$	$p = 0.0027$

Table S5. Tukey's post-hoc multiple comparisons test for significant timepoints in the central canal diameters of adult and juvenile zebrafish.

Timepoints	**Adults**	**Juveniles**
Control vs. 7dpi	$p = 0.0049$	$p = 0.0079$
Sham vs. 7dpi	$p = 0.0015$	$p = 0.0115$
12hpi vs. 7dpi	$p = 0.008$	$p = 0.0360$
1dpi vs. 7dpi	$p = 0.0018$	$p = 0.0164$
3dpi vs. 7dpi	$p = 0.0046$	_____
Control vs. 14dpi	$p = 0.0005$	_____
Sham vs. 14dpi	$p = 0.0002$	_____
12hpi vs. 14dpi	$p = 0.0001$	_____
1dpi vs. 14dpi	$p = 0.0002$	_____
3dpi vs. 14dpi	$p = 0.0005$	_____

Table S6. Dunnetts's multiple comparisons test for significant timepoints in total distance swam within adult and juvenile zebrafish.

Timepoints	**Adults**	**Juveniles**
Control vs. D0	$p = 0.0002$	$p < 0.0001$
Control vs. D1	$p = 0.0005$	$p < 0.0001$
Control vs. D3	$p = 0.0004$	$p = 0.0002$
Control vs. D5	$p = 0.0010$	$p = 0.0007$
Control vs. D7	_____	$p = 0.0424$

Table S7. Bonferroni's multiple comparisons test for significant timepoints in total distance swam between adult and juvenile zebrafish.

Timepoint	**P value**
Day 20	$p = 0.0054$
Day 22	$p = 0.0199$
Day 24	$p = 0.0195$
Day 26	$p = 0.0278$
Day 28	$p < 0.0001$

Table S8. List of common solutions and recipes used.

Solution	**Recipe**
0.4% Tricaine	400mg Tricaine powder, 97.9mL MilliQ water, ~2.1mL 1M Tris (pH 9)
10mM EdU	50mg EdU powder, 19.84mL 1X-PBS, 200uL DMSO to aid in dissolving
2% PFA	0.8g PFA powder, 40mL 1X-PBS
EDTA/Sucrose	100mL 0.5M EDTA, 22g Sucrose, 11mL 10X-PBS
8% Fish Gelatin	20g Sucrose, 8g fish gelatin, 100mL 1X-PBS
1X-PBS	900ml MilliQ water, 100mL 10X-PBS
PBS-Tx	997mL 1X-PBS, 3mL Triton
DAPI	1mg DAPI powder in 1mL 1X-PBS
50mM Tris Buffer	1mL 2M Tris, 39mL MilliQ water
2M Tris Buffer	242.2g Tris base, 800mL MilliQ water
PDT	2mL 10X-PBS, 0.02mL DMSO, 0.02mL Tween, 20mL MilliQ top up
0.5M L-Ascorbic Acid	4.4g 1M L-Ascorbic Acid, 49.9mL MilliQ water